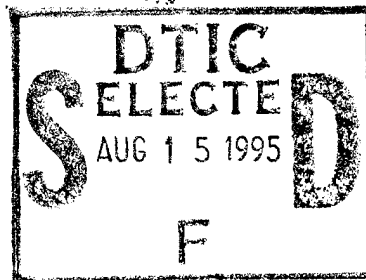


AFIT/GE/ENG/95J-04



19950811 061

**DETERMINATION OF THE TEMPERATURE  
COEFFICIENTS OF SELECTED MATERIAL  
CONSTANTS OF DILITHIUM  
TETRABORATE**

THESIS

Gregory S. Weaver, 2nd Lieutenant, USAF

AFIT/GE/ENG/95J-04

Approved for public release; distribution unlimited.

# DETERMINATION OF THE TEMPERATURE COEFFICIENTS OF SELECTED MATERIAL CONSTANTS OF DILITHIUM TETRABORATE

## THESIS

Presented to the Faculty of the Graduate School of Engineering  
of the Air Force Institute of Technology  
Air University  
In Partial Fulfillment of the  
Requirements for the Degree of  
Master of Science in Electrical Engineering

Accession For	
NTIS CRA&I	<input checked="" type="checkbox"/>
DTIC TAB	<input type="checkbox"/>
Unannounced	<input type="checkbox"/>
Justification .....	
By .....	
Distribution /	
Availability Codes	
Dist	Avail and/or Special
A-1	

Gregory S. Weaver  
2nd Lieutenant, USAF

June 1995

## Table of Contents

List of Figures	iii
List of Tables	v
Acknowledgments	vi
Abstract	vii
Chapter 1 - Introduction	1-1
1.1 Background	1-1
1.2 Problem Statement	1-4
1.3 Scope	1-5
1.4 Approach and Presentation	1-5
Chapter 2 - Fundamentals	2-1
2.1 Concepts	2-1
2.2 Tensor Notation	2-5
2.3 Measurement Procedure (The "Resonator Method")	2-8
2.4 Temperature Dependence	2-10
Chapter 3 - Theory	3-1
3.1 Acoustic Wave Propagation in Piezoelectric Materials	3-1
3.2 Coordinate Transformations and Symmetry Conditions	3-6
3.3 Pure-Mode Solutions and Sample Set Determination	3-9
Chapter 4 - Experimental Procedure	4-1
4.1 Introduction	4-1
4.2 Experimental Setup	4-4
4.3 Experimental Method	4-6
4.4 Experimental Procedure	4-8

Chapter 5 - Data Analysis	5-1
5.1 Data Analysis Overview	5-1
5.2 Third Order Power Series Fit for Antiresonant Frequencies	5-2
5.3 Stiffness Eigenvalue Determination	5-2
5.4 Linear Least Squares Extraction of Material Constants	5-6
5.5 Determination of Material Constants and Their Temperature Coefficients	5-9
5.6 Summary of Experimental Results	5-10
Chapter 6 - Conclusions and Recommendations	6-1
6.1 Comparisons of Results	6-1
6.2 Recommendations for Further Study	6-2
Appendix A	A-1
Bibliography	Bib-1
Vita	Vita-1

## List of Figures

Fig 1-1. Example of a high frequency delay line.....	1-2
Fig 1-2. Example of a piezoelectric transmitter/receiver.....	1-3
Fig 1-3. Examples of a bulk acoustic wave (BAW) and a surface acoustic wave (SAW) devices.....	1-4
Fig 2-1. Crystal possessing trifold symmetry.....	2-1
Fig 2-2. The structure of dilithium tetraborate.....	2-2
Fig 2-3. Mechanical model of crystal and equivalent electrical model.....	2-3
Fig 2-4. Equivalent circuit for a BAW resonator.....	2-4
Fig 2-5. Illustration of stress tensor directions.....	2-6
Fig 2-6. Experimental setup. BAW resonator with thickness $2h$ .....	2-9
Fig 3-1. Infinite, flat piezoelectric plate.....	3-1
Fig 3-2. Doubly rotated plate with $(YXwl)\phi, \theta$ notation.....	3-7
Fig 4-1. Crystal test fixture.....	4-4
Fig 4-2. Experimental setup.....	4-5
Fig 4-3. Graphical representation of transcendental equation (4.1).....	4-8
Fig 4-4. Example of TE fundamental resonance peak measurement.....	4-10
Fig 4-5. Example of LE fundamental resonance peak measurement.....	4-10
Fig 5-1. Plot of $c_{11}^E$ and its power series fit.....	5-12
Fig 5-2. Plot of $c_{12}^E$ and its power series fit.....	5-12
Fig 5-3. Plot of $c_{44}^E$ and its power series fit.....	5-13

Fig 5-4. Plot of  $c_{66}^E$  and its power series fit.....5-13

Fig 5-5. Plot of  $e_{15}$  and its power series fit.....5-14

## List of Tables

Table 3-1. Pure-Mode Loci in Dilithium Tetraborate.....	3-11
Table 3-2. Symmetry Class Pure-Mode Eigenvalue Expressions for Dilithium Tetraborate.....	3-12
Table 3-3. Material-Specific Pure-Mode Eigenvalue Expressions for Dilithium Tetraborate...	3-13
Table 3-4. Suggested Sample Set Summary for Dilithium Tetraborate.....	3-15
Table 4-1. Sample Set and Eigenvalue Expressions.....	4-3
Table 5-1. First and Second Order Coefficients of Thermal Expansion of $\text{Li}_2\text{B}_4\text{O}_7$ .....	5-3
Table 5-2. A Comparison of the Calculated Values of Room Temperature $\bar{c}$ .....	5-6
Table 5-3. Values for Room Temperature Dielectric Constant of $\text{Li}_2\text{B}_4\text{O}_7$ and First and Second Order Temperature Coefficients.....	5-10
Table 5-4. Comparison of the Room Temperature Selected Material Constants with Those of Kosinski [2] and Others.....	5-11
Table 5-5. Calculated First and Second Order Temperature Coefficients of Selected Material Constants of $\text{Li}_2\text{B}_4\text{O}_7$ .....	5-11
Table 6-1. Comparison of First Order Temperature Coefficients ( $\times 10^{-6}/\text{K}$ ) with Previously Published Values.....	6-1
Table 6-2. Comparison of Second Order Temperature Coefficients ( $\times 10^{-9}/\text{K}$ ) with those of Shiosaki, et. al.....	6-2

## Acknowledgments

The help and guidance I've received since I've been at AFIT has come from many sources. My deepest gratitude goes to Dr. John Kosinski of the US Army Research Laboratory. Dr. Kosinski's guidance in every aspect of my research was critical to the development of my knowledge of piezoelectrics and research techniques. Whether traveling to Ohio to examine my experimental setup or faxing me copies of published papers, Dr. Kosinski went far beyond my expectations of a sponsor. I consider myself very lucky to have been able to work him.

Much thanks goes to my advisor, Dr. Victor Bright. Dr. Bright's insights about research and his experience in presenting results made this a better thesis. Thanks are due to Chris O'Brien and Bill Trop, whose experience and helpfulness in lab was much appreciated. I would also like to thank Charlie Powers and Captain Gary Mauersberger, whose professionalism and knowledge greatly aided me in my work. Finally I would like to thank my fiancée, Barbara Antonio, for her patience and her proofreading skills.



## Abstract

The first and second order temperature coefficients of the material constants  $c_{11}^E$ ,  $c_{12}^E$ ,  $c_{44}^E$ ,  $c_{66}^E$ , and  $e_{15}$  of dilithium tetraborate ( $\text{Li}_2\text{B}_4\text{O}_7$ ) have been measured over a temperature range of 20°C to 150°C. An improved resonator method was used to measure the fundamental zero mass loading antiresonant frequencies of selected pure-mode orientations of  $\text{Li}_2\text{B}_4\text{O}_7$ . Material constants extraction was performed using a linear least squares matrix method. The resulting material constant curves were fit with a third order power series to obtain their corresponding temperature coefficients. The calculated temperature coefficients of the material constants  $c_{11}^E$ ,  $c_{12}^E$ ,  $c_{44}^E$ ,  $c_{66}^E$ , and  $e_{15}$  of  $\text{Li}_2\text{B}_4\text{O}_7$  were used to predict the zero mass loading antiresonant frequencies of the crystal samples with average errors of 1.20% for thickness excitation and 0.285% for lateral excitation.

# **Determination of the Temperature Coefficients of Selected Material Constants of Dilithium Tetraborate**

## **Chapter 1 - Introduction**

This chapter provides the background material necessary to understand the importance of piezoelectric crystals to present day electronic systems. Various applications of piezoelectric crystals are discussed. The two main categories of acoustic piezoelectric devices (bulk and surface acoustic wave) are presented and described. Problem Statement and Scope sections cover the goals of this thesis research as well as the experimental methods utilized. Finally, the Approach and Presentation section provides an outline for the remaining chapters of the thesis.

### **1.1 Background**

Piezoelectric materials have become essential to the operation of many electronic systems both in commercial and military use due to the fact that they are natural transducers. Their use as transducers - converting electrical to mechanical energy or vice versa - is an electric tap into the very desirable mechanical properties of crystals. Exploiting these desirable properties of crystals, such as very high Q values, allows the production of very accurate resonators. Highly accurate crystal resonators are needed for use in clocks and oscillators whose accuracies are critical to the performance of many types of electronic systems in the fields of navigation, communication, digital systems, space tracking, guidance systems, radar, and electronic warfare.

One of the desirable properties into which piezoelectricity taps is the high elastic constants associated with crystals. The interatomic bonds in a crystal hold the atoms rigidly in an orderly lattice structure. The extreme stiffness of these bonds is what gives crystals their characteristic hardness and correspondingly their high elastic constant values. As the value of the elastic

constant increases, so does the ability of the atoms in the crystal to return to their equilibrium positions after being perturbed. The ability of a material to transmit high frequency mechanical signals is directly related to how quickly the signal carriers can oscillate; therefore, the high elastic constants associated with crystals allow them to be used in high frequency applications such as filters and delay lines (Figure 1-1).

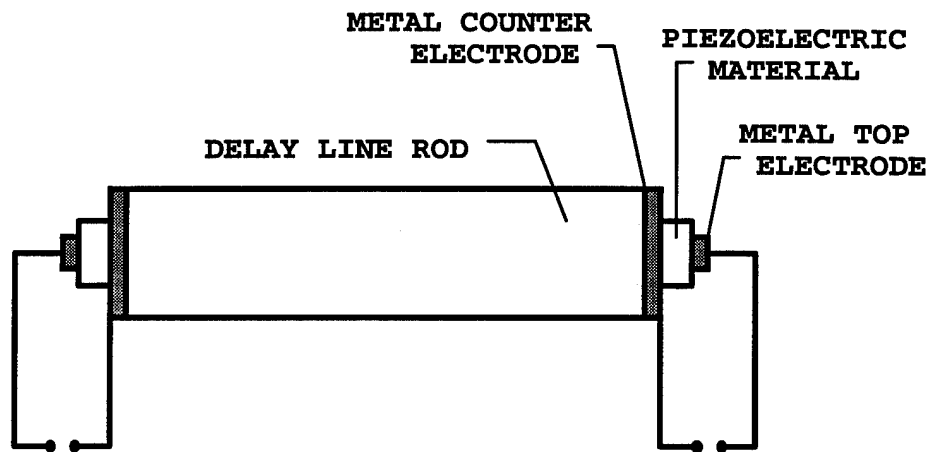


Fig 1-1. Example of a high frequency delay line [1]. The delay line rod is not a piezoelectric crystal. Only the ends of the rod are piezoelectric (transducers). This allows the delay line rod to be a material possessing more desirable mechanical properties than the piezoelectric.

The “natural transducer” characteristic of piezoelectric materials lends them for use as tactile sensors on a robotic finger or in bomb fuses to indicate when the bomb has hit the target. Another transducer-type application is piezoelectric transmitters and receivers that send out and receive vibrational signals. Piezoelectric transmitters/receivers find use as underwater communication systems or as the ultrasound machines used in medicine (Figure 1-2). In addition to their high Q values, piezoelectric materials have other benefits such as: stability over a wide range of parameters; low noise; low power; small size; fast warm-up; and low life-cost cycle. The

importance of piezoelectric materials to modern electrical systems cannot be overemphasized. As our knowledge about piezoelectric materials grows, so does our ability to design and build more advanced systems.

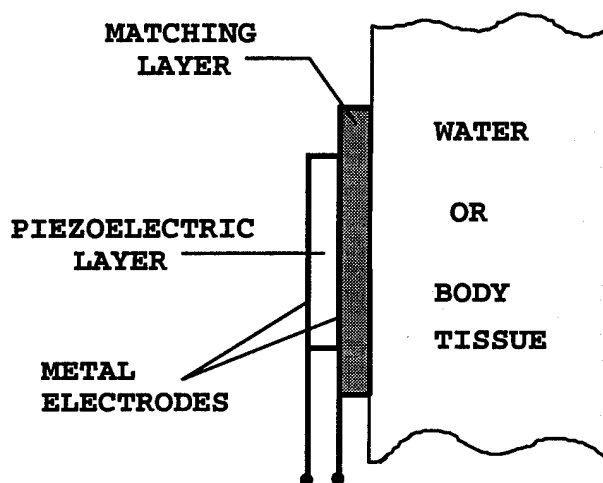


Fig 1-2. Example of a piezoelectric transmitter/receiver [1]. The matching layer serves to match the acoustic impedances of the piezoelectric crystal and the material in which it transmits.

There are two general classifications of acoustic piezoelectric devices: bulk acoustic wave (BAW) and surface acoustic wave (SAW), as shown in Figure 1-3. The difference between the two types of devices lies in the type of elastic waves generated in the crystal. The BAW device has “sending” electrodes that create acoustic waves that travel through the bulk of the material and are picked up by “receiving” electrodes that can be on either side of the crystal. Types of BAW devices include resonators, filters, transducers from audio frequencies to the UHF band, and oscillators [2]. The SAW devices have “sending” electrodes that create acoustic waves which travel on the surface of the crystal and are picked up on the same surface by the “receiving” electrodes. Types of SAW devices include resonators, delay lines, filters, and correlators [2].

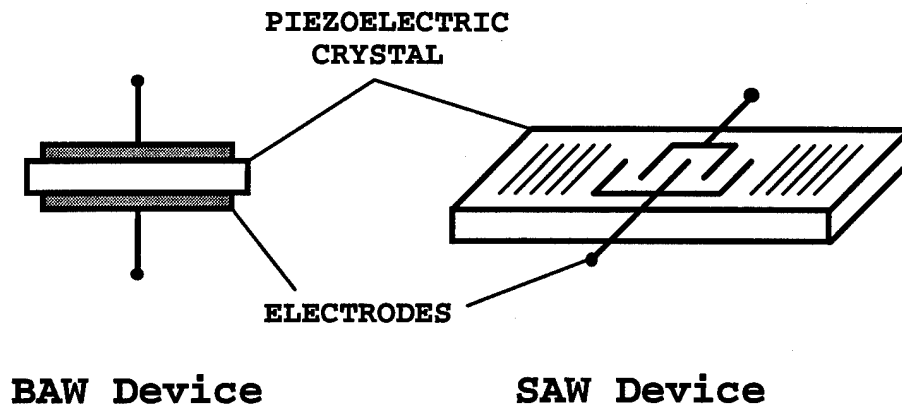


Fig 1-3. Examples of a bulk acoustic wave (BAW) and a surface acoustic wave (SAW) devices [3].

## 1.2 Problem Statement

With the importance of piezoelectric materials fully realized, it is understood that knowledge about the material properties of piezoelectric materials is necessary in order to develop and advance the electrical systems that use them. Quartz crystals have been the most studied and most used piezoelectric crystals to date; however, studies of dilithium tetraborate ( $\text{Li}_2\text{B}_4\text{O}_7$ ) have demonstrated that this material might do a better job than quartz in many applications [2]. Given the correct temperature coefficients of the relevant material constants (elastic constant, piezoelectric constant, dielectric constant), the resonator frequencies of a material may be predicted at any temperature. The temperature coefficients of the material constants of  $\text{Li}_2\text{B}_4\text{O}_7$  published to date have not been able to accurately predict the temperature behavior of its resonator frequencies [4]. In order to fully realize the abilities of dilithium tetraborate, accurate knowledge of the temperature coefficients of its material constants must be obtained. The goal of

this thesis research is to determine the temperature dependence of selected material constants of dilithium tetraborate.

### **1.3 Scope**

Samples of dilithium tetraborate were obtained from Dr. John A. Kosinski, Army Research Laboratory, Fort Monmouth, NJ. It was necessary to design and build a test fixture to hold the  $\text{Li}_2\text{B}_4\text{O}_7$  crystal samples. The resulting test fixture serves the dual purpose of holding the crystals and stabilizing the temperature of the crystals. The antiresonant frequencies of the samples were measured over a range of temperatures. The resulting frequency dependences of temperature were modeled by a third order power fit. Using previously published values for the zero mass-loading room temperature material constants of  $\text{Li}_2\text{B}_4\text{O}_7$  [2], the mass-loading effect was removed from the fitted frequency versus temperature curves. The resulting set of frequency versus temperature curves were used in a linear least squares extraction of the selected material constants of  $\text{Li}_2\text{B}_4\text{O}_7$  over a range of temperatures. Temperature coefficient curves for the selected material constants of  $\text{Li}_2\text{B}_4\text{O}_7$  were then constructed from the results of the material constants extraction. Results are compared with other results published in the literature. Suggestions for further work are also presented.

### **1.4 Approach and Presentation**

The goal of this research was to obtain accurate values for the temperature coefficients of selected material constants of dilithium tetraborate. Chapter 2 presents basic theory beginning with the conceptual fundamentals of piezoelectricity along with a review of tensor notation in the context of the piezoelectric constitutive equations. Chapter 2 concludes with a description of the "resonator method" used in this thesis as well as a definition of the temperature coefficients whose

determination is the ultimate goal of this research. Chapter 3 presents a detailed derivation of the eigenvalue expressions used to obtain pure-mode solutions to the piezoelectric wave equation. Chapter 4 describes the experimental setup as well as the methods used to extract the temperature coefficients of the material constants. Chapter 5 contains the results of this research as well as a comparison with other published results. Chapter 6 presents conclusions drawn from this research and suggestions for further investigation.

## Chapter 2 - Fundamentals

This chapter provides an overview of the theory of piezoelectricity. Basic concepts of piezoelectricity are presented as well as the physical models and mathematical formulas on which piezoelectric phenomena are based. A review of tensor notation is presented in the context of the piezoelectric constitutive relations. The experimental method used in this thesis for determining the material constants of a piezoelectric crystal, the “resonator method,” is reviewed. Finally, there is a brief discussion of the temperature dependence of material constants.

### 2.1 Concepts

Piezoelectric properties are found in many crystals. A piezoelectric material will deform when an electric field is applied across it, and conversely, an electric field will be generated across a piezoelectric material when it is stressed. The cause of piezoelectricity is rooted in the symmetry of a material. Materials lacking a center of symmetry (non-centrosymmetric) are piezoelectric. Figure 2-1 shows a material that possesses trifold symmetry. The electric dipole

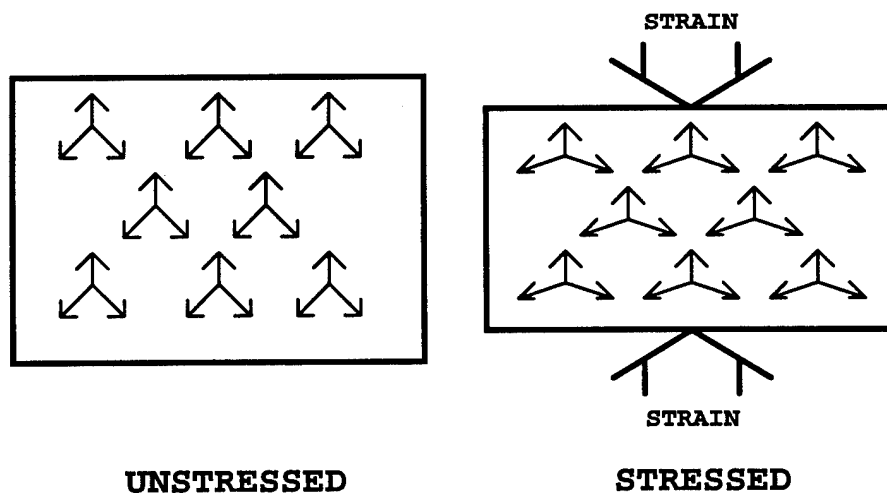


Fig 2-1. Crystal possessing trifold symmetry [1].



moments (arrows) add up to zero in the unstressed case; however, in the stressed case the dipole moments add up to give a net electric dipole moment upwards. The crystal structure of  $\text{Li}_2\text{B}_4\text{O}_7$  is shown in Figure 2-2.

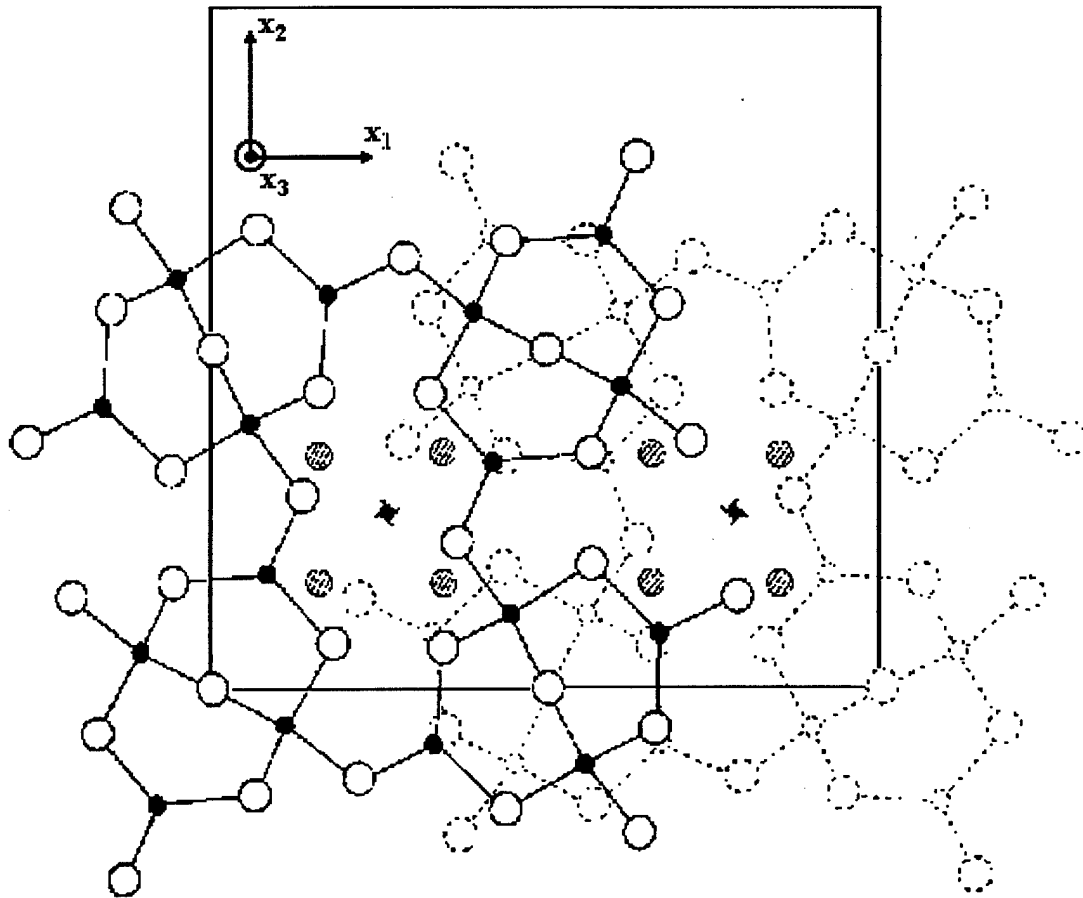


Fig 2-2. The structure of dilithium tetraborate as viewed along the  $x_3$ -axis [5]. The black spheres represent boron atoms, the white spheres represent oxygen atoms, and the shaded spheres represent lithium atoms. The square represents a unit cell.

The basic structural unit of dilithium tetraborate consists of two non-planar six membered rings combined in one group [5]. Because the group is slightly twisted, it has no true mirror-plane symmetry in the  $x_3$  direction; thus, dilithium tetraborate is a piezoelectric material. There is, however, a four-fold symmetry about the  $x_3$ -axis, which places  $\text{Li}_2\text{B}_4\text{O}_7$  in the  $4mm$  crystal class.

A crystal can be modeled as a damped mass-spring system in which the atoms (mass) are held together in a lattice by chemical bonds (springs) which have some form of damping associated with them (dashpot). A mass-spring system behaves as an oscillator, so one can offer another equivalent model for the crystal. This model is an electrical resonator, or RCL circuit. Both models are shown in Figure 2-3.

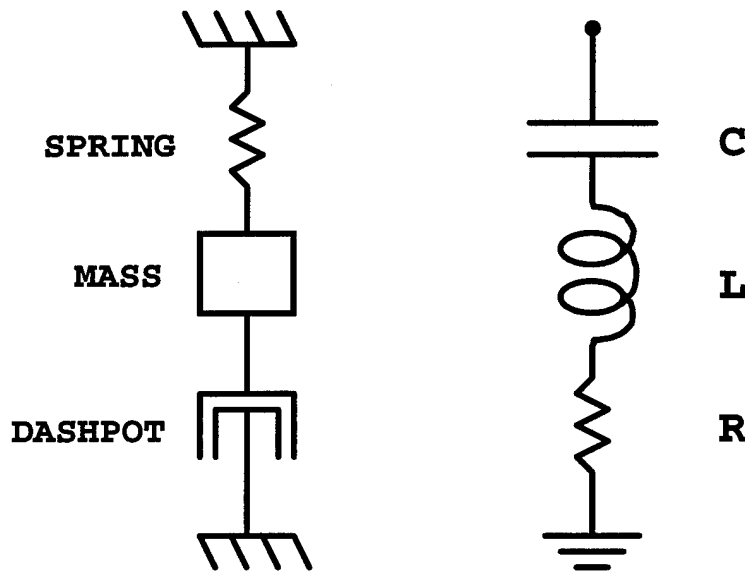


Fig 2-3. Mechanical model of crystal and equivalent electrical model [3].

For comparison, the mass in the mechanical model corresponds to the inductor in the electrical model. Both the mass and the inductor are a resistance to change (mass resists change in motion, inductor resists change in current). The spring in the mechanical system corresponds to the capacitor in the electrical system. Both the spring and the capacitor store energy (the spring stores mechanical energy, the capacitor stores electrical energy). The dashpot corresponds to the resistor. Both are resistant to “motion”, whether it's mechanical motion or the electrical

“motion” of current, and both represent loss. Solving the differential equations governing these systems, one would obtain solutions in the form of waves. In Chapter 3 the governing differential equations are solved to yield wave solutions that are dependent on the material constants as well as the orientation of the sample relative to the crystallographic axes. The waves in a piezoelectric material can be either transverse (shear), longitudinal, or a combination of both.

From the RCL model of a piezoelectric resonator it is possible to obtain the equivalent circuit for the bulk acoustic wave resonator shown in Figure 1-3. The equivalent circuit is shown in Figure 2-4. The resistor (R), capacitor (C), and inductor (L) represent electrical equivalent model for the vibrating crystal and the capacitance  $C_0$  is the capacitance resulting from the attachment of electrodes to the crystal in order to create the acoustic waves. Since the electrical components of the equivalent circuit correspond to the mechanical components of the crystal, the characteristic resonances can be used to measure the material constants of piezoelectric crystal.

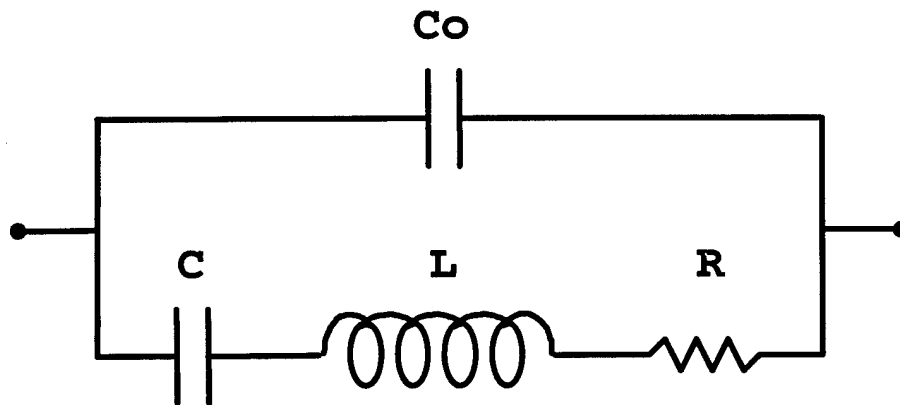


Fig 2-4. Equivalent circuit for a BAW resonator [3]. Where  $C$  is the capacitance,  $L$  is the inductance, and  $R$  is the resistance associated with the electrical equivalent model of the crystal.  $C_0$  is capacitance added as a result of the deposition of electrodes onto the crystal surface.

The electric and mechanical properties of a crystal are coupled together through the piezoelectric constitutive relations [1]:

$$T_i = c_{ij}^E \cdot S_j - e_{ij} \cdot E_j \quad (2.1a)$$

$$D_i = \epsilon_{ij}^S \cdot E_j + e_{ij} \cdot S_j \quad (2.1b)$$

where: T is stress;  $c^E$  is elastic stiffness at a constant electric field; S is strain; e is piezoelectric constant; E is electric field; D is electric displacement;  $\epsilon^S$  is dielectric constant at a constant strain. Stress (T) is the force per unit area that is applied to a solid. Strain (S) is the fractional particle displacement that occurs due to stress. The elastic constant ( $c^E$ ) is a measure of how strongly the atoms of a material are bound to each other at a constant electric field value. The piezoelectric constant (e) is a measure of how strongly the electrical and mechanical properties of a solid are coupled. The elastic, piezoelectric, and dielectric constants are the material properties that govern the piezoelectric effects of a material. These material constants are tensors, and the piezoelectric effects seen in crystals are generally anisotropic. In the design of piezoelectric devices it is necessary to know these material constants to a high degree of accuracy.

## 2.2 Tensor Notation

The piezoelectric constitutive relations may be written in a matrix form [3]:

$$\begin{bmatrix} T_1 \\ T_2 \\ T_3 \\ T_4 \\ T_5 \\ T_6 \\ D_1 \\ D_2 \\ D_3 \end{bmatrix} = \begin{bmatrix} c_{11}^E & c_{12}^E & c_{13}^E & c_{14}^E & c_{15}^E & c_{16}^E & -e_{11} & -e_{12} & -e_{13} \\ c_{21}^E & c_{22}^E & c_{23}^E & c_{24}^E & c_{25}^E & c_{26}^E & -e_{21} & -e_{22} & -e_{23} \\ c_{31}^E & c_{32}^E & c_{33}^E & c_{34}^E & c_{35}^E & c_{36}^E & -e_{31} & -e_{32} & -e_{33} \\ c_{41}^E & c_{42}^E & c_{43}^E & c_{44}^E & c_{45}^E & c_{46}^E & -e_{41} & -e_{42} & -e_{43} \\ c_{51}^E & c_{52}^E & c_{53}^E & c_{54}^E & c_{55}^E & c_{56}^E & -e_{51} & -e_{52} & -e_{53} \\ c_{61}^E & c_{62}^E & c_{63}^E & c_{64}^E & c_{65}^E & c_{66}^E & -e_{61} & -e_{62} & -e_{63} \\ e_{11} & e_{12} & e_{13} & e_{14} & e_{15} & e_{16} & \epsilon_{11}^S & \epsilon_{12}^S & \epsilon_{13}^S \\ e_{21} & e_{22} & e_{23} & e_{24} & e_{25} & e_{26} & \epsilon_{21}^S & \epsilon_{22}^S & \epsilon_{23}^S \\ e_{31} & e_{32} & e_{33} & e_{34} & e_{35} & e_{36} & \epsilon_{31}^S & \epsilon_{32}^S & \epsilon_{33}^S \end{bmatrix} \cdot \begin{bmatrix} S_1 \\ S_2 \\ S_3 \\ S_4 \\ S_5 \\ S_6 \\ E_1 \\ E_2 \\ E_3 \end{bmatrix} \quad (2.2)$$

The tensor values represent the fact that the material is anisotropic, but they also represent the fact that there are two ways to apply stress to a material. Stress can be applied either longitudinally (normal) or transversely (shear) to a material surface. The components of the stress tensor are shown pictorially in Figure 2-5. The first subscript denotes the coordinate axis normal

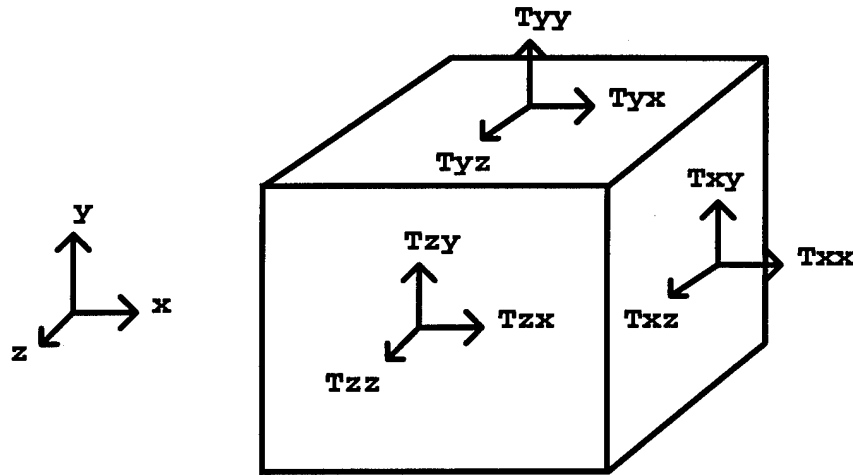


Fig 2-5. Illustration of stress tensor directions [1].

to a stressed plane, and the second subscript denotes the axis along which the stress is applied. The diagonal element of the stress tensor, for example  $T_{xx}$ , represents a stress in the x direction due to a force in the x direction. The off diagonal element of stress, for example  $T_{xy}$ , represents a stress on the x plane due to a force in the y direction. Equation (2.2) makes use of Voigt's prescription which takes into account the inherent symmetry of crystals. The use of Voigt's prescription reduces the rank of a symmetric tensor by one half, thereby greatly simplifying the problem. Voigt's prescription is as follows [6]:

ij or kl	11	22	33	23,32	31,13	12,21
$\lambda$ or $\mu$	1	2	3	4	5	6

where the subscripts  $ij$  or  $kl$  may be replaced with the corresponding value of  $\lambda$  or  $\mu$ . The values  $T_1, T_2,$  and  $T_3$  correspond to  $T_{xx}, T_{yy},$  and  $T_{zz}$  which are the longitudinal stresses in the  $x, y,$  and  $z$  directions respectively; the values  $T_4, T_5,$  and  $T_6$  correspond  $T_{yz}$  or  $T_{zy}, T_{zx}$  or  $T_{xz}, T_{xy}$  or  $T_{yx}$  which are shear stresses about the  $x, y,$  and  $z,$  axis respectively. Equation (2.2) gives nine coupled equations that relate stresses, strains, piezoelectric constants, elastic constants, electric fields, dielectric constants, and electric displacements in different directions.

It appears necessary to obtain values for eighty one material constants in order to completely characterize a piezoelectric material! In practice, however, the number of independent entries in the material constants matrix in Equation (2.2) is greatly reduced due to symmetries arising from the crystal structure. Dilithium tetraborate, for example, belongs to symmetry class  $4mm$  crystal with two independent values for dielectric constant, three independent values for piezoelectric constant, and six independent values for elastic constant [2]. The dielectric constant matrix of dilithium tetraborate is as follows [7]:

$$[\epsilon] = \begin{bmatrix} \epsilon_{11} & 0 & 0 \\ 0 & \epsilon_{11} & 0 \\ 0 & 0 & \epsilon_{33} \end{bmatrix} \quad (2.3a)$$

The piezoelectric constant matrix of dilithium tetraborate is as follows [7]:

$$[e] = \begin{bmatrix} 0 & 0 & 0 & 0 & e_{15} & 0 \\ 0 & 0 & 0 & e_{15} & 0 & 0 \\ e_{31} & e_{31} & e_{33} & 0 & 0 & 0 \end{bmatrix} \quad (2.3b)$$

The elastic constant matrix of dilithium tetraborate is as follows [7]:

$$[c] = \begin{bmatrix} c_{11} & c_{12} & c_{13} & 0 & 0 & 0 \\ c_{12} & c_{11} & c_{13} & 0 & 0 & 0 \\ c_{13} & c_{13} & c_{33} & 0 & 0 & 0 \\ 0 & 0 & 0 & c_{44} & 0 & 0 \\ 0 & 0 & 0 & 0 & c_{44} & 0 \\ 0 & 0 & 0 & 0 & 0 & c_{66} \end{bmatrix} \quad (2.3c)$$

So the characterization of  $\text{Li}_2\text{B}_4\text{O}_7$  is reduced to a problem of finding eleven independent variables.

### 2.3 Measurement Procedure (The “Resonator Method”)

A measurement technique presented by Kosinski [2] has advantages over other methods arising from the exploitation of pure-mode excitation of the material combined with an engineering methodology for pure-mode calculations. The measurement technique is described in detail in Chapter 4; however, a basic overview is presented here.

The technique employs the “resonator method” in which a sample’s characteristic antiresonance frequencies are measured. Multiple odd harmonics of the fundamental antiresonance frequencies are measured in order to increase the accuracy of the results. The characteristic antiresonance frequencies depend on the material constants and the geometry of the device. The crystals used in the technique are cut into discs that measure 0.2 mm in thickness and 14 mm in diameter [2]. Consider the experimental setup in Figure 2-6. This setup can be used to produce longitudinal waves (pure-mode device), shear waves (pure-mode device), or a combination of longitudinal and shear waves (non pure-mode device).

After determining the antiresonance frequencies of the crystal plates, the stiffness eigenvalues ( $\bar{c}$ ) may be determined using the following equation [2]:

$$f_A = \frac{M}{2(2h)} \left[ \frac{\bar{c}}{\rho} \right]^{1/2} \quad (2.4)$$

where  $f_A$  is the antiresonance frequency,  $M$  is the mode of vibration,  $2h$  is the thickness of the plate, and  $\rho$  is the mass density of the crystal. The stiffness eigenvalues are related to the stiffened elastic constants by the following differential equation (wave equation):

$$\bar{c}_{\lambda\mu} \frac{\partial^2 u}{\partial x^2} + \bar{c}u = 0 \quad (2.5)$$

where  $u$  is particle displacement, and  $\bar{c}_{\lambda\mu}$  is the stiffened elastic constant. Equation (2.5) and the eigenvalue expressions are derived in Chapter 3.

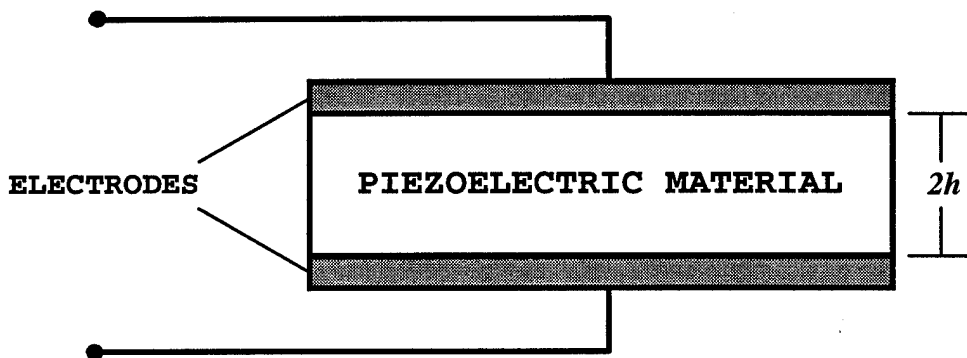


Fig 2-6. Experimental setup. BAW resonator with thickness  $2h$ .

The eigenvalue expressions for the stiffness eigenvalues of a piezoelectric plate form an overdetermined set of equations relating the unknown material constants to the known stiffened elastic constants. The antiresonant frequency data from different crystal orientations as well as different excitation methods is combined with the eigenvalue expressions in a linear least squares



extraction process. The result of the linear least squares extraction is the desired material constants.

## 2.4 Temperature Dependence

It is desirable to produce devices that give the same performance no matter what the operating temperature. Therefore, the temperature dependence of the material constants is an important characteristic to investigate. The temperature dependence of a function is modeled by a power series expansion about a reference temperature. Using a reference temperature of 25°C, the resonant frequency as a function of temperature is represented in the following equation:

$$f(\theta) = f(\theta = 25^\circ C) \cdot \left[ \begin{array}{l} 1 + T_1(\theta - 25) + T_2(\theta - 25)^2 + \dots \\ \dots + T_n(\theta - 25)^n \end{array} \right] \quad (2.6)$$

The value  $\theta$  is the temperature and the values  $T_1, T_2, \dots, T_n$  are the first through  $n$ th order temperature coefficients. In the case of some important piezoelectric materials which have zero temperature dependence of frequency or delay along specific cuts, the temperature coefficients in the power series expansion are very small. As the temperature coefficients get very small, the power series expansion of frequency or delay loses its dependency on temperature.

Since the resonator method uses measurements of antiresonant frequencies to extract the material constants, when the antiresonant frequencies change with temperature so will the material constants. The plate thickness ( $2h$ ), mass density ( $\rho$ ), and dielectric constant ( $\epsilon$ ) are also functions of temperature. Because they are functions of temperature,  $2h$ ,  $\rho$ , and  $\epsilon$  also have their own power series expansions. If the correct temperature coefficients for each of the power series expansions were known, it would be possible to predict the values of the material constants at every temperature. In order to investigate the temperature dependence of the material constants,

it is necessary to determine the temperature dependence of frequency, plate thickness, mass density, and dielectric constant. Fortunately, the temperature dependences of plate thickness and mass density are the result of simple thermal expansion. The coefficients of thermal expansion have been determined by other researchers [8-14].

It is desired to have materials that possess little or no temperature dependence for certain device characteristics such as frequency or delay. With accurate knowledge of the room temperature values for the material constants and their temperature coefficients it will be possible to predict the material's behavior at any orientation and at any temperature, thus allowing full exploitation of the material.

## Chapter 3 - Theory

This chapter provides the reader with a detailed derivation of acoustic plane wave propagation in piezoelectric materials. Once a solution for acoustic wave propagation is obtained, generalized rotation matrices are presented so that wave propagation in any direction through a material may be examined. Applying conditions for pure-mode solutions allows the determination of a set of crystal orientations that propagate pure-mode waves. Selected crystal orientations that propagate pure-mode waves are used in the experimental procedure described in Chapter 4.

### 3.1 Acoustic Wave Propagation in Piezoelectric Materials

In order to determine the crystal orientations that will yield pure-mode waves when excited, it is necessary to examine how acoustic waves travel in a piezoelectric crystal. The derivation in this section is taken from Tiersten's paper on thickness vibrations in piezoelectric plates [15]. Some steps were filled in where appropriate.

Consider an unrotated flat piezoelectric plate of infinite extent (Figure 3-1). Using the rectangular Cartesian coordinate system, let the piezoelectric plate be infinite in the  $x_1$  and  $x_3$  directions, and choose the faces of the plate to be defined at  $x_2 = \pm h$ .

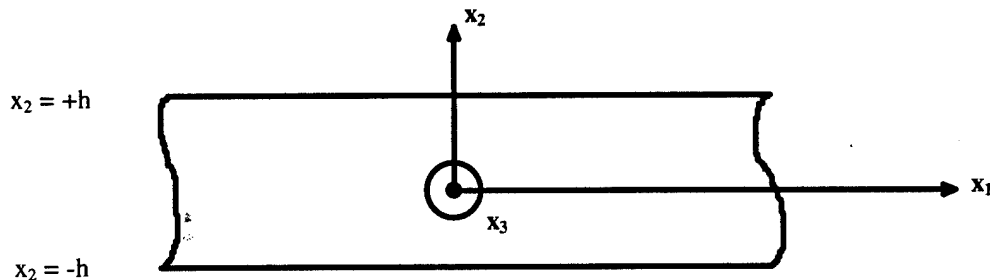


Fig 3-1. Infinite flat piezoelectric plate [2].

Differentiation with respect to a spatial coordinate will be denoted by preceding the differentiation index by a comma. The dot notation for differentiation with respect to time and the summation convention for repeated indices are also employed.

The system of governing equations for this infinite piezoelectric plate includes the stress equations of motion:

$$T_{ij,i} = \rho \ddot{u}_j \quad (3.1)$$

The charge equation of electrostatics:

$$D_{i,i} = 0 \quad (3.2)$$

The mechanical strain displacement relations:

$$S_{kl} = \frac{1}{2}(u_{k,l} + u_{l,k}) \quad (3.3)$$

The equation of electrostatics:

$$E_k = -\varphi_{,k} \quad (3.4)$$

The linear, piezoelectric constitutive relations:

$$T_{ij} = c_{ijkl}^E \cdot S_{kl} - e_{kij} \cdot E_k \quad (3.5a)$$

$$D_i = \epsilon_{ik}^S \cdot E_k + e_{ikl} \cdot S_{kl} \quad (3.5b)$$

where all symbols in equations 3.1 through 3.5 have been defined in Chapter 2 except for  $\varphi$ , which is electric potential.

An alternating electric potential is applied to the faces of the plate. Assuming no external forces are applied to the plate face, the boundary conditions for the infinite plate are:

$$T_{2j} = 0 \quad \text{at} \quad x_2 = \pm h \quad (3.6)$$

$$\varphi = \pm \varphi_0 e^{-i\omega t} \quad \text{at} \quad x_2 = \pm h \quad (3.7)$$

where  $\phi_0$  is a constant, and  $\omega$  is angular frequency.

Now Equations (3.3) and (3.4) may be substituted into Equation (3.5a) to yield:

$$T_{ij} = c_{ijkl}^E u_{k,l} + e_{kij} \phi_{,k} \quad (3.8a)$$

Equations (3.3) and (3.4) may be substituted into Equation (3.5b) to yield:

$$D_i = e_{ikl} u_{k,l} - \epsilon_{ik}^S \phi_{,k} \quad (3.8b)$$

Since there are no boundaries in the  $x_1$  and  $x_3$  directions and the applied voltage is independent of the  $x_1$  and  $x_3$  directions, all derivatives with respect to these directions will vanish. Substituting Equation (3.8a) into Equation (3.1) gives:

$$c_{2jk2}^E u_{k,22} + e_{22j} \phi_{,22} = \rho \ddot{u}_j \quad (3.9a)$$

Substituting Equation (3.8b) into Equation (3.2) yields:

$$e_{2k2} u_{k,22} - \epsilon_{22}^S \phi_{,22} = 0 \quad (3.9b)$$

Now substituting Equation (3.8a) into Equation (3.6) gives the boundary condition:

$$c_{2jk2}^E u_{k,2} + e_{22j} \phi_{,2} = 0 \quad \text{at} \quad x_2 = \pm h \quad (3.10)$$

along with the other boundary condition (3.7). Rearranging Equation (3.9b) gives:

$$\phi_{,22} = \frac{e_{2k2}}{\epsilon_{22}^S} u_{k,22} \quad (3.11)$$

Substituting Equation (3.11) into Equation (3.9a) yields:

$$c_{2jk2}^E u_{k,22} + e_{22j} \left( \frac{e_{2k2}}{\epsilon_{22}^S} u_{k,22} \right) - \rho \ddot{u}_j = 0 \quad (3.12)$$

Assuming an  $e^{-i\omega t}$  time dependence and combining terms, Equation (3.12) becomes:

$$\bar{c}_{2jk2} u_{k,22} + \rho \omega^2 u_j = 0 \quad (3.13a)$$

where: 
$$\bar{c}_{2jk2} = c_{2jk2}^E + \frac{e_{22j}e_{22k}}{\epsilon_{22}^S} \quad (3.13b)$$

The value  $\bar{c}_{2jk2}$  is the stiffened elastic constant. Equation (3.13) is the governing differential equation for thickness vibrations in an infinite, flat piezoelectric plate. Solutions to this wave equation are of the form:

$$u_j = A_j \sin(\eta x_2) \quad (3.14)$$

The value  $\eta$  is the wave number defined by Equation (3.15).

$$\eta = \frac{2\pi}{\lambda} \quad (3.15)$$

The value  $\lambda$  is the acoustic wavelength. Substituting Equation (3.14) into the governing differential equation (3.13) gives:

$$\left( \bar{c}_{2jk2} - \frac{\rho\omega^2}{\eta^2} \delta_{jk} \right) A_k = 0 \quad (3.16)$$

where  $\delta_{jk}$  is the Kronecker delta. For non-trivial solutions:

$$|\bar{c}_{2jk2} - \bar{c} \delta_{jk}| = 0 \quad (3.17a)$$

where: 
$$\bar{c} = \frac{\rho\omega^2}{\eta^2} \quad (3.17b)$$

Equation (3.17) is the governing eigenvalue equation for acoustic waves in a piezoelectric plate.

It is a cubic equation in  $\bar{c}$  that yields three positive, real roots ( $\bar{c}^{(1)}, \bar{c}^{(2)}, \bar{c}^{(3)}$ ) called the stiffness eigenvalues. The eigenvectors,  $A_k$ , may then be found using Equation (3.16).

For the infinite flat piezoelectric plate of Figure 3-1, acoustic resonance occurs when the thickness of the plate equals an odd integer multiple of acoustic half-wavelengths. This condition is given in Equation (3.18).

$$2h = \frac{M}{2}\lambda \quad \text{where } M = 1, 3, 5, \dots \quad (3.18)$$

When this condition is met, the acoustic plane waves traveling in the  $x_2$  direction will be completely reflected at the plate face. When the crystal resonator of Figure 2-6 is connected to a transmission line circuit, this complete reflectance corresponds to an open-circuit (infinite impedance) condition. The frequencies at which the crystal resonator acts like an open circuit are the antiresonant frequencies ( $f_{A0}$ ) of the circuit. In order to determine the  $f_{A0}$ 's, Equation (3.18) is solved for  $\lambda$  and substituted into Equation (3.15) to yield:

$$\eta = \frac{M\pi}{2h} \quad (3.19)$$

Equation (3.19) is then substituted into Equation (3.17b) to give:

$$\bar{c} = \rho \left( \frac{2(2h)f_{A0}}{M} \right)^2 \quad (3.20)$$

For the fundamental zero mass loading antiresonant frequency ( $f_{A0}^{(1)}$ ), Equation (3.20) reduces to the following:

$$\bar{c} = \rho (2(2h)f_{A0}^{(1)})^2 \quad (3.21)$$

Equation (3.21) is used to obtain the stiffness eigenvalues from measurements of  $\rho$ ,  $2h$ , and  $f_{A0}^{(1)}$  using unelectroded crystal (zero mass loading).

### 3.2 Coordinate Transformations and Symmetry Conditions

The remainder of Chapter 3 is based on the method presented by Kosinski to determine crystal orientations that propagate pure-mode waves [2]. Once pure-mode orientations are determined, it is possible to construct a sample set of crystal orientations. Use of the sample set

with the resonator method utilizes the advantages of pure-mode waves in the determination of the material constants.

Symmetry considerations allow the governing eigenvalue equation (3.17a) to be written using Voigt's prescription described in Chapter 2:

$$\begin{vmatrix} (\bar{c}_{66})' - \bar{c} & (\bar{c}_{26})' & (\bar{c}_{46})' \\ (\bar{c}_{26})' & (\bar{c}_{22})' - \bar{c} & (\bar{c}_{24})' \\ (\bar{c}_{46})' & (\bar{c}_{24})' & (\bar{c}_{44})' - \bar{c} \end{vmatrix} = 0 \quad (3.22)$$

Equation (3.13b) may be written with Voigt's prescription as:

$$(\bar{c}_{\lambda\mu})' = (c_{\lambda\mu}^E)' + \frac{(e_{2\lambda})'(e_{2\mu})'}{(\epsilon_{22}^S)'} \quad (3.23)$$

In Equations (3.22) and (3.23) the prime (') indicates a transformation from the crystallographic coordinate system to the coordinate system of the piezoelectric plate. In matrix notation, the transformations are as follows [16]:

$$\left[ (\epsilon^S)' \right] = [a] [\epsilon^S] [a]^T \quad (3.24)$$

$$[e'] = [a] [e] [M]^T \quad (3.25)$$

$$\left[ (c^E)' \right] = [M] [c^E] [M]^T \quad (3.26)$$

The matrix  $[a]$  consists of direction cosines for a doubly rotated crystal plate. The matrix  $[M]$  is a rotation matrix formed from matrix  $[a]$ . The superscript "T" denotes the transpose of a matrix.

The crystal orientations presented in this thesis are based on the standard IEEE notation  $(YXwl)\phi,\theta$  for a doubly rotated plate as shown in Figure 3-2 [17]. The first letter in the IEEE



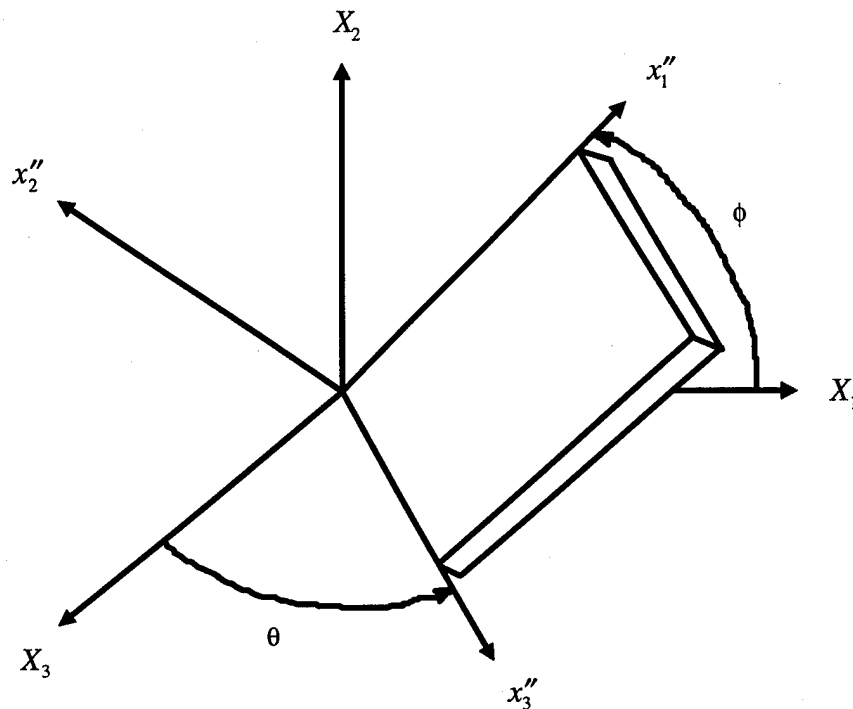


Fig 3-2. Doubly rotated plate with (YXwl) $\phi,\theta$  notation [17]. The unprimed coordinates  $X_1$ ,  $X_2$ , and  $X_3$ , correspond to the crystallographic axes. The double primed coordinates are the doubly rotated axes corresponding to the actual crystal cut.

notation (YXwl) $\phi,\theta$  denotes the crystal axis which is normal to the unrotated plate surface (see Figure 3-1). Thus, plate thickness of the unrotated plate is along the y-axis ( $X_2$ -axis). The second letter in (YXwl) $\phi,\theta$  denotes the direction of the length of the plate; the unrotated plate length is along the x-axis ( $X_1$ -axis). The width of the crystal plate, then, is along the z-axis ( $X_3$ -axis). The "w" denotes the first right-handed rotation about the width axis ( $X_3$ -axis) of  $\phi$  degrees. This rotation results in a new coordinate system for the crystal plate of  $x'_1$ ,  $x'_2$ , and  $x'_3$  ( $x'_3$  equals  $X_3$ ). The "l" denotes the second right-handed rotation about the singly rotated length axis ( $x'_1$ -axis) of  $\theta$  degrees. The result is a doubly rotated plate with rotated crystal axis of  $x''_1$ ,  $x''_2$ , and  $x''_3$ .

Based on the standard IEEE rotation convention of Figure 3-2, the direction cosine matrix is [16]:

$$[a] = \begin{bmatrix} \cos\phi & \sin\phi & 0 \\ -\sin\phi \cos\theta & \cos\phi \cos\theta & \sin\theta \\ \sin\phi \sin\theta & -\cos\phi \sin\theta & \cos\theta \end{bmatrix} \quad (3.27)$$

The rotation matrix, [M], is then given by [16]:

$$[M] = \begin{bmatrix} a_{11}^2 & a_{12}^2 & a_{13}^2 & 2a_{12}a_{13} & 2a_{13}a_{11} & 2a_{11}a_{12} \\ a_{21}^2 & a_{22}^2 & a_{23}^2 & 2a_{22}a_{23} & 2a_{23}a_{21} & 2a_{21}a_{22} \\ a_{31}^2 & a_{32}^2 & a_{33}^2 & 2a_{32}a_{33} & 2a_{33}a_{31} & 2a_{31}a_{32} \\ a_{21}a_{31} & a_{22}a_{32} & a_{23}a_{33} & a_{22}a_{33} + a_{23}a_{32} & a_{21}a_{33} + a_{23}a_{31} & a_{22}a_{31} + a_{21}a_{32} \\ a_{31}a_{11} & a_{32}a_{12} & a_{33}a_{13} & a_{12}a_{33} + a_{13}a_{32} & a_{13}a_{31} + a_{11}a_{33} & a_{11}a_{32} + a_{12}a_{31} \\ a_{11}a_{21} & a_{12}a_{22} & a_{13}a_{23} & a_{12}a_{23} + a_{13}a_{22} & a_{13}a_{21} + a_{11}a_{23} & a_{11}a_{22} + a_{12}a_{21} \end{bmatrix} \quad (3.28)$$

The transformation equations (3.24) through (3.26) are applied to the material constant matrices (2.3a) through (2.3c). The result is a set of analytic expressions that are used to define the elements of the eigenvalue equation (3.22) in terms of untransformed material constants and rotation angles [2]:

$$(\epsilon_{22}^S)' = \cos^2\theta(\epsilon_{11}^S) + \sin^2\theta(\epsilon_{33}^S) \quad (3.29)$$

$$(e_{22})' = \cos^2\theta \sin\theta(2e_{15} + e_{31}) + \sin^3\theta(e_{33}) \quad (3.30)$$

$$(e_{24})' = \cos^3\theta(e_{15}) + \cos\theta \sin^2\theta(e_{33} - e_{15} - e_{31}) \quad (3.31)$$

$$(e_{26})' = 0 \quad (3.32)$$

$$(c_{22}^E)' = \cos^4\theta \left[ c_{11}^E - (2\sin^2\phi \cos^2\phi)(c_{11}^E - (c_{12}^E + c_{66}^E)) \right] \\ + 2\cos^2\theta \sin^2\theta(c_{13}^E + 2c_{44}^E) + \sin^4\theta(c_{33}^E) \quad (3.33)$$

$$\begin{aligned} (c_{24}^E)' &= \cos^3 \theta \sin \theta \left[ (c_{13}^E + 2c_{44}^E) - c_{11}^E + (2 \sin^2 \phi \cos^2 \phi) (c_{11}^E - (c_{12}^E + 2c_{66}^E)) \right] \\ &\quad + \cos \theta \sin^3 \theta (c_{33}^E - (c_{13}^E + 2c_{44}^E)) \end{aligned} \quad (3.34)$$

$$(c_{26}^E)' = \cos^3 \theta \left[ \sin \phi \cos \phi (\cos^2 \phi - \sin^2 \phi) (c_{11}^E - (c_{12}^E + 2c_{66}^E)) \right] \quad (3.35)$$

$$\begin{aligned} (c_{44}^E)' &= \cos^4 \theta (c_{44}^E) + \cos^2 \theta \sin^2 \theta \left[ (c_{11}^E + c_{33}^E) - 2(c_{13}^E + c_{44}^E) \right. \\ &\quad \left. - (2 \sin^2 \phi \cos^2 \phi) (c_{11}^E - (c_{12}^E + 2c_{66}^E)) \right] + \sin^4 \theta (c_{44}^E) \end{aligned} \quad (3.36)$$

$$(c_{46}^E)' = \cos^2 \theta \sin \theta \left[ \sin \phi \cos \phi (\sin^2 \phi - \cos^2 \phi) (c_{11}^E - (c_{12}^E + 2c_{66}^E)) \right] \quad (3.37)$$

$$(c_{66}^E)' = \cos^2 \theta \left[ c_{66}^E + (2 \sin^2 \phi \cos^2 \phi) (c_{11}^E - (c_{12}^E + 2c_{66}^E)) \right] + \sin^2 \theta (c_{44}^E) \quad (3.38)$$

### 3.3 Pure-Mode Solutions and Sample Set Selection

Now that Equation (3.22) may be defined in terms of untransformed material constants and rotation angles, it is possible to determine which crystal orientations will propagate pure-mode waves. Pure-mode solutions to Equation (3.22) are obtained whenever two or more of the off diagonal stiffened elastic constant terms  $\left[ (\bar{c}_{24})', (\bar{c}_{26})', (\bar{c}_{46})' \right]$  are zero [2]. When two of the off diagonal elements are zero, there is a single distinct root. When all three of the off diagonal elements are zero, there are three distinct roots. In analyzing the zeros of the off diagonal elements, it is necessary to examine the zeros of  $(c_{\lambda\mu}^E)'$ ,  $(e_{2\lambda})'$ , and  $(e_{2\mu})'$ .

Examining Equations (3.30) - (3.32), (3.34), (3.35), and (3.37), it is apparent that certain rotation angles will produce zero values for  $(c_{\lambda\mu}^E)'$ ,  $(e_{2\lambda})'$ , or  $(e_{2\mu})'$  independent of the material constant values. These zeros are classified as global symmetry class zeros [2]. The other class of

zero loci occurs when combinations of the material constants sum to produce a zero result for  $(c_{\lambda\mu}^E)'$ ,  $(e_{2\lambda})'$ , or  $(e_{2\mu})'$ . These zeros are classified as material-specific zeros [2]. For dilithium tetraborate, only  $(c_{24}^E)'$  has material-specific zero loci [2]. The piezoelectric contribution to  $(\bar{c}_{24})'$  is small, therefore it shares the same material-specific zero loci as  $(c_{24}^E)'$  [2]. At  $\phi = 0^\circ$ , material-specific zeros for  $(c_{24}^E)'$  occur at  $\theta = 22.7^\circ, 157.3^\circ, 202.7^\circ$ , and  $337.3^\circ$  [2]. As  $\phi$  increases from  $0^\circ$  to  $45^\circ$ , the zeros shift until at  $\phi = 45^\circ$  they are located at  $\theta = 32.4^\circ, 147.6^\circ, 212.4^\circ$ , and  $327.6^\circ$  [2].

Finding the pure-mode solutions for dilithium tetraborate then becomes a problem of finding which rotation angles ( $\phi$  and  $\theta$ ) produce zeros for at least two of  $(\bar{c}_{24})'$ ,  $(\bar{c}_{26})'$ , and  $(\bar{c}_{46})'$  simultaneously. The symmetry of class 4mm materials limits the rotation angles to  $0^\circ \leq \phi \leq 45^\circ$  and  $0^\circ \leq \theta \leq 90^\circ$ . The pure-mode eigenvalues for  $\text{Li}_2\text{B}_4\text{O}_7$  are listed in Table 3-1. The pure-mode eigenvalues  $(\bar{c}_{66})'$  and  $(\bar{c}_{44})'$  correspond to shear waves propagating through the plate in the  $x_2$  direction. The pure-mode eigenvalue  $(\bar{c}_{22})'$  corresponds to longitudinal waves propagating in the  $x_2$  direction.

The eigenvalue equation (3.22) may now be solved at the pure mode orientations to yield eigenvalue expressions that define the relationships between the eigenvalues  $(\bar{c}_{66})'$ ,  $(\bar{c}_{22})'$ , and  $(\bar{c}_{44})'$  and the material constants. The eigenvalue expressions for  $\text{Li}_2\text{B}_4\text{O}_7$  are listed in Tables 3-2 and 3-3. Measuring the antiresonant frequencies of crystals cut at the pure-mode orientations

yields a set of pure-mode eigenvalues through Equation (3.21). Along with the eigenvalue expressions of Table 3-2 and Table 3-3, this set of pure-mode eigenvalues yields an overdetermined system of equations for the extraction of the material constants.

Table 3-1. Pure-Mode Loci in Dilithium Tetraborate [2].

Locus	Distinct Eigenvalues
$0^\circ < \phi < 45^\circ, \theta = 0^\circ$	$(\bar{c}_{44})'$
$0^\circ \leq \phi \leq 45^\circ, \theta = 90^\circ$	$(\bar{c}_{66})', (\bar{c}_{22})', (\bar{c}_{44})'$
$\phi = 0^\circ, \theta = 0^\circ$	$(\bar{c}_{66})', (\bar{c}_{22})', (\bar{c}_{44})'$
$\phi = 0^\circ, 0^\circ < \theta < 90^\circ, \theta \neq 22.7^\circ$	$(\bar{c}_{66})'$
$\phi = 0^\circ, \theta = 22.7^\circ$	$(\bar{c}_{66})', (\bar{c}_{22})', (\bar{c}_{44})'$
$\phi = 45^\circ, \theta = 0^\circ$	$(\bar{c}_{66})', (\bar{c}_{22})', (\bar{c}_{44})'$
$\phi = 45^\circ, 0^\circ < \theta < 90^\circ, \theta \neq 32.4^\circ$	$(\bar{c}_{66})'$
$\phi = 45^\circ, \theta = 32.4^\circ$	$(\bar{c}_{66})', (\bar{c}_{22})', (\bar{c}_{44})'$

In order to measure the antiresonant frequencies of the pure-mode crystal orientations, it is necessary to excite the proper longitudinal waves (corresponding to  $(\bar{c}_{22})'$ ) and shear waves (corresponding to  $(\bar{c}_{66})'$  and  $(\bar{c}_{44})'$ ). The acoustic waves are excited with electric fields directed

Table 3-2. Symmetry Class Pure-Mode Eigenvalue Expressions for Dilithium Tetraborate [2].

Locus	Eigenvalue Expressions
$0^\circ < \phi < 45^\circ, \theta = 0^\circ$	$(\bar{c}_{44})' = c_{44}^E + \frac{e_{15}^2}{\epsilon_{11}^S}$
$0^\circ \leq \phi \leq 45^\circ, \theta = 90^\circ$	$(\bar{c}_{66})' = c_{44}^E$ $(\bar{c}_{22})' = c_{33}^E + \frac{e_{33}^2}{\epsilon_{33}^S}$ $(\bar{c}_{44})' = c_{44}^E$
$\phi = 0^\circ, \theta = 0^\circ$	$(\bar{c}_{66})' = c_{66}^E$ $(\bar{c}_{22})' = c_{11}^E$ $(\bar{c}_{44})' = c_{44}^E + \frac{e_{15}^2}{\epsilon_{11}^S}$
$\phi = 0^\circ, 0^\circ < \theta < 90^\circ$	$(\bar{c}_{66})' = \cos^2 \theta (c_{66}^E) + \sin^2 \theta (c_{44}^E)$
$\phi = 45^\circ, \theta = 0^\circ$	$(\bar{c}_{66})' = \frac{1}{2} c_{11}^E - \frac{1}{2} c_{12}^E$ $(\bar{c}_{22})' = \frac{1}{2} c_{11}^E + \frac{1}{2} c_{12}^E + c_{66}^E$ $(\bar{c}_{44})' = c_{44}^E + \frac{e_{15}^2}{\epsilon_{11}^S}$
$\phi = 45^\circ, 0^\circ < \theta < 90^\circ$	$(\bar{c}_{66})' = \cos^2 \theta \left( \frac{1}{2} c_{11}^E - \frac{1}{2} c_{12}^E \right) + \sin^2 \theta (c_{44}^E)$

through the thickness of the crystal plate (thickness excitation, designated TE) or with electric fields directed along the surface of the crystal plate (lateral excitation, designated LE). The lateral field excitation field may be applied in any direction along the face of the crystal, however, in

Table 3-3. Material-Specific Pure-Mode Eigenvalue Expressions for Dilithium Tetraborate [2].

Locus	Eigenvalue Expressions
$\phi=0^\circ, \theta=22.7^\circ$	$(\bar{c}_{66})' = 0.85(c_{66}^E) + 0.15(c_{44}^E)$ $(\bar{c}_{22})' = 0.72(c_{11}^E) + 0.25(c_{13}^E + 2c_{44}^E) + 0.02(c_{33}^E) + [0.33(2e_{15} + e_{31}) + 0.06(e_{33})]^2 / [0.85(\epsilon_{11}^S) + 0.15(\epsilon_{33}^S)]$ $(\bar{c}_{44})' = 0.49(c_{44}^E) + 0.13(c_{11}^E + c_{33}^E - 2c_{13}^E) + [0.79(e_{15}) + 0.14(e_{33} - e_{15} - e_{31})]^2 / [0.85(\epsilon_{11}^S) + 0.15(\epsilon_{33}^S)]$
$\phi=45^\circ, \theta=32.4^\circ$	$(\bar{c}_{66})' = 0.36(c_{11}^E) - 0.36(c_{12}^E) + 0.29(c_{44}^E)$ $(\bar{c}_{22})' = 0.25(c_{11}^E + c_{12}^E + 2c_{66}^E) + 0.41(c_{13}^E + 2c_{44}^E) + 0.08(c_{33}^E) + [0.38(2e_{15} + e_{31}) + 0.15(e_{33})]^2 / [0.71(\epsilon_{11}^S) + 0.29(\epsilon_{33}^S)]$ $(\bar{c}_{44})' = 0.18(c_{44}^E) + 0.10(c_{11}^E + c_{12}^E + 2c_{33}^E + 2c_{66}^E - 4c_{13}^E) + [0.60(e_{15}) + 0.24(e_{33} - e_{15} - e_{31})]^2 / [0.71(\epsilon_{11}^S) + 0.29(\epsilon_{33}^S)]$

order to completely characterize the crystal's response it is only necessary to define two orthogonal excitation directions along the face of the crystal. It is necessary to define another rotation angle,  $\psi$ , resulting in the IEEE triply rotated plate designation (YXwlt) $\phi, \theta, \psi$  [17]. The "t" denotes a third right-handed rotation about the doubly rotated thickness axis ( $x''_2$ -axis) of  $\psi$  degrees. The orientation (YXwlt) $\phi, \theta, 0$  corresponds to lateral field excitation in the  $\psi=0^\circ$  direction of a (YXwl) $\phi, \theta$  doubly rotated crystal. This orientation/excitation combination has the

designation LE0. The orientation  $(YXwl)\phi,\theta,90$  corresponds to a  $(YXwl)\phi,\theta$  doubly rotated crystal with lateral field excitation in the  $\psi=90^\circ$  direction. This orientation/excitation combination has the designation LE90. Therefore, the only remaining question is which modes may be excited electrically. This question is addressed by Kosinski who concludes that all but two of the pure-modes may be excited electrically [2]. The pure-modes that cannot be excited electrically are the modes associated with  $(\bar{c}_{66})'$  for the  $(YXwl)0,0$  (Y-cut) and  $(YXwl)45,0$  orientations [2]. In general, modes may be excited by both thickness and lateral excitation, however, some modes may only be excited by either TE, LE0, or LE90 [2]. A sample set suggested by Kosinski for the determination of all of the material constants of  $Li_2B_4O_7$  is given in Table 3-4 [2]. Seventeen different crystal orientation/excitation combinations are utilized in the sample set [2].



Table 3-4. Suggested Sample Set Summary for Dilithium Tetraborate [2].  
Shown are the orientation/excitation combinations recommended for the extraction  
of the various constants or combinations of constants.

Constant(s)	Orientation	Excitation
$\epsilon_{11}^S$	(YXwl)0,0 (Y-cut)	TE
$\epsilon_{33}^S$	(YXwl)0,90 (Z-cut) (YXwl)0,45	TE TE
$\epsilon_{11}^S, \epsilon_{33}^S$	(YXwl)45,45 (YXwl)0,22.7 (YXwl)45,32.4	TE TE TE
$e_{15}$	(YXwl)0,0 (Y-cut) (YXwl)45,0	TE TE
$e_{33}$	(YXwl)0,90 (Z-cut)	TE
$e_{15}, e_{31}, e_{33}$	(YXwl)0,22.7 (YXwlt)0,22.7,90 (YXwl)45,32.4 (YXwlt)45,32.4,90	TE LE90 TE LE90
$c_{11}^E$	(YXwlt)0,0,90 (Y-cut)	LE90
$c_{33}^E$	(YXwl)0,90 (Z-cut)	TE
$c_{44}^E$	(YXwl)0,0 (Y-cut) (YXwlt)0,90,0 (Z-cut) (YXwlt)0,90,90 (Z-cut) (YXwl)45,0	TE LE0 LE90 TE
$c_{44}^E, c_{66}^E$	(YXwlt)0,45,0 (YXwlt)0,22.7,0	LE0 LE0
$c_{11}^E, c_{12}^E, c_{44}^E$	(YXwlt)45,45,0 (YXwlt)45,32.4,0	LE0 LE0
$c_{11}^E, c_{12}^E, c_{66}^E$	(YXwlt)45,0,90	LE90
$c_{11}^E, c_{13}^E, c_{33}^E, c_{44}^E$	(YXwl)0,22.7 (YXwlt)0,22.7,90	TE LE90
$c_{11}^E, c_{12}^E, c_{13}^E, c_{33}^E, c_{44}^E, c_{66}^E$	(YXwl)45,32.4 (YXwlt)45,32.4,90	TE LE90

## Chapter 4 - Experimental Procedure

This chapter presents the experimental approach utilized in this thesis. The first section provides an introduction to the piezoelectric material constants measurement technique used in this thesis. The second section describes the equipment and the crystal samples as well as the experimental setup. The third section discusses the experimental method. The fourth section describes the experimental procedure.

### 4.1 Introduction

The purpose of the experimental technique utilized in this thesis is to determine the values for the stiffness eigenvalues of multiple samples of  $\text{Li}_2\text{B}_4\text{O}_7$  over a range of temperatures. In order to accomplish this goal, a sample set composed of  $\text{Li}_2\text{B}_4\text{O}_7$  resonators cut at selected pure-mode orientations is utilized. The orientations of the sample set crystals are chosen to provide an overdetermined set of eigenvalue equations (see Tables 3-2 and 3-3) for use in the extraction of the selected material constants of  $\text{Li}_2\text{B}_4\text{O}_7$ . Using eigenvalue expressions along with the determined values of stiffness eigenvalues for each selected crystal orientation, the selected material constants may be extracted using a data analysis process discussed in Chapter 5.

Choosing the crystal orientations that will be included in the sample set involves the analysis of the eigenvalue expressions of Tables 3-2 and 3-3. Assuming the value  $\epsilon_{11}^s$  is known (obtained from the measurements of Shiosaki [10]), the squared value of  $e_{15}$  may be considered a linear term in the symmetry class pure-mode eigenvalue equations. Nine of the eleven material constants of  $\text{Li}_2\text{B}_4\text{O}_7$  appear in the linear symmetry class pure-

mode eigenvalue equations. The remaining two,  $c_{13}^E$  and  $e_{31}$ , appear only in the nonlinear material-specific eigenvalue equations. Three of the nine that appear in linear equations,  $c_{33}^E$ ,  $e_{33}$ ,  $\epsilon_{33}^S$ , appear in only one linear equation. The eigenvalue equation for  $(\bar{c}_{22})'$  for  $(YXwl)0^\circ \leq \phi \leq 45^\circ, \theta = 90^\circ$  is the only linear equation relating these three constants, therefore, they cannot be obtained from a linear least squares extraction. The five remaining material constants of  $\text{Li}_2\text{B}_4\text{O}_7$ ,  $c_{11}^E$ ,  $c_{12}^E$ ,  $c_{44}^E$ ,  $c_{66}^E$ , and  $e_{15}$ , occur in multiple linear eigenvalue equations which form an overdetermined set of linear equations. These are the selected material constants whose temperature coefficients will be determined with the use of a linear least squares matrix process derived in Chapter 5. All but one of the symmetry class eigenvalue expressions of Table 3-2 are linear equations containing the selected material constants. Therefore, all but one symmetry class pure-mode crystal orientation/excitation combinations may be used for the determination of the selected material constants. The experimental procedure in this thesis utilizes seven different crystal orientations; with two of the selected orientations excited using both TE and LE. Table 4-1 shows the sample set chosen for this thesis as well as the corresponding eigenvalue expressions. When these orientation/excitations are used to measure the stiffness eigenvalues, the sample set gives nine equations for the determination of five unknowns. The accuracy of the calculated material constants is improved because the sample set results in an overdetermined system of equations. Since the value  $\epsilon_{11}^S$  is obtained from previously published work, the value of  $e_{15}^2$  may be obtained through the linear least squares method of Chapter 5.

Table 4-1. Sample Set and Eigenvalue Expressions.

Number of Crystal Samples	Orientation and Excitation	Eigenvalue Expression
4	(YXwl)0,0 TE	$(\bar{c}_{44})' = c_{44}^E + \frac{e_{15}^2}{\epsilon_{11}^S}$
4	(YXwlt)0,0 LE90	$(\bar{c}_{22})' = c_{11}^E$
4	(YXwlt)0,45,0 LE0	$(\bar{c}_{66})' = \frac{1}{2}(c_{66}^E) + \frac{1}{2}(c_{44}^E)$
2	(YXwl)45,0 TE	$(\bar{c}_{44})' = c_{44}^E + \frac{e_{15}^2}{\epsilon_{11}^S}$
4	(YXwlt)45,0,90 LE90	$(\bar{c}_{22})' = \frac{1}{2}c_{11}^E + \frac{1}{2}c_{12}^E + c_{66}^E$
4	(YXwlt)45,45,0 LE0	$(\bar{c}_{66})' = \frac{1}{2}(\frac{1}{2}c_{11}^E - \frac{1}{2}c_{12}^E) + \frac{1}{2}(c_{44}^E)$
4	(YXwlt)0,90,90 LE90	$(\bar{c}_{66})' = c_{44}^E$
4	(YXwlt)0,28.2,0 LE0	$(\bar{c}_{66})' = 0.78(c_{66}^E) + 0.22(c_{44}^E)$
4	(YXwlt)45,56.1,0 LE0	$(\bar{c}_{66})' = 0.31(\frac{1}{2}c_{11}^E - \frac{1}{2}c_{12}^E) + 0.69(c_{44}^E)$

In order to determine the stiffness eigenvalues of the pure-mode crystal orientations, it is necessary to measure the zero mass loading fundamental antiresonance frequency of the crystal. Knowing  $f_{A0}^{(1)}$ , mass density, and thickness of the crystal resonator sample, the value for its stiffness eigenvalue may be determined through Equation (3.21). Measurements of the mass density of the crystal samples ranged from 2414.6 kg/m<sup>3</sup> to 2453.2 kg/m<sup>3</sup> with a relative accuracy of 0.1% [2]. Measurements of the thicknesses of the samples ranged from 196.0 μm to 206.9μm with a relative accuracy of

0.1% [2]. The  $f_{A0}^{(1)}$ 's are measured using the experimental setup described in the following section. A complete description of all crystal samples and  $f_{A0}^{(1)}$  data is presented in Appendix A.

#### 4.2 Experimental Setup

The measurements of the  $f_{A0}^{(1)}$ 's of the crystal samples were performed using a Hewlett-Packard HP 4195A Network/Spectrum Analyzer and Measurement Unit, an Anzac Mod H1 Hybrid Junction, a General Radio Company 874-VCL Variable Capacitor, and a crystal test fixture. The crystal test fixture contained nine Augat 8000-AG1 crystal mounts that were fastened inside a 0.25 inch thick aluminum box shown in Figure 4-1.

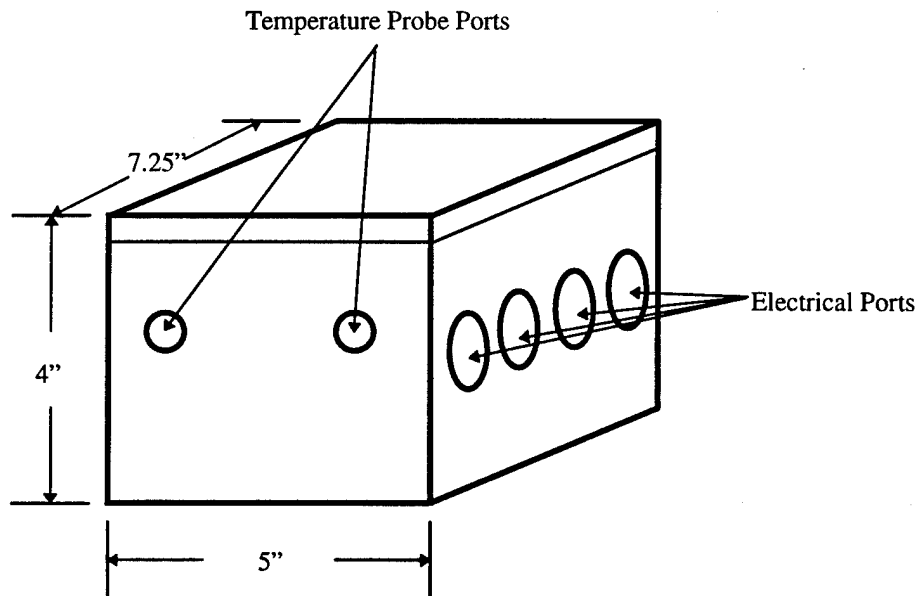


Fig. 4-1. Crystal test fixture.

Temperature was controlled by a Lab-Line Ultra-Clean 100 Oven Model 3490M and measured with an Omega Model DP95 RTD Thermometer equipped with two Omega PRP-1 High Precision RTD Probes. The experimental setup is shown in Figure 4-2.

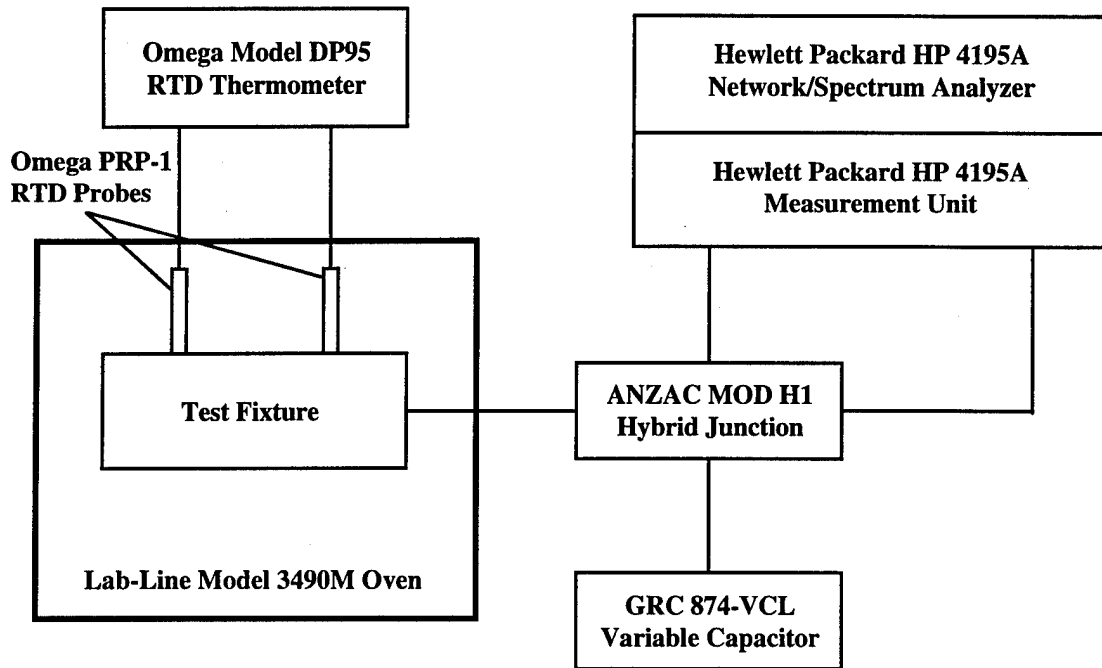


Fig 4-2. Experimental Setup.

Accuracy in the temperature measurements is a critical parameter for extracting accurate results for the temperature coefficients of the material constants. The issue of temperature accuracy was addressed by the construction of the test fixture and the use of dual thermometry for temperature measurement. The test fixture serves the dual purpose of holding the crystals and stabilizing the temperature. By completely enclosing the crystals in a box of aluminum, the test fixture stabilizes the temperature of the crystal samples in two ways. First, the aluminum acts like a “heat capacitor,” storing the heat

energy of the oven. Once the aluminum temperature has stabilized at the average oven temperature, small changes or instabilities in the oven temperature have little effect on the aluminum temperature due to the metal's high thermal capacity. The aluminum box, therefore, serves to stabilize temperature by surrounding its contents with a layer of stable heat energy. The test fixture also stabilizes the temperature of the crystal samples by reducing the effect of convection. By completely enclosing the crystals, the test fixture prevents the thermal convection currents of the oven from reaching the crystals.

In order to accurately measure the temperature of the crystals, two temperature probes were used. In addition to providing two temperature measurements at each data point, this dual thermometry provided a rough measurement of thermal gradients in the test fixture. The difference in the temperature measurements of each probe was used in determining the stability of the temperature for each data point. Therefore, the use of dual thermometry provided more accurate temperature measurements.

### **4.3 Experimental Method**

In order to determine the stiffness eigenvalues of Equation (3.21), it is necessary to measure mass density, thickness, and fundamental zero mass-loading antiresonant frequency ( $f_{A0}^{(1)}$ ) of the crystal. The accuracy of the  $f_{A0}^{(1)}$  measurements is another parameter critical to the accurate determination of the temperature coefficients of the material constants. The experimental procedure utilized in this thesis enhances the accuracy of the  $f_{A0}^{(1)}$  measurements. The accuracy of the antiresonant frequencies is enhanced through the measurement of multiple harmonics. Using the exact transmission line analog for an infinite piezoelectric plate resonator [18-25], it can be shown that

measuring multiple harmonics of the mass loaded resonant frequency ( $f_{R\mu}^{(M)}$ ) eliminates the effect of piezoelectric coupling. For thickness excitation, the resonance frequencies are related through the following exact transmission line equation [26]:

$$\tan(X) = \frac{X}{k^2 + \mu X^2}, \quad X = \frac{\pi}{2} \frac{f_{R\mu}^{(M)}}{f_{Ao}^{(1)}} \quad (4.1)$$

The value  $\mu$  is a unitless parameter called the mass loading,  $f_{Ao}^{(1)}$  is the zero mass loading fundamental antiresonant frequency,  $f_{R\mu}^{(M)}$  is the Mth order mass loaded resonant frequency, and  $k$  is the piezoelectric coupling constant defined as follows [2]:

$$k^2 = \frac{e^2}{\epsilon^s \bar{c}} \quad (4.2)$$

As the harmonic number increases in Equation (4.1),  $f_{R\mu}^{(M)}/M$  converges to the fundamental mass loaded antiresonant frequency. In other words, at higher harmonics  $f_{R\mu}^{(M)}$  becomes an odd integer multiple of the fundamental mass loaded antiresonant frequency. This is shown graphically in Figure 4-3.

In order to obtain the fundamental zero mass loading antiresonant frequencies to be used with Equation (3.21), it is necessary to consider the effects of mass loading. The mass loading of a crystal resonator is defined as the ratio of the mass of the plated electrodes to the mass of the underlying crystal [27]. Mass loading has the effect of lowering the antiresonant frequencies of a crystal resonator. Since neither the mass of the electrodes or the mass of the crystal are functions of temperature, mass loading is not a function of temperature. Therefore, in order to eliminate the effects of mass loading on frequency versus temperature curves it is sufficient to normalize the curve to its room



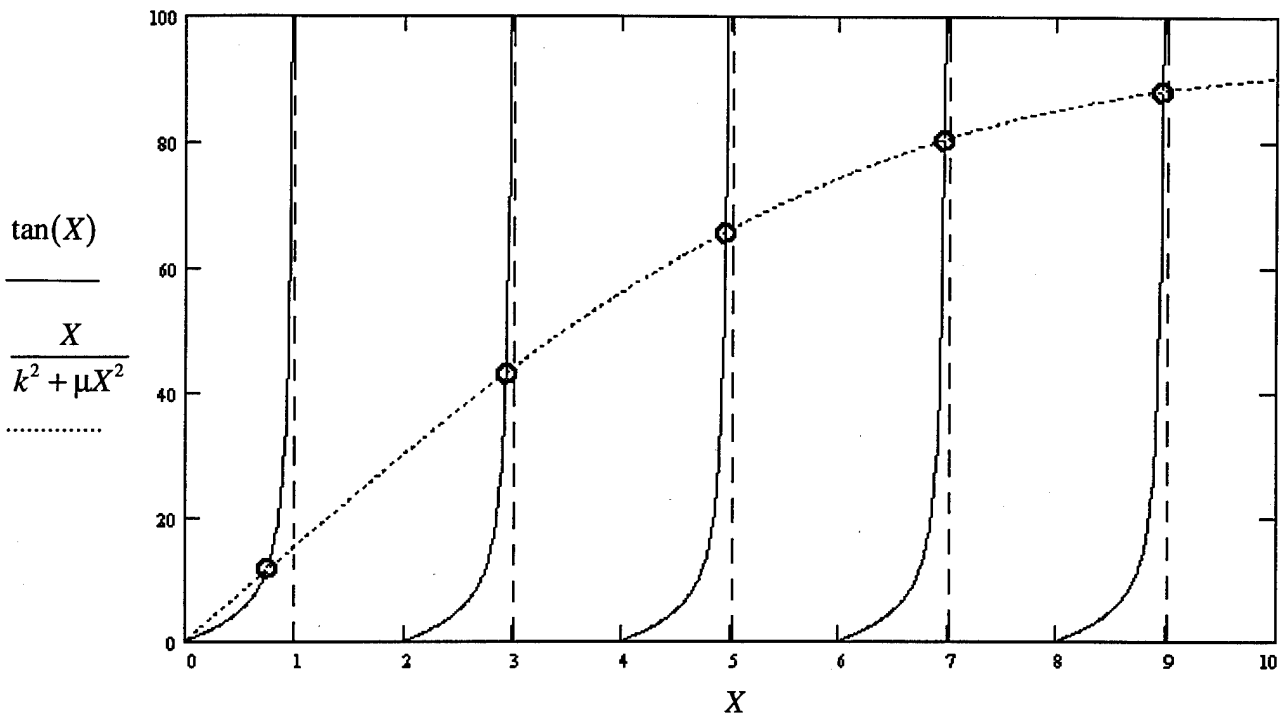


Figure 4-3. Graphical representation of the transcendental Equation (4.1) with  $k = .25$  and  $\mu = .0015$ . As the order of the harmonic increases, the solutions (circled) approach odd integer values, thus the value  $\frac{f_{R\mu}^{(M)}}{f_{A0}^{(1)}}$  approaches  $M$ .

temperature zero mass loading antiresonant frequency. This technique is used in Chapter 5 to build the antiresonant frequency versus temperature curves used in the data analysis. The higher order mass loaded resonant frequencies of the LE modes converge even more quickly to their corresponding fundamental mass loaded resonant frequencies, so measuring the  $f_{R\mu}^{(M)}$ 's of LE crystals and normalizing is also sufficient to obtain frequency values for use in Equation (3.21) [26].

#### 4.4 Experimental Procedure

The experimental procedure involved measurements of multiple harmonics of the  $f_{R\mu}^{(M)}$ 's of each crystal sample over a temperature range of 20°C to 150°C. The temperature was incremented in 10°C steps. The values of  $f_{R\mu}^{(M)}/M$  converged into the  $f_{A\sigma}^{(1)}$ 's. A measurement trial constitutes a complete set of  $f_{A\sigma}^{(1)}$ 's measured at each temperature point for one crystal sample. There were 53 measurement trials completed; each crystal in the sample set of Table 4-1 is measured at least once. A complete list of all measurements is given in Appendix A. Harmonics up to and including the ninth harmonic were measured on most of the crystal samples. On some of the crystal samples, however, only one mode was measured because the other modes could not be resolved. The TE resonance peaks had full width half maximum (FWHM) values of approximately 5 kHz, while the LE resonance peaks had a FWHM of approximately 1 kHz. Figures 4-4 and 4-5 show example TE and LE resonance peak measurements.

Temperature was measured to within  $\pm 0.1^\circ\text{C}$ , and a temperature gradient (difference measured between probes) greater than the accuracy of the thermometer occurred only for the 111.2°C (0.11°C disparity) and 120.9°C (0.12°C disparity) measurements of crystals #5-12 and #20. With the  $f_{A\sigma}^{(1)}$ 's (from the convergence of  $f_{R\mu}^{(M)}/M$ ) measured at each data point, the corresponding stiffness eigenvalues may be calculated from Equation (3.21). The next step is data analysis described in Chapter 5.

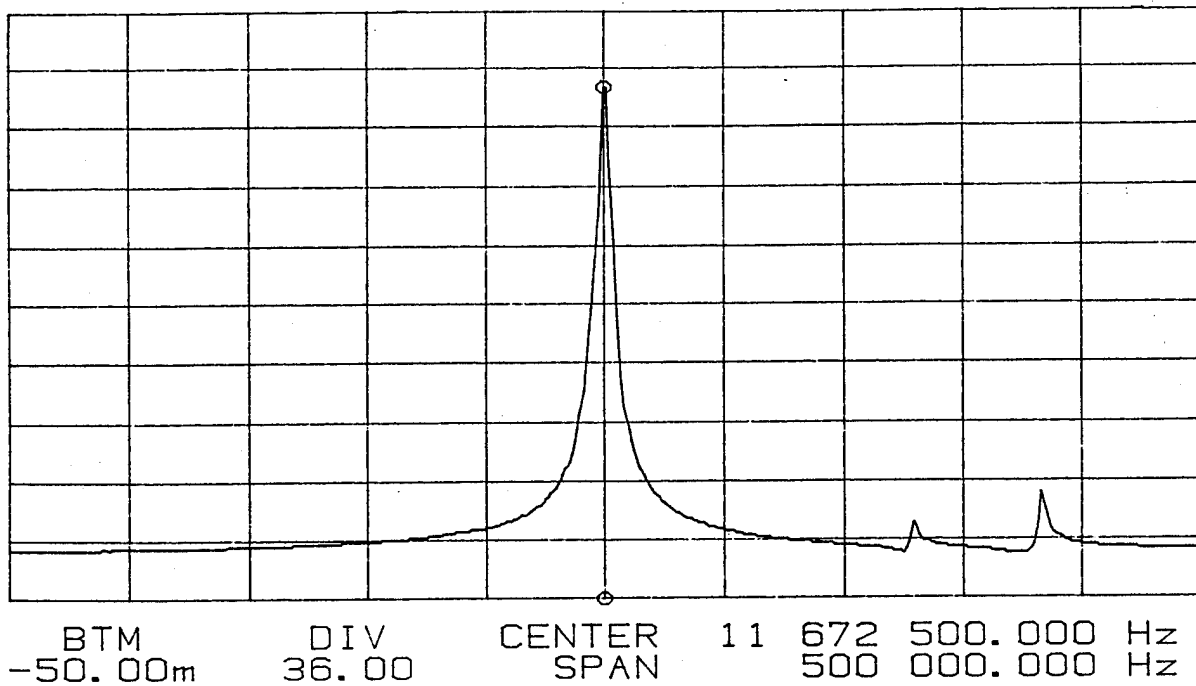


Fig. 4-4. Example of TE fundamental resonance peak measurement for crystal #4, (YXwl)0,0 TE.

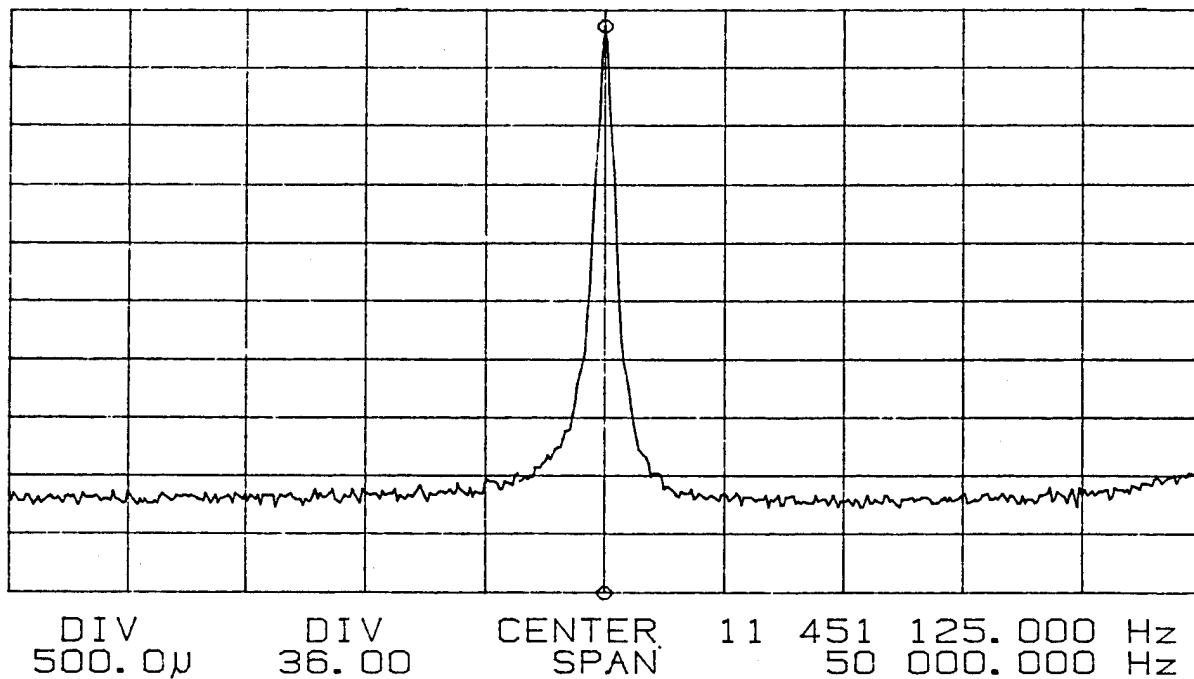


Fig. 4-5. Example of LE fundamental resonance peak measurement for crystal #12, (YXwlt)0,45,0 LE0.

## Chapter 5 - Data Analysis

This chapter presents the method used to extract the temperature coefficients of the selected material constants of dilithium tetraborate. The first section is an overview of the data analysis procedure. The second section describes the purpose of the third order power series fit to the measured antiresonant frequencies. The third section details the calculation of the stiffness eigenvalues from the antiresonant frequency curves. The third section also includes a comparison of the calculated room temperature stiffness eigenvalues with the results obtained by Kosinski [2] using the same crystals. The fourth section describes the linear least squares extraction process for the material constants. The fifth section describes the calculation of the temperature coefficients of the material constants. The sixth section is a summary of the results.

### 5.1 Data Analysis Overview

Now that the mass loaded antiresonant frequencies have been obtained for each crystal orientation using the experimental procedure of Chapter 4, the first step in the data analysis is the normalization of the frequency versus temperature curves. The next step is the calculation of the stiffness eigenvalues using Equation (3.21). Both the mass density and the thickness of the crystals are functions of temperature, so each must be calculated over the appropriate temperature range. The resulting room temperature stiffness eigenvalues were compared with those of Kosinski [2] in order to check the data extraction program. The next step is a linear least squares fit of the stiffness eigenvalue data. Using the eigenvalue expressions found in Table 3-2 for the selected sample set orientations results in an overdetermined system of equations relating stiffness eigenvalue

data to the material constants. The linear least squares process is used for the extraction of the material constants from the overdetermined system. The accuracy of the values for the material constants is enhanced by using an overdetermined system of equations in the extraction process. The data extraction was performed using MathCAD Plus 5.0 [28]. The data extraction program is given in Appendix A.

## 5.2 Third Order Power Series Fit for Antiresonant Frequencies

Once the antiresonant frequencies were measured, it was necessary to construct antiresonant frequency versus temperature curves so that the data could be used in the extraction process. A third order power series with a reference temperature of 25°C (see Equation (2.6)) was used to fit the antiresonant frequency data for each trial. Because the crystal samples had electrodes plated to their surface, the antiresonant frequency data was normalized to the room temperature, unelectroded measurements of Kosinski [2]. The maximum deviations of the measured fundamental mass loaded antiresonant frequencies from Kosinski's  $f_{A0}^{(1)}$  values were only 1.3% for TE measurements and 0.6% for LE measurements. The unelectroded  $f_{A0}^{(1)}$  measurements of Kosinski were used to ensure zero-mass loading conditions. Replacing the zeroth order fundamental mass loaded antiresonant frequency temperature coefficients with the unelectroded measurements of Kosinski should completely eliminate mass loading effects in this thesis' fundamental mass loaded antiresonant frequency data. The third order power series fit provided an easy opportunity to normalize the measured antiresonant frequencies. Once the temperature coefficients of antiresonant frequency were calculated, the zeroth order temperature coefficient was replaced with the room temperature, unelectroded measurements of

Kosinski. The resulting normalized antiresonant frequency versus temperature curves were used in the calculation of the stiffness eigenvalues for each crystal orientation at the temperature points: 20°C, 30°C, 40°C,... 150°C.

### 5.3 Stiffness Eigenvalue Determination

Once the antiresonance frequency versus temperature curves have been determined, the next step is the determination of the stiffness eigenvalues for each crystal orientation. The stiffened elastic constants are calculated at each temperature point.

In order to calculate the stiffness eigenvalues from the antiresonant frequency data, Equation (3.21) is used. Equation (3.21) shows that the stiffness eigenvalues are functions of zero mass loading fundamental antiresonant frequency, mass density, and crystal thickness. Both the mass density and the thickness of the crystal samples change with temperature, therefore, it is necessary to calculate their values at the appropriate temperature points.

In order to calculate the values of mass density and crystal thickness at the temperature points, previously reported values of the coefficients of thermal expansion of  $\text{Li}_2\text{B}_4\text{O}_7$  were used. The first and second order coefficients of thermal expansion were obtained from Shiosaki, et. al. [10] and are listed in Table 5-1. Shiosaki, et. al., uses a reference temperature of 25°C for the coefficients of thermal expansion of  $\text{Li}_2\text{B}_4\text{O}_7$  [10]. The thermal expansion coefficients for the unrotated  $x_1$  direction ( $\alpha_{11}$ 's) are identical to the thermal expansion coefficients for the unrotated  $x_2$  direction ( $\alpha_{22}$ 's). The first and

Table 5-1. First and Second Order Coefficients of Thermal Expansion of  $\text{Li}_2\text{B}_4\text{O}_7$  Obtained from Shiosaki, et al. [10].

	First Order ( $\times 10^{-6}/\text{K}$ )	Second Order ( $\times 10^{-9}/\text{K}^2$ )
$\alpha_{11}$	11.1	5.6
$\alpha_{33}$	-3.74	21

second order temperature coefficients of mass density were calculated with Equation (5.1).

$$T\rho^{(n)} = -(\alpha_{11}^{(n)} + \alpha_{22}^{(n)} + \alpha_{33}^{(n)}) \quad (5.1)$$

The value  $T\rho^{(n)}$  is the nth order temperature coefficient of mass density and  $\alpha_{ij}^{(n)}$  are the nth order thermal expansion coefficients. The mass density of the crystal samples was calculated using a second order power series, Equation (5.2).

$$\rho = \rho_0 [1 + T\rho^{(1)}(\theta - 25) + T\rho^{(2)}(\theta - 25)^2] \quad (5.2)$$

The value  $\rho$  is the mass density,  $\rho_0$  is the room temperature (25°C) mass density, and  $\theta$  is the temperature. The room temperature values of mass density for the crystal samples were measured by Kosinski to an accuracy of 0.1% [2].

Because the coefficients of thermal expansion of  $\text{Li}_2\text{B}_4\text{O}_7$  depend on crystal cut orientation, calculating the thicknesses of the crystal samples at each temperature point is more complicated. In order to use the coefficients of thermal expansion of Table 5-1, they must first be transformed to the appropriate crystal orientation using Equation (5.3) [16].

$$[\alpha''^{(n)}] = [a][\alpha^{(n)}][a]^T \quad (5.3)$$

The matrix  $[a]$  is the direction cosine matrix defined in Chapter 3, and matrix  $[\alpha^{(n)}]$  is a matrix of the coefficients of thermal expansion defined in Equation 5.4.

$$[\alpha^{(n)}] = \begin{bmatrix} \alpha_{11}^{(n)} & 0 & 0 \\ 0 & \alpha_{11}^{(n)} & 0 \\ 0 & 0 & \alpha_{33}^{(n)} \end{bmatrix} \quad (5.4)$$

When  $[\alpha^{(n)}]$  is transformed using Equation (5.3) for a given crystal cut orientation, the resulting matrix may have off-diagonal elements as shown in Equation (5.5).

$$[\alpha''^{(n)}] = \begin{bmatrix} \alpha_{11}''^{(n)} & \alpha_{12}''^{(n)} & \alpha_{13}''^{(n)} \\ \alpha_{21}''^{(n)} & \alpha_{22}''^{(n)} & \alpha_{23}''^{(n)} \\ \alpha_{31}''^{(n)} & \alpha_{32}''^{(n)} & \alpha_{33}''^{(n)} \end{bmatrix} \quad (5.5)$$

Since the crystal samples' thicknesses are directed along the  $x_2''$  axis, the  $\alpha_{22}''^{(n)}$  element is the nth order coefficient of thermal expansion for the thickness of the doubly rotated crystal plate. Using the value for  $\alpha_{22}''^{(n)}$ , the thickness of a crystal sample at the appropriate temperature points is calculated with a second order power series, Equation (5.6).

$$l = l_0 \left[ 1 + \alpha_{22}''^{(1)}(\theta - 25) + \alpha_{22}''^{(2)}(\theta - 25)^2 \right] \quad (5.6)$$

In Equation (5.6),  $l$  is the crystal thickness and  $l_0$  is the room temperature (25°C) crystal thickness. The room temperature crystal thicknesses of the investigated crystal samples were measured by Kosinski to within 0.1% [2].

Once the values of mass density and crystal thickness are calculated over the range of temperatures, the next step in the data analysis is to use Equation (3.21) to calculate the stiffness eigenvalues at the temperature points for each measurement trial. Table 5-2



shows a comparison between the calculated room temperature values for the stiffness eigenvalues and those obtained by Kosinski using the same crystal samples [2].

Table 5-2. A Comparison of the Calculated Values of Room Temperature  $\bar{c}$  with the Values Obtained by Kosinski Using the Same Crystals [2].

Crystal Orientation/ Excitation	Results of this thesis:		Kosinski $\bar{c}$ 's (x10 <sup>9</sup> Pa)	Error (%)
	Calculated $\bar{c}$ 's (x10 <sup>9</sup> Pa)	Standard Deviation (%)		
(YXwl)0,0 TE	59.21	0.29	59.12	0.155
(YXwlt)0,0,90 LE90	135.95	0.23	135.9	0.038
(YXwlt)0,45,0 LE0	52.46	0.23	52.49	0.067
(YXwl)45,0 TE	59.00	0.29	58.95	0.079
(YXwlt)45,0,90 LE90	115.54	0.28	115.4	0.117
(YXwlt)45,45,0 LE0	62.61	0.30	62.49	0.194
(YXwlt)0,90,90 LE90	57.04	0.40	57.06	0.031
(YXwlt)0,28.2,0 LE0	49.757	0.27	49.76	0.006
(YXwlt)45,56.1,0 LE0	60.48	0.25	60.49	0.016

The utility of Table 5-2 is merely to check the validity of the data analysis program used in this thesis. The errors in Table 5-2 may be attributed to the fact that Kosinski used slightly different weightings for each crystal sample used in calculating the  $\bar{c}$ 's.

The values of stiffness eigenvalues are the pure-mode stiffened elastic constants

$\left( (\bar{c}_{66})', (\bar{c}_{22})', (\bar{c}_{44})' \right)$  derived in Chapter 3 and listed in Table 4-1. The eigenvalue

expressions in Table 4-1 constitute an overdetermined system relating the known values of the stiffened elastic constants to the unknown values of the material constants

$\left( c_{11}^E, c_{12}^E, c_{44}^E, c_{66}^E, \frac{e_{15}^2}{\epsilon_{11}^S} \right)$ . A linear least squares extraction process is used to extract the

values of the material constants from this overdetermined system.

#### 5.4 Linear Least Squares Extraction of Material Constants

Every measured antiresonant frequency produces a calculated stiffened elastic constant value. Each stiffened elastic constant value corresponds to one of the eigenvalue expressions of Table 4-1. In this thesis nine different crystal orientation/excitation combinations were used as shown in Table 4-1. There were 53 measurements of antiresonant frequency made at each temperature point.. Therefore, at each temperature point there are 53 equations relating five unknowns. In order to extract the values of the five unknowns, a linear least squares method is used. The data extraction method used in this thesis follows the linear least squares method derived by Nye [7].

Each stiffened elastic constant is a function of five values  $\left( c_{11}^E, c_{12}^E, c_{44}^E, c_{66}^E, \frac{e_{15}^2}{\epsilon_{11}^S} \right)$

and thus may be written as shown in Equation (5.7).

$$\bar{c} = b_1 c_{11}^E + b_2 c_{12}^E + b_3 c_{44}^E + b_4 c_{66}^E + b_5 \frac{e_{15}^2}{\epsilon_{11}^S} \quad (5.7)$$

The coefficients ( $b_n$ 's) are constants that depend on the crystal orientation/excitation. For example, the eigenvalue equation of the (YXwlt)45,0,90 orientation with LE90 excitation has coefficient values of 1/2, 1/2, 0,1,0 respectively. In general there may be N values of

$\bar{c}$  measured ( $N = 53$  for this thesis) resulting in a system of  $N$  equations as shown in Equation (5.8).

$$\begin{aligned}
 \bar{c}_1 &= b_{11}c_{11}^E + b_{12}c_{12}^E + b_{13}c_{44}^E + b_{14}c_{66}^E + b_{15}\frac{e_{15}^2}{\epsilon_{11}^S} \\
 \bar{c}_2 &= b_{21}c_{11}^E + b_{22}c_{12}^E + \dots \\
 &\vdots \\
 \bar{c}_N &= b_{N1}c_{11}^E + b_{N2}c_{12}^E + b_{N3}c_{44}^E + b_{N4}c_{66}^E + b_{N5}\frac{e_{15}^2}{\epsilon_{11}^S}
 \end{aligned} \tag{5.8}$$

Each measurement results in the true value of  $\bar{c}$  plus some error,  $v$ . Rewriting Equation (5.8) to include the error results in the following:

$$\begin{aligned}
 v_1 &= b_{11}c_{11}^E + b_{12}c_{12}^E + b_{13}c_{44}^E + b_{14}c_{66}^E + b_{15}\frac{e_{15}^2}{\epsilon_{11}^S} - \bar{c}_1 \\
 v_2 &= b_{21}c_{11}^E + b_{22}c_{12}^E + \dots \\
 &\vdots \\
 v_N &= b_{N1}c_{11}^E + b_{N2}c_{12}^E + b_{N3}c_{44}^E + b_{N4}c_{66}^E + b_{N5}\frac{e_{15}^2}{\epsilon_{11}^S} - \bar{c}_N
 \end{aligned} \tag{5.9}$$

Equation (5.9) is rewritten in matrix form to obtain Equation (5.10).

$$v_i = b_{ij}z_j - \bar{c}_j \tag{5.10}$$

where,

$$z_j = \begin{bmatrix} c_{11}^E \\ c_{12}^E \\ c_{44}^E \\ c_{66}^E \\ e_{15}^2 / \epsilon_{11}^S \end{bmatrix} \tag{5.11}$$

Following the principle of least squares, the value of  $z_j$  should be such that the sum of the squares of the errors is a minimum. This condition is given by Equation (5.12).

$$\frac{\partial}{\partial z_j} (v_1^2 + v_2^2 + v_3^2 + \dots + v_N^2) = \frac{\partial}{\partial z_j} (v_i \bullet v_i) = 0 \quad (5.12)$$

Using the product rule, Equation (5.12) may be written as Equation (5.13).

$$\begin{aligned} v_i \frac{\partial v_i}{\partial z_j} + v_i \frac{\partial v_i}{\partial z_j} &= 0 \\ 2v_i \frac{\partial v_i}{\partial z_j} &= 0 \\ v_i \frac{\partial v_i}{\partial z_j} &= 0 \end{aligned} \quad (5.13)$$

By taking the derivative with respect to  $z_j$  of both sides of Equation (5.10) and then multiplying through by  $v_i$ , Equation (5.14) is obtained.

$$v_i \frac{\partial v_i}{\partial z_j} = v_i \frac{\partial (b_{ij} z_j)}{\partial z_j} - v_i \frac{\partial \bar{c}_j}{\partial z_j} \quad (5.14)$$

Since  $\bar{c}_j$  is a vector of measured constants, its partial derivative is equal to zero.

Applying the result of Equation (5.13) yields the following:

$$v_i b_{ij} = 0 \quad (5.15)$$

Now multiplying Equation (5.10) by  $b_{ij}$  results in Equation (5.16).

$$v_i b_{ij} = (b_{ij} z_j - \bar{c}_j) b_{ij} \quad (5.16)$$

Applying the result of Equation (5.15) and solving for  $z_j$  gives Equation (5.17).

$$z_k = (b_{ji}^T b_{ik})^{-1} b_{ji}^T \bar{c}_i \quad (5.17)$$

Equation (5.17) is the defining equation for the linear least squares method of extracting the material constants from N stiffened eigenvalue measurements. Substituting Equation (5.17) into Equation (5.10) gives an equation for the accuracy of the measurements:

$$v_i = \left( b_{ij} (b_{ji}^T b_{ik})^{-1} b_{ji}^T - I \right) \bar{c}_j \quad (5.18)$$

where  $I$  is the identity matrix.

### 5.5 Determination of Material Constants and Their Temperature Coefficients

The material constants extraction involves the construction of the N by 5 matrix of coefficients,  $b_{ij}$ . Performing the appropriate matrix operations on  $b_{ij}$  and multiplying by a vector containing the corresponding stiffened elastic constant measurements produces  $z_k$ ,

a vector composed of material constants  $\left( c_{11}^E, c_{12}^E, c_{44}^E, c_{66}^E, \frac{e_{15}^2}{\epsilon_{11}^S} \right)$ . In order to calculate the

value of  $e_{15}$ , it is necessary to know the value of  $\epsilon_{11}^S$ . The room temperature value of  $\epsilon_{11}^S$  was obtained from Kosinski [2] and its corresponding first and second order temperature coefficients were obtained from Shiosaki, et. al. [10], and are listed in Table 5-3.

Table 5-3. Values for Room Temperature Dielectric Constant of  $\text{Li}_2\text{B}_4\text{O}_7$  ( $\epsilon_{11_0}^S$ ) and First and Second Order Temperature Coefficients ( $T\epsilon_{11}^{S(1)}, T\epsilon_{11}^{S(2)}$ ) [10].

$\epsilon_{11_0}^S$ ( $10^{-12}\text{F/m}$ )	$T\epsilon_{11}^{S(1)}$ ( $10^{-6}/\text{K}$ )	$T\epsilon_{11}^{S(2)}$ ( $10^{-9}/\text{K}^2$ )
76.69	97.1	2800

Values for  $\epsilon_{11}^s$  at the appropriate temperature points are calculated using a second order power series equation identical to Equation (5.6).

The material constants extraction is repeated at each of the 14 temperature points (20°C through 150°C) to obtain values for the material constants over the temperature range. The values of  $e_{15}$  are calculated from the fifth element of the  $z_k$  vectors using the  $\epsilon_{11}^s$  values at the respective temperature points. In order to obtain the temperature coefficients of the material constants, a third order power series is fit to the calculated material constants values.

## 5.6 Summary of Experimental Results

The zeroth through second order temperature coefficients of the material constants of  $\text{Li}_2\text{B}_4\text{O}_7$  were obtained from the third order power series fit to the material constants. The zeroth order (room temperature values) serve as a check for the data extraction program. These values are compared to the room temperature material constants obtained by Kosinski [2] and other researchers in Table 5-4. The results obtained for the first and second order temperature coefficients of the selected material constants of  $\text{Li}_2\text{B}_4\text{O}_7$  are listed in Table 5-5.

Table 5-4. Comparison of the Calculated Selected Material Constants with those Determined by Kosinski [2] and Others at Room Temperature.

	Results of this Thesis	[2]	[12]	[29]	[30]	[31]	[32]	[33]
$c_{11}^E$ (GPa)	135.955	135.823	135.27	126.7	127.1	135	135.2	127.6
$c_{12}^E$ (GPa)	-0.288	-0.285	0.109	0.5	0.6	3.57	0.8	8.9
$c_{44}^E$ (GPa)	57.057	57.072	57.39	55.0	53.8	58.5	55.9	57.5
$c_{66}^E$ (GPa)	47.700	47.680	47.38	46.0	57.4	46.7	47.3	48.2
$e_{15}$ (C/m <sup>2</sup> )	.4017	0.3918	0.36	0.36	0.278	0.472	0.35	0.39

Table 5-5. Calculated First and Second Order Temperature Coefficients of Selected Material Constants of Li<sub>2</sub>B<sub>4</sub>O<sub>7</sub>.

	First Order (x10 <sup>-6</sup> /K)	Second Order (x10 <sup>-9</sup> /K)
$c_{11}^E$	-70.26	-193.1
$c_{12}^E$	-67310	114939
$c_{44}^E$	-14.53	-398.1
$c_{66}^E$	-418.6	504.4
$e_{15}$	-1320	5163

Figures 5-1 through 5-5 are plots of the calculated material constants and their corresponding third order power series fits.

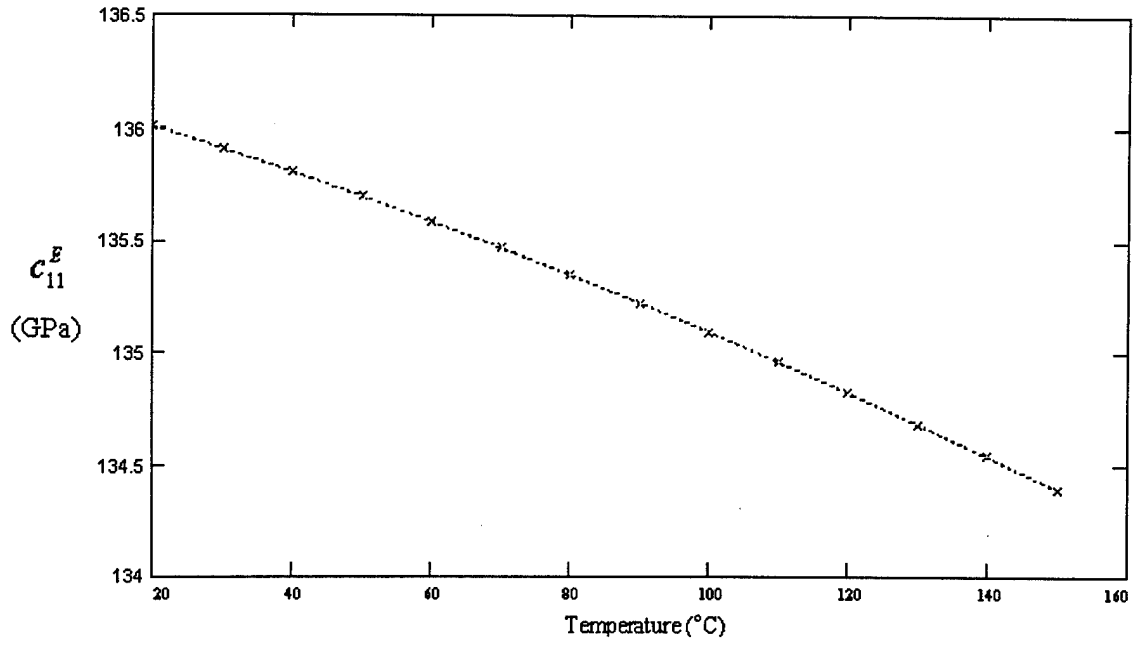


Fig. 5-1. Plot of  $c_{11}^E$  and its power series fit.

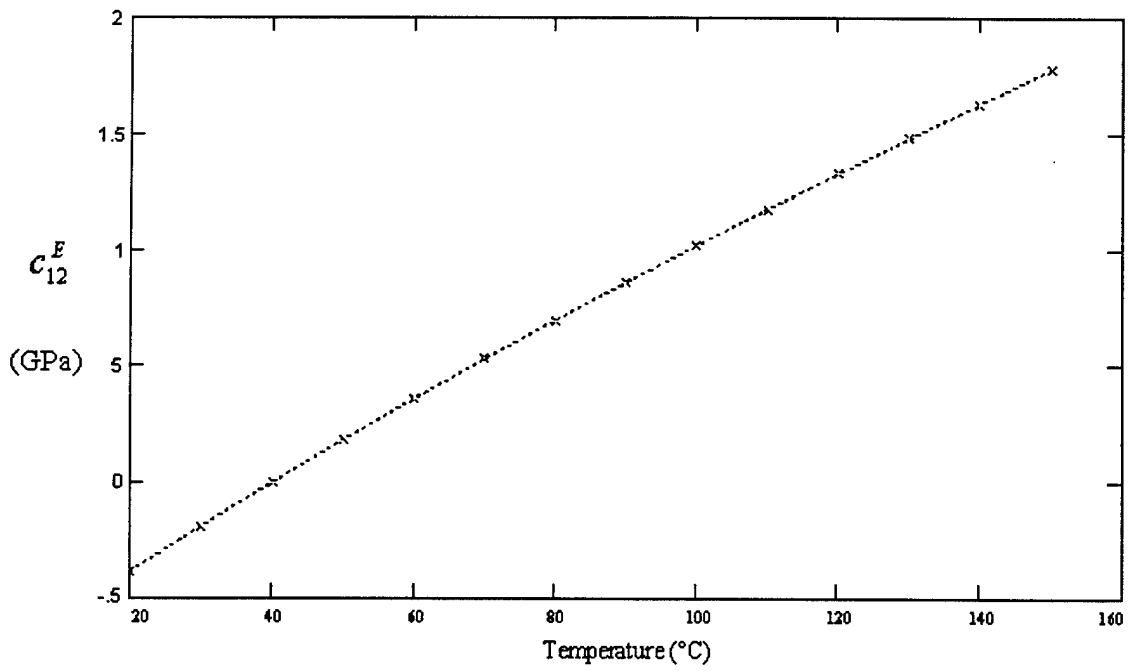


Fig. 5-2. Plot of  $c_{12}^E$  and its power series fit.



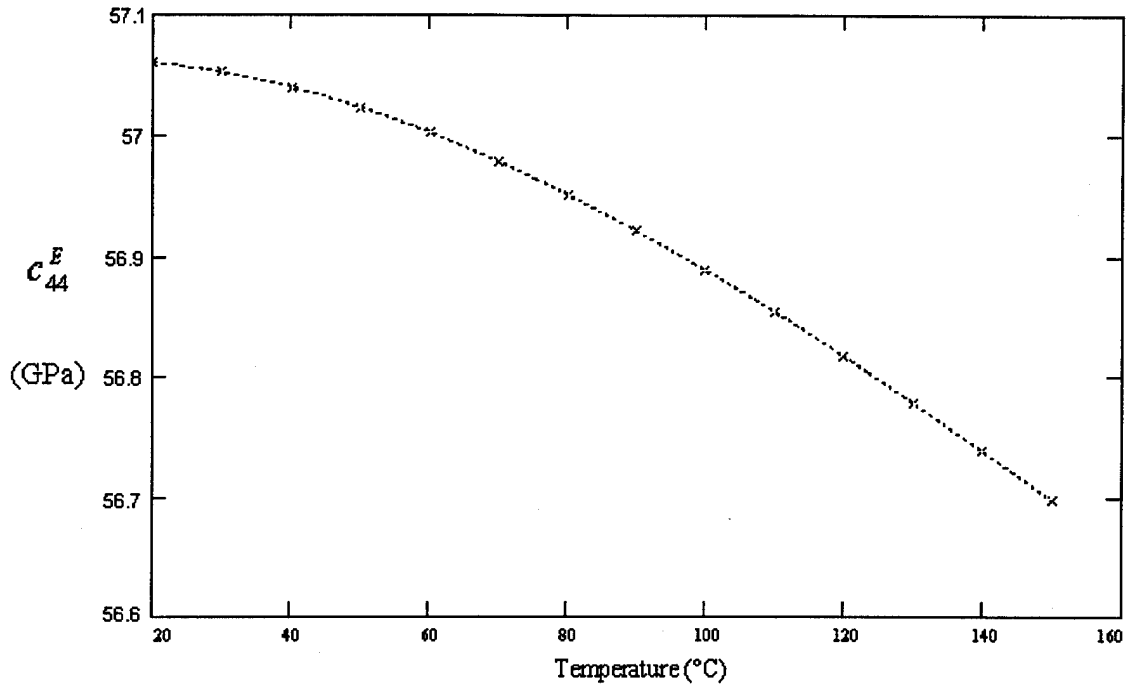


Fig. 5-3. Plot of  $c_{44}^E$  and its power series fit.

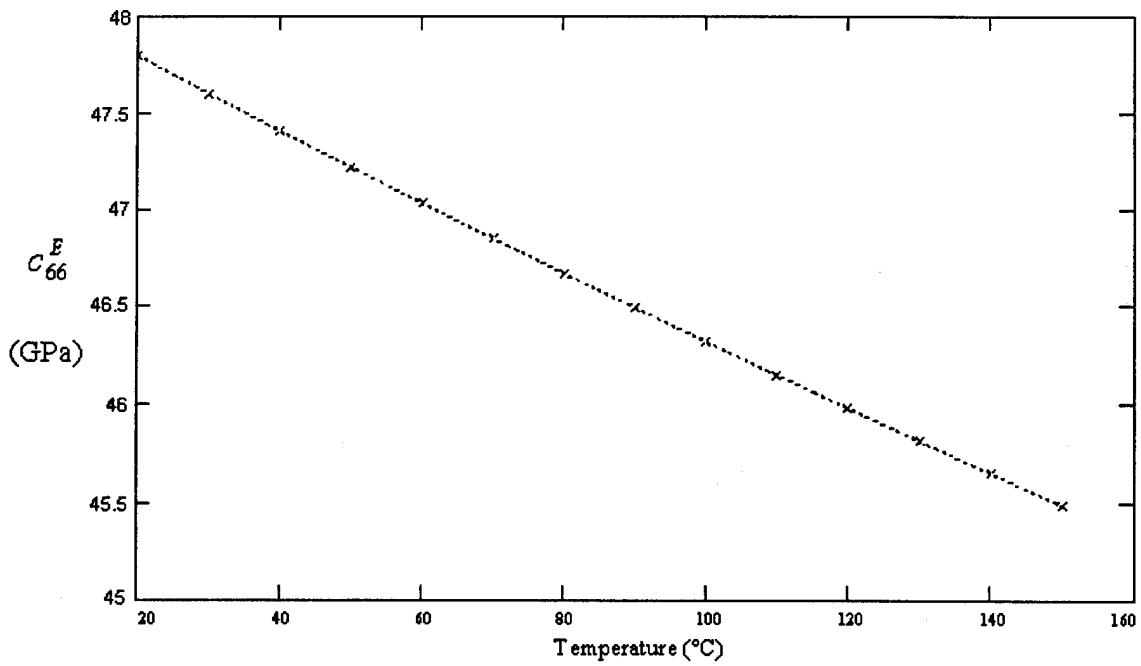


Fig. 5-4. Plot of  $c_{66}^E$  and its power series fit.

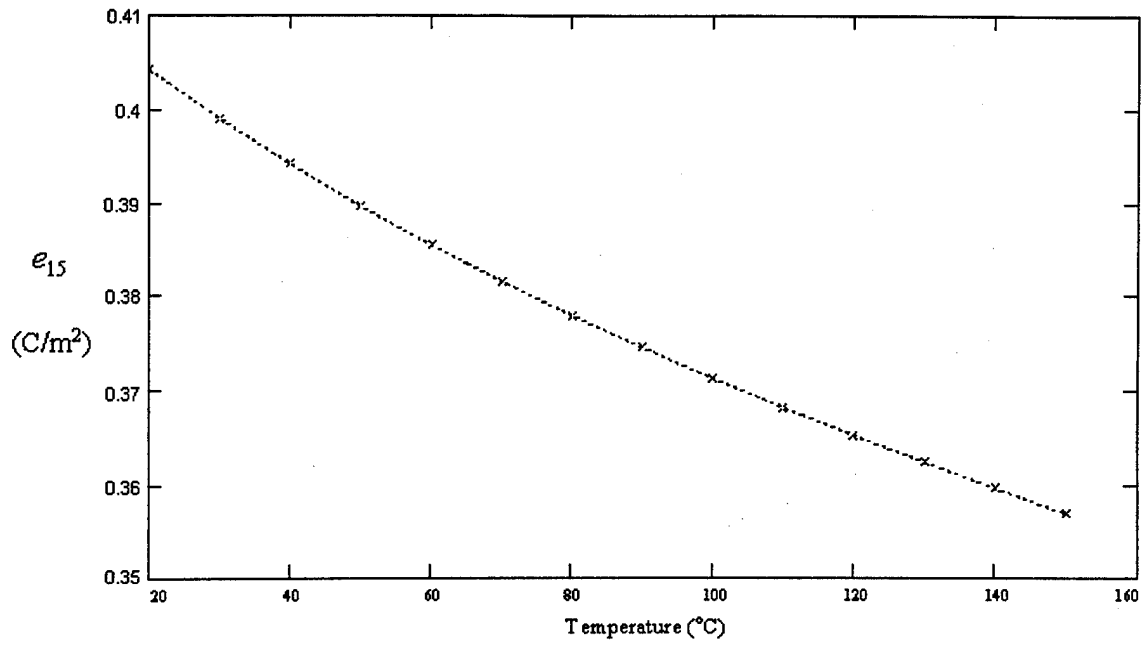


Fig. 5-5. Plot of  $e_{15}$  and its power series fit.

## Chapter 6 - Conclusions and Recommendations

This chapter presents a summary of the experimental results as well as recommendations for further study. The first section presents a comparison of the calculated temperature coefficients of the selected material constants of  $\text{Li}_2\text{B}_4\text{O}_7$  to previously published values. The second section discusses how the knowledge gained in this thesis might be applied and improved upon.

### 6.1 Comparison of Results

The first and second order temperature coefficients of the material constants  $c_{11}^E$ ,  $c_{12}^E$ ,  $c_{44}^E$ ,  $c_{66}^E$ , and  $e_{15}$  of  $\text{Li}_2\text{B}_4\text{O}_7$  have been calculated using an improved resonator method described by Kosinski [26]. Table 6-1 compares the calculated first order temperature coefficients with previously published values.

Table 6-1. Comparison of Calculated First Order Temperature Coefficients  
( $\times 10^{-6}/\text{K}$ ) with Previously Published Values.

	Results of this thesis	[29]	[30]	[31]	[12]	[13]
$c_{11}^E$	-71.26	-125	-51	-81	-80	-65
$c_{12}^E$	-67310	14000	1600	3370	20000	-8390
$c_{44}^E$	-14.53	-23	-22	-18	13	108
$c_{66}^E$	-418.6	-480	-200	-272	-480	-220
$e_{15}$	-1320	-1300	-349	-1050		

Table 6-2 presents a comparison of the second order temperature coefficients with those of Shiosaki, et. al. [34]

Table 6-2. Comparison of Second Order Temperature Coefficients ( $\times 10^{-9}/K$ ) with Those of Shiosaki, et. al. [34].

	Results of this thesis	[34]
$c_{11}^E$	-193.1	-440
$c_{12}^E$	-114939	-17400
$c_{44}^E$	-398.1	500
$c_{66}^E$	504.4	-450
$e_{15}$	5163	-900

The calculated values of the temperature coefficients of the selected material constants were used to predict the measured  $f_{A0}^{(1)}$  data. This serves as a check for the calculated results. When designing piezoelectric plate resonators and transducers, it is desirable that the  $f_{A0}^{(1)}$ 's are known with an accuracy of at least 1% [2]. The mean error between the measured and calculated  $f_{A0}^{(1)}$ 's was 1.20% with a standard deviation of 0.005% for TE and 0.285% with a standard deviation of 0.031% for LE. The difference in the accuracies of the predictions is attributed to the fact that the measured higher harmonic resonant frequencies of TE modes converge more slowly than the higher

harmonic resonance frequencies of LE modes. Appendix A contains the complete comparison between all measured and calculated values of  $f_{A0}^{(1)}$ .

## 6.2 Recommendations for Further Study

The knowledge gained in this thesis should be useful in the development of  $\text{Li}_2\text{B}_4\text{O}_7$  based electronics. The most desirable benefit obtained from the results of this thesis will probably be the prediction of new zero temperature coefficient orientations of  $\text{Li}_2\text{B}_4\text{O}_7$ . These new zero temperature coefficient orientations of  $\text{Li}_2\text{B}_4\text{O}_7$  might also have advantages over current zero temperature coefficient cuts. In order to test the validity of the results presented here, zero temperature coefficient cuts of  $\text{Li}_2\text{B}_4\text{O}_7$  may be predicted using the calculated temperature coefficients and tested in later research.

Further studies of  $\text{Li}_2\text{B}_4\text{O}_7$  should focus on the temperature coefficients for the remaining material constants. Also, the temperature coefficients of expansion and dielectric constant should be measured. Accomplishing these two research goals will allow the complete thermal characterization of  $\text{Li}_2\text{B}_4\text{O}_7$  without the need of previously published material.

Another possible area of further research is below-room-temperature measurements of  $\text{Li}_2\text{B}_4\text{O}_7$ . The results of this thesis are limited to roughly 20°C to 150°C. The power series fits that were used to obtain the temperature coefficients of the selected material constants should be most accurate in the middle of the temperature range and least accurate near the extremes of the temperature range. In order to improve the overall accuracy of the calculated temperature coefficients, especially at room temperature

values, measurements should be made of the below-room-temperature characteristics of the material constants of  $\text{Li}_2\text{B}_4\text{O}_7$ .

# Appendix A - Data Extraction

Crystal Sample Data: crystal sample number, orientation, excitation, thickness, mass density, and room temperature antiresonant frequency [35]:

Crystal Sample Number	Orientation	Excitation	Thickness ( $\mu\text{m}$ )	Mass Density ( $\text{kg/m}^3$ )	$f_{A0}^{(1)}$ (MHz) [35]
1	(YXwt)0,0	TE	206.6	2436.0	11.94
2	(YXwt)0,0	TE	206.6	2453.2	11.90
3	(YXwt)0,0	TE	206.6	2437.2	11.89
4	(YXwt)0,0	TE	206.6	2437.5	11.93
5	(YXwt)0,0,90	LE90	206.6	2450.1	18.058
6	(YXwt)0,0,90	LE90	206.6	2442.7	18.059
7	(YXwt)0,0,90	LE90	206.6	2446.0	18.035
8	(YXwt)0,0,90	LE90	206.6	2440.4	18.037
9	(YXwt)0,45,0	LE0	202.2	2437.5	11.470
10	(YXwt)0,45,0	LE0	202.2	2441.2	11.473
11	(YXwt)0,45,0	LE0	202.2	2437.2	11.477
12	(YXwt)0,45,0	LE0	202.2	2417.7	11.493

Crystal Sample Number	Orientation	Excitation	Thickness ( $\mu\text{m}$ )	Mass Density ( $\text{kg}/\text{m}^3$ )	$f_{A0}^{(1)}$ (MHz) [35]
18	(YXwl)45,0	TE	206.9	2435.3	11.87
20	(YXwl)45,0	TE	206.9	2423.8	11.935
21	(YXwlt)45,0,90	LE90	206.9	2436.3	16.670
22	(YXwlt)45,0,90	LE90	206.9	2437.0	16.621
23	(YXwlt)45,0,90	LE90	206.9	2425.2	16.658
24	(YXwlt)45,0,90	LE90	206.9	2436.2	16.626
25	(YXwlt)45,45,0	LE0	200.1	2437.5	12.670
26	(YXwlt)45,45,0	LE0	200.1	2428.1	12.668
27	(YXwlt)45,45,0	LE0	200.1	2444.6	12.675
28	(YXwlt)45,45,0	LE0	200.1	2424.8	12.677
37	(YXwlt)0,90,90	LE90	201.5	2437.7	12.022
38	(YXwlt)0,90,90	LE90	201.5	2436.4	12.009
39	(YXwlt)0,90,90	LE90	201.5	2431.6	11.999



Crystal Sample Number	Orientation	Excitation	Thickness ( $\mu\text{m}$ )	Mass Density ( $\text{kg}/\text{m}^3$ )	$f_{A0}^{(1)}$ (MHz) [35]
40	(YXwt)0,90,90	LE90	201.5	2422.8	12.001
49	(YXwt)0,28.2,0	LE0	196.0	2438.6	11.538
50	(YXwt)0,28.2,0	LE0	196.0	2433.7	11.530
51	(YXwt)0,28.2,0	LE0	196.0	2428.3	11.524
52	(YXwt)0,28.2,0	LE0	196.0	2435.4	11.544
61	(YXwt)45,56.1,0	LE0	203.8	2414.6	12.276
62	(YXwt)45,56.1,0	LE0	203.8	2433.3	12.227
63	(YXwt)45,56.1,0	LE0	203.8	2423.9	12.238
64	(YXwt)45,56.1,0	LE0	203.8	2429.5	12.265

**Sample calculation of third order power series fit to the measured antiresonant frequency data for crystal #1 (YXw)0,0 TE:**

For Crystal #1 (0-0 TE):

Measured Data:

22.0	11.796
30.7	11.790
40.3	11.784
49.7	11.778
59.2	11.771
68.7	11.765
78.3	11.758
87.6	11.751
101.0	11.742
110.3	11.735
120.1	11.728
129.6	11.721
140.9	11.713
150.5	11.705

temps1 :=

guess :=

10
10 <sup>-6</sup>
10 <sup>-9</sup>
10 <sup>-12</sup>

Fit1 := genfit(temps1, freqs1, guess, Fitfunction1)

Third Order Power Fit Function:

$$\text{Fitfunction1}(\theta, F) = \frac{F_0 \cdot \left[ \frac{1 + F_1 \cdot (\theta - 25) + F_2 \cdot (\theta - 25)^2 + F_3 \cdot (\theta - 25)^3}{1 + F_1 \cdot (\theta - 25) + F_2 \cdot (\theta - 25)^2 + F_3 \cdot (\theta - 25)^3} \right]}{F_0 \cdot \left[ \frac{1 + (\theta - 25) + F_2 \cdot (\theta - 25)^2 + F_3 \cdot (\theta - 25)^3}{1 + F_1 \cdot (\theta - 25) + (\theta - 25)^2 + F_3 \cdot (\theta - 25)^3} \right]}$$

Zeroth through third order temperature coeffs of antiresonant frequency:

$$\text{Fit1} \cdot \begin{bmatrix} 1 \\ 10^6 \\ 10^9 \\ 10^{12} \end{bmatrix} = \begin{bmatrix} 11.79 \\ -54.96 \\ -45.51 \\ 48.84 \end{bmatrix}$$

Zeroth order (MHz)  
 First order (x10<sup>-6</sup>/K)  
 Second order (x10<sup>-9</sup>/K)  
 Third order (x10<sup>-12</sup>/K)

Now plot the data and the power series fit on the same graph. Check the fit using Chauvenet's criterion.

Crystal #1:

N := 14

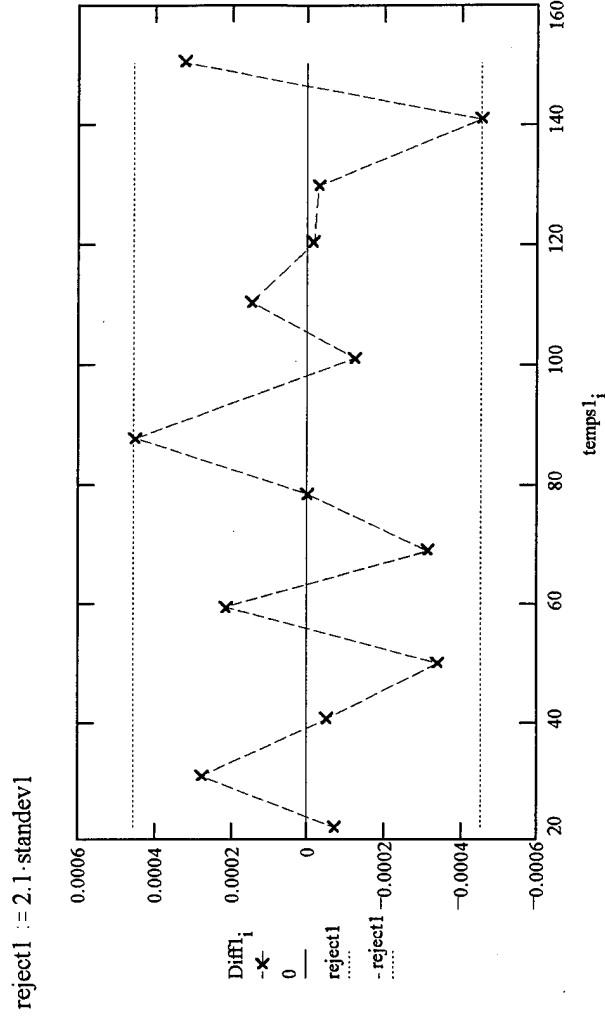
i := 0..N - 1

$$\text{Powfit1}_i := \text{Fit1}_0 \cdot [1 + \text{Fit1}_1 \cdot (\text{temps1}_i - 25) + \text{Fit1}_2 \cdot (\text{temps1}_i - 25)^2 + \text{Fit1}_3 \cdot (\text{temps1}_i - 25)^3]$$

$$\text{Diff1}_i := (\text{Powfit1}_i - \text{freqs1}_i)$$

$$\text{standev1} := \frac{1}{N - 1} \cdot \sum_i \sqrt{(\text{Diff1}_i)^2} \quad \text{standev1} = 0.00022$$

Using Chauvenet's criterion for 14 data points, data points lying more than 2.1 standard deviations from the mean may be considered for rejection. This comes from the assumption of a Gaussian distribution of the data points along with the criterion of rejection when less than half an event is expected:



## Data from Power Series Fits of Measured Antiresonant Frequencies:

Crystal Cut Data (listed by Trial #): First order temperature coefficients ( $\times 10^{-6}/K$ ):

Coef1<sub>1</sub> := -54.963 Coef5<sub>1</sub> := -37.97 Coef9<sub>1</sub> := -91.632 Coef18<sub>1</sub> := -55.128 Coef21<sub>1</sub> := -70.822 Coef25<sub>1</sub> := -56.219 Coef37a<sub>1</sub> := 5.657 Coef49<sub>1</sub> := -155.566 Coef61<sub>1</sub> := -31.49  
 Coef2<sub>1</sub> := -57.834 Coef6<sub>1</sub> := -37.98 Coef10<sub>1</sub> := -94.749 Coef20a<sub>1</sub> := -57.447 Coef22<sub>1</sub> := -56.772 Coef26<sub>1</sub> := -55.393 Coef37b<sub>1</sub> := 5.775 Coef50<sub>1</sub> := -158.307 Coef62<sub>1</sub> := -33.31  
 Coef3<sub>1</sub> := -56.59 Coef7<sub>1</sub> := -37.53 Coef11<sub>1</sub> := -87.625 Coef20b<sub>1</sub> := -54.98 Coef23<sub>1</sub> := -70.253 Coef27<sub>1</sub> := -56.68 Coef38<sub>1</sub> := 3.813 Coef51<sub>1</sub> := -158.18 Coef63<sub>1</sub> := -34.27  
 Coef4<sub>1</sub> := -57.323 Coef8<sub>1</sub> := -36.98 Coef12<sub>1</sub> := -95.971 Coef18b<sub>1</sub> := -56.93 Coef24<sub>1</sub> := -69.549 Coef28<sub>1</sub> := -55.187 Coef39<sub>1</sub> := 10.461 Coef52<sub>1</sub> := -154.904 Coef64<sub>1</sub> := -31.521  
 Coef1b<sub>1</sub> := -55.9 Coef10b<sub>1</sub> := -94.09 Coef20c<sub>1</sub> := -55.45 Coef21b<sub>1</sub> := -68.2 Coef25b<sub>1</sub> := -54.9 Coef40<sub>1</sub> := 3.268 Coef49b<sub>1</sub> := -156.41 Coef61b<sub>1</sub> := -34.65  
 Coef2b<sub>1</sub> := -54.35 Coef20d<sub>1</sub> := -56.07  
 Coef51b<sub>1</sub> := -157.36 Coef63b<sub>1</sub> := -34.41  
 Coef52b<sub>1</sub> := -155.58 Coef64b<sub>1</sub> := -33.16

Crystal Cut Data (listed by Trial #): Second order temperature coefficients ( $\times 10^{-9}/K$ ):

Coef1<sub>2</sub> := -45.513 Coef5<sub>2</sub> := -88.95 Coef9<sub>2</sub> := -53.932 Coef18<sub>2</sub> := -37.229 Coef21<sub>2</sub> := 9.798 Coef25<sub>2</sub> := -50.789 Coef37a<sub>2</sub> := -208.565 Coef49<sub>2</sub> := 99.042 Coef61<sub>2</sub> := -159.803  
 Coef2<sub>2</sub> := 18.379 Coef6<sub>2</sub> := -88.96 Coef10<sub>2</sub> := 12.921 Coef20a<sub>2</sub> := -7.786 Coef22<sub>2</sub> := -31.533 Coef26<sub>2</sub> := -56.458 Coef37b<sub>2</sub> := -196.708 Coef50<sub>2</sub> := 147.228 Coef62<sub>2</sub> := -128.477  
 Coef3<sub>2</sub> := -26.335 Coef7<sub>2</sub> := -87.6 Coef11<sub>2</sub> := -74.408 Coef20b<sub>2</sub> := -43.055 Coef23<sub>2</sub> := 13.268 Coef27<sub>2</sub> := -42.876 Coef38<sub>2</sub> := -187.375 Coef51<sub>2</sub> := 152.064 Coef63<sub>2</sub> := -97.537  
 Coef4<sub>2</sub> := 4.181 Coef8<sub>2</sub> := -111.1 Coef12<sub>2</sub> := 50.08 Coef18b<sub>2</sub> := -24.58 Coef24<sub>2</sub> := -11.041 Coef28<sub>2</sub> := -58.374 Coef39<sub>2</sub> := -382.362 Coef52<sub>2</sub> := 78.414 Coef64<sub>2</sub> := -159.96  
 Coef1b<sub>2</sub> := -31.29 Coef10b<sub>2</sub> := 18.28 Coef20c<sub>2</sub> := -53.21 Coef21b<sub>2</sub> := -24.26 Coef25b<sub>2</sub> := -50.22 Coef40<sub>2</sub> := -151.183 Coef49b<sub>2</sub> := 118.99 Coef61b<sub>2</sub> := -98.88  
 Coef2b<sub>2</sub> := -59.46 Coef20d<sub>2</sub> := -27.43  
 Coef51b<sub>2</sub> := 143.57 Coef63b<sub>2</sub> := -99.15  
 Coef52b<sub>2</sub> := 106.52 Coef64b<sub>2</sub> := -129.43

Crystal Cut Data (listed by Trial #): Third order temperature coefficients ( $\times 10^{-12}/K$ ):

Coef1<sub>3</sub> := 48.842 Coef5<sub>3</sub> := 124.42 Coef9<sub>3</sub> := 336.452 Coef18<sub>3</sub> := -7.453 Coef21<sub>3</sub> := -64.863 Coef25<sub>3</sub> := -23.962 Coef37a<sub>3</sub> := 462.048 Coef49<sub>3</sub> := -65.961 Coef61<sub>3</sub> := 414.943  
 Coef2<sub>3</sub> := -304.611 Coef6<sub>3</sub> := 124.43 Coef10<sub>3</sub> := -5.673 Coef20a<sub>3</sub> := -130.139 Coef22<sub>3</sub> := 22.418 Coef26<sub>3</sub> := -31.683 Coef37b<sub>3</sub> := 339.522 Coef50<sub>3</sub> := -301.694 Coef62<sub>3</sub> := 273.789  
 Coef3<sub>3</sub> := 13.017 Coef7<sub>3</sub> := 94.91 Coef11<sub>3</sub> := 341.173 Coef20b<sub>3</sub> := 5.516 Coef23<sub>3</sub> := -138.437 Coef27<sub>3</sub> := -81.576 Coef38<sub>3</sub> := 404.301 Coef51<sub>3</sub> := -326.64 Coef63<sub>3</sub> := 43.408  
 Coef4<sub>3</sub> := -218.802 Coef8<sub>3</sub> := 255.28 Coef12<sub>3</sub> := -253.164 Coef18b<sub>3</sub> := -9.14 Coef24<sub>3</sub> := 25.7 Coef28<sub>3</sub> := -41.2 Coef39<sub>3</sub> := 1450.392 Coef52<sub>3</sub> := 33.18 Coef64<sub>3</sub> := 415.35  
 Coef1b<sub>3</sub> := 3.41 Coef10b<sub>3</sub> := -94.56 Coef20c<sub>3</sub> := 151.0 Coef21b<sub>3</sub> := 76.46 Coef25b<sub>3</sub> := -102.55 Coef40<sub>3</sub> := 224.52 Coef49b<sub>3</sub> := -147.76 Coef61b<sub>3</sub> := 105.66  
 Coef2b<sub>3</sub> := 111.84 Coef20d<sub>3</sub> := -32.14  
 Coef51b<sub>3</sub> := -298.61 Coef63b<sub>3</sub> := 103.04  
 Coef52b<sub>3</sub> := -132.51 Coef64b<sub>3</sub> := 256.12

Now combine the temperature coeff of antires. frequency data with the values for room temperature antires. frequency of Kosinski [34] and calculate the stiffness eigenvalues for each crystal cut at various temperatures:

$$j := 0..13$$

$$\text{Fit1}_j := 11.94 \cdot \left[ 1 + \text{Coef1}_1 \cdot 10^{-6} \cdot (j \cdot 10 - 5) + \text{Coef1}_2 \cdot 10^{-9} \cdot (j \cdot 10 - 5)^2 + \text{Coef1}_3 \cdot 10^{-12} \cdot (j \cdot 10 - 5)^3 \right]$$

$$\text{Fit1b}_j := 11.94 \cdot \left[ 1 + \text{Coef1b}_1 \cdot 10^{-6} \cdot (j \cdot 10 - 5) + \text{Coef1b}_2 \cdot 10^{-9} \cdot (j \cdot 10 - 5)^2 + \text{Coef1b}_3 \cdot 10^{-12} \cdot (j \cdot 10 - 5)^3 \right]$$

$$\text{Fit2}_j := 11.90 \cdot \left[ 1 + \text{Coef2}_1 \cdot 10^{-6} \cdot (j \cdot 10 - 5) + \text{Coef2}_2 \cdot 10^{-9} \cdot (j \cdot 10 - 5)^2 + \text{Coef2}_3 \cdot 10^{-12} \cdot (j \cdot 10 - 5)^3 \right]$$

$$\text{Fit2b}_j := 11.90 \cdot \left[ 1 + \text{Coef2b}_1 \cdot 10^{-6} \cdot (j \cdot 10 - 5) + \text{Coef2b}_2 \cdot 10^{-9} \cdot (j \cdot 10 - 5)^2 + \text{Coef2b}_3 \cdot 10^{-12} \cdot (j \cdot 10 - 5)^3 \right]$$

$$\text{Fit3}_j := 11.89 \cdot \left[ 1 + \text{Coef3}_1 \cdot 10^{-6} \cdot (j \cdot 10 - 5) + \text{Coef3}_2 \cdot 10^{-9} \cdot (j \cdot 10 - 5)^2 + \text{Coef3}_3 \cdot 10^{-12} \cdot (j \cdot 10 - 5)^3 \right]$$

$$\text{Fit4}_j := 11.93 \cdot \left[ 1 + \text{Coef4}_1 \cdot 10^{-6} \cdot (j \cdot 10 - 5) + \text{Coef4}_2 \cdot 10^{-9} \cdot (j \cdot 10 - 5)^2 + \text{Coef4}_3 \cdot 10^{-12} \cdot (j \cdot 10 - 5)^3 \right]$$

$$\text{Fit5}_j := 18.058 \cdot \left[ 1 + \text{Coef5}_1 \cdot 10^{-6} \cdot (j \cdot 10 - 5) + \text{Coef5}_2 \cdot 10^{-9} \cdot (j \cdot 10 - 5)^2 + \text{Coef5}_3 \cdot 10^{-12} \cdot (j \cdot 10 - 5)^3 \right]$$

$$\text{Fit6}_j := 18.059 \cdot \left[ 1 + \text{Coef6}_1 \cdot 10^{-6} \cdot (j \cdot 10 - 5) + \text{Coef6}_2 \cdot 10^{-9} \cdot (j \cdot 10 - 5)^2 + \text{Coef6}_3 \cdot 10^{-12} \cdot (j \cdot 10 - 5)^3 \right]$$

$$\text{Fit7}_j := 18.037 \cdot \left[ 1 + \text{Coef7}_1 \cdot 10^{-6} \cdot (j \cdot 10 - 5) + \text{Coef7}_2 \cdot 10^{-9} \cdot (j \cdot 10 - 5)^2 + \text{Coef7}_3 \cdot 10^{-12} \cdot (j \cdot 10 - 5)^3 \right]$$

$$\text{Fit8}_j := 18.037 \cdot \left[ 1 + \text{Coef8}_1 \cdot 10^{-6} \cdot (j \cdot 10 - 5) + \text{Coef8}_2 \cdot 10^{-9} \cdot (j \cdot 10 - 5)^2 + \text{Coef8}_3 \cdot 10^{-12} \cdot (j \cdot 10 - 5)^3 \right]$$

$$\text{Fit9}_j := 11.470 \cdot \left[ 1 + \text{Coef9}_1 \cdot 10^{-6} \cdot (j \cdot 10 - 5) + \text{Coef9}_2 \cdot 10^{-9} \cdot (j \cdot 10 - 5)^2 + \text{Coef9}_3 \cdot 10^{-12} \cdot (j \cdot 10 - 5)^3 \right]$$

$$\text{Fit10}_j := 11.473 \cdot \left[ 1 + \text{Coef10}_1 \cdot 10^{-6} \cdot (j \cdot 10 - 5) + \text{Coef10}_2 \cdot 10^{-9} \cdot (j \cdot 10 - 5)^2 + \text{Coef10}_3 \cdot 10^{-12} \cdot (j \cdot 10 - 5)^3 \right]$$

$$\text{Fit10b}_j := 11.473 \cdot \left[ 1 + \text{Coef10b}_1 \cdot 10^{-6} \cdot (j \cdot 10 - 5) + \text{Coef10b}_2 \cdot 10^{-9} \cdot (j \cdot 10 - 5)^2 + \text{Coef10b}_3 \cdot 10^{-12} \cdot (j \cdot 10 - 5)^3 \right]$$

$$\text{Fit11}_j := 11.477 \cdot \left[ 1 + \text{Coef11}_1 \cdot 10^{-6} \cdot (j \cdot 10 - 5) + \text{Coef11}_2 \cdot 10^{-9} \cdot (j \cdot 10 - 5)^2 + \text{Coef11}_3 \cdot 10^{-12} \cdot (j \cdot 10 - 5)^3 \right]$$

$$\text{Fit12}_j := 11.493 \cdot \left[ 1 + \text{Coef12}_1 \cdot 10^{-6} \cdot (j \cdot 10 - 5) + \text{Coef12}_2 \cdot 10^{-9} \cdot (j \cdot 10 - 5)^2 + \text{Coef12}_3 \cdot 10^{-12} \cdot (j \cdot 10 - 5)^3 \right]$$

$$\text{Fit18}_j := 11.87 \cdot \left[ 1 + \text{Coef18}_1 \cdot 10^{-6} \cdot (j \cdot 10 - 5) + \text{Coef18}_2 \cdot 10^{-9} \cdot (j \cdot 10 - 5)^2 + \text{Coef18}_3 \cdot 10^{-12} \cdot (j \cdot 10 - 5)^3 \right]$$

$$\text{Fit18b}_j := 11.87 \cdot \left[ 1 + \text{Coef18b}_1 \cdot 10^{-6} \cdot (j \cdot 10 - 5) + \text{Coef18b}_2 \cdot 10^{-9} \cdot (j \cdot 10 - 5)^2 + \text{Coef18b}_3 \cdot 10^{-12} \cdot (j \cdot 10 - 5)^3 \right]$$





Mass density, crystal thickness, and dielectric constant all vary with temperature. Therefore, they must be calculated for each temperature. Crystal thickness is also a function of orientation, so the proper rotations must also be applied.

Mass density changes with temperature, but does not change with crystal orientation:

From Shiosaki, et al. [10], the first and second order coefficients of thermal expansion for  $\text{Li}_2\text{B}_4\text{O}_7$  are:

$$\alpha_1 := \begin{pmatrix} 11.1 & 0 & 0 \\ 0 & 11.1 & 0 \\ 0 & 0 & -3.74 \end{pmatrix} \cdot 10^{-6} \quad \alpha_2 := \begin{pmatrix} 5.6 & 0 & 0 \\ 0 & 5.6 & 0 \\ 0 & 0 & 20.8 \end{pmatrix} \cdot 10^{-9}$$

Both are  
at a reference  
temperature of  
25 degrees C.

The mass density changes inversely with volume, so the first and second order temperature coefficients of density are:

$$\rho_1 := -(\alpha_{1,0,0} + \alpha_{1,1,1} + \alpha_{1,2,2}) \quad \rho_2 := -(\alpha_{2,0,0} + \alpha_{2,1,1} + \alpha_{2,2,2})$$

$$\rho_1 = -1.846 \cdot 10^{-5} \quad \rho_2 = -3.2 \cdot 10^{-8}$$

The mass density as a function of temperature is therefore:

$$\rho = \rho_0 \cdot [1 + \rho_1 \cdot (10 \cdot j - 5) + \rho_2 \cdot (10 \cdot j - 5)^2]$$



For each of the 30 crystals in the sample set, the densities over our temperature range are:

$$\begin{aligned} \rho1_j &:= 2436.0 \cdot [1 + \rho_1 \cdot (10j - 5) + \rho_2 \cdot (10j - 5)^2] \\ \rho2_j &:= 2453.2 \cdot [1 + \rho_1 \cdot (10j - 5) + \rho_2 \cdot (10j - 5)^2] \\ \rho3_j &:= 2437.2 \cdot [1 + \rho_1 \cdot (10j - 5) + \rho_2 \cdot (10j - 5)^2] \\ \rho4_j &:= 2437.5 \cdot [1 + \rho_1 \cdot (10j - 5) + \rho_2 \cdot (10j - 5)^2] \\ \rho5_j &:= 2450.1 \cdot [1 + \rho_1 \cdot (10j - 5) + \rho_2 \cdot (10j - 5)^2] \\ \rho6_j &:= 2442.7 \cdot [1 + \rho_1 \cdot (10j - 5) + \rho_2 \cdot (10j - 5)^2] \\ \rho7_j &:= 2446.0 \cdot [1 + \rho_1 \cdot (10j - 5) + \rho_2 \cdot (10j - 5)^2] \\ \rho8_j &:= 2440.4 \cdot [1 + \rho_1 \cdot (10j - 5) + \rho_2 \cdot (10j - 5)^2] \\ \rho9_j &:= 2437.5 \cdot [1 + \rho_1 \cdot (10j - 5) + \rho_2 \cdot (10j - 5)^2] \\ \rho10_j &:= 2441.2 \cdot [1 + \rho_1 \cdot (10j - 5) + \rho_2 \cdot (10j - 5)^2] \\ \rho11_j &:= 2437.2 \cdot [1 + \rho_1 \cdot (10j - 5) + \rho_2 \cdot (10j - 5)^2] \\ \rho12_j &:= 2417.7 \cdot [1 + \rho_1 \cdot (10j - 5) + \rho_2 \cdot (10j - 5)^2] \\ \rho18_j &:= 2435.3 \cdot [1 + \rho_1 \cdot (10j - 5) + \rho_2 \cdot (10j - 5)^2] \\ \rho20_j &:= 2423.8 \cdot [1 + \rho_1 \cdot (10j - 5) + \rho_2 \cdot (10j - 5)^2] \\ \rho21_j &:= 2436.3 \cdot [1 + \rho_1 \cdot (10j - 5) + \rho_2 \cdot (10j - 5)^2] \\ \rho22_j &:= 2437.0 \cdot [1 + \rho_1 \cdot (10j - 5) + \rho_2 \cdot (10j - 5)^2] \end{aligned}$$

$$\begin{aligned} \rho23_j &:= 2425.2 \cdot [1 + \rho_1 \cdot (10j - 5) + \rho_2 \cdot (10j - 5)^2] \\ \rho24_j &:= 2436.2 \cdot [1 + \rho_1 \cdot (10j - 5) + \rho_2 \cdot (10j - 5)^2] \\ \rho25_j &:= 2437.5 \cdot [1 + \rho_1 \cdot (10j - 5) + \rho_2 \cdot (10j - 5)^2] \\ \rho26_j &:= 2428.1 \cdot [1 + \rho_1 \cdot (10j - 5) + \rho_2 \cdot (10j - 5)^2] \\ \rho27_j &:= 2444.6 \cdot [1 + \rho_1 \cdot (10j - 5) + \rho_2 \cdot (10j - 5)^2] \\ \rho28_j &:= 2424.8 \cdot [1 + \rho_1 \cdot (10j - 5) + \rho_2 \cdot (10j - 5)^2] \\ \rho37_j &:= 2437.7 \cdot [1 + \rho_1 \cdot (10j - 5) + \rho_2 \cdot (10j - 5)^2] \\ \rho38_j &:= 2436.4 \cdot [1 + \rho_1 \cdot (10j - 5) + \rho_2 \cdot (10j - 5)^2] \\ \rho39_j &:= 2431.6 \cdot [1 + \rho_1 \cdot (10j - 5) + \rho_2 \cdot (10j - 5)^2] \\ \rho40_j &:= 2422.8 \cdot [1 + \rho_1 \cdot (10j - 5) + \rho_2 \cdot (10j - 5)^2] \end{aligned}$$

$$\begin{aligned} \rho49_j &:= 2438.6 \cdot [1 + \rho_1 \cdot (10j - 5) + \rho_2 \cdot (10j - 5)^2] \\ \rho50_j &:= 2433.7 \cdot [1 + \rho_1 \cdot (10j - 5) + \rho_2 \cdot (10j - 5)^2] \\ \rho51_j &:= 2428.3 \cdot [1 + \rho_1 \cdot (10j - 5) + \rho_2 \cdot (10j - 5)^2] \\ \rho52_j &:= 2435.4 \cdot [1 + \rho_1 \cdot (10j - 5) + \rho_2 \cdot (10j - 5)^2] \\ \rho61_j &:= 2414.6 \cdot [1 + \rho_1 \cdot (10j - 5) + \rho_2 \cdot (10j - 5)^2] \\ \rho62_j &:= 2433.3 \cdot [1 + \rho_1 \cdot (10j - 5) + \rho_2 \cdot (10j - 5)^2] \\ \rho63_j &:= 2423.9 \cdot [1 + \rho_1 \cdot (10j - 5) + \rho_2 \cdot (10j - 5)^2] \\ \rho64_j &:= 2429.5 \cdot [1 + \rho_1 \cdot (10j - 5) + \rho_2 \cdot (10j - 5)^2] \end{aligned}$$

Crystal thickness varies with temperature and with crystal orientation:

Shiosaki's values for the coefficients of thermal expansion [10] must be transformed using the following rotation matrix:

$$a(\phi, \theta) = \begin{bmatrix} \cos(\phi) & \sin(\phi) & 0 \\ -\sin(\phi) \cdot \cos(\theta) & \cos(\phi) \cdot \cos(\theta) & \sin(\theta) \\ \sin(\phi) \cdot \sin(\theta) & -\cos(\phi) \cdot \sin(\theta) & \cos(\theta) \end{bmatrix}$$

After the rotation, the appropriate expansion is in the  $x'_2$  direction, so the  $\alpha'_{22}$  is the appropriate value:

For the (YXw)0,0 orientation:

$$a(0,0) \cdot \alpha_1 \cdot a(0,0)^T = \begin{bmatrix} 1.11 \cdot 10^{-5} & 0 & 0 \\ 0 & 1.11 \cdot 10^{-5} & 0 \\ 0 & 0 & -3.74 \cdot 10^{-6} \end{bmatrix} \quad a(0,0) \cdot \alpha_2 \cdot a(0,0)^T = \begin{bmatrix} 5.6 \cdot 10^{-9} & 0 & 0 \\ 0 & 5.6 \cdot 10^{-9} & 0 \\ 0 & 0 & 2.08 \cdot 10^{-8} \end{bmatrix}$$

The first order coeff is:  $\alpha_{0\_0\_1} := 1.11 \cdot 10^{-5}$

The second order coeff is:  $\alpha_{0\_0\_2} := 5.6 \cdot 10^{-9}$

The thickness as a function of temperature is:  $t_{0\_j} := 206.6 \cdot 10^{-6} \cdot [1 + \alpha_{0\_0\_1} \cdot (10j - 5) + \alpha_{0\_0\_2} \cdot (10j - 5)^2]$

For the (YXw)0,45 orientation:

$$a\left(0, \frac{45}{180} \cdot \pi\right) \cdot \alpha_1 \cdot a\left(0, \frac{45}{180} \cdot \pi\right)^T = \begin{bmatrix} 1.11 \cdot 10^{-5} & 0 & 0 \\ 0 & 3.68 \cdot 10^{-6} & -7.42 \cdot 10^{-6} \\ 0 & -7.42 \cdot 10^{-6} & 3.68 \cdot 10^{-6} \end{bmatrix} \quad a\left(0, \frac{45}{180} \cdot \pi\right) \cdot \alpha_2 \cdot a\left(0, \frac{45}{180} \cdot \pi\right)^T = \begin{bmatrix} 5.6 \cdot 10^{-9} & 0 & 0 \\ 0 & 1.32 \cdot 10^{-8} & 7.6 \cdot 10^{-9} \\ 0 & 7.6 \cdot 10^{-9} & 1.32 \cdot 10^{-8} \end{bmatrix}$$

The first order coeff is:  $\alpha_{0\_45\_1} = 3.68 \cdot 10^{-6}$

The second order coeff is:  $\alpha_{0\_45\_2} := 1.32 \cdot 10^{-8}$

The thickness as a function of temperature is:  $t_{0\_45\_j} := 202.2 \cdot 10^{-6} \cdot [1 + \alpha_{0\_45\_1} \cdot (10j - 5) + \alpha_{0\_45\_2} \cdot (10j - 5)^2]$

For the (YXw)45,0 orientation:

$$a \begin{pmatrix} \frac{45}{180} \cdot \pi, 0 \\ \alpha_1 \cdot a \left( \frac{45}{180} \cdot \pi, 0 \right) \end{pmatrix}^T = \begin{bmatrix} 1.11 \cdot 10^{-5} & 0 & 0 \\ 0 & 1.11 \cdot 10^{-5} & 0 \\ 0 & 0 & -3.74 \cdot 10^{-6} \end{bmatrix}$$

$$a \begin{pmatrix} \frac{45}{180} \cdot \pi, 0 \\ \alpha_2 \cdot a \left( \frac{45}{180} \cdot \pi, 0 \right) \end{pmatrix}^T = \begin{bmatrix} 5.6 \cdot 10^{-9} & 0 & 0 \\ 0 & 5.6 \cdot 10^{-9} & 0 \\ 0 & 0 & 2.08 \cdot 10^{-8} \end{bmatrix}$$

The first order coeff is:  $\alpha_{45\_0\_1} = 1.11 \cdot 10^{-5}$

The second order coeff is:  $\alpha_{45\_0\_2} := 5.6 \cdot 10^{-9}$

The thickness as a function of temperature is:  $t_{45\_0_j} := 206.9 \cdot 10^{-6} \cdot [1 + \alpha_{45\_0\_1} \cdot (10j - 5) + \alpha_{45\_0\_2} \cdot (10j - 5)^2]$

For the (YXw)45,45 orientation:

$$a \begin{pmatrix} \frac{45}{180} \cdot \pi, \frac{45}{180} \cdot \pi \\ \alpha_1 \cdot a \left( \frac{45}{180} \cdot \pi, \frac{45}{180} \cdot \pi \right) \end{pmatrix}^T = \begin{bmatrix} 1.11 \cdot 10^{-5} & 0 & 0 \\ 0 & 3.68 \cdot 10^{-6} & -7.42 \cdot 10^{-6} \\ 0 & -7.42 \cdot 10^{-6} & 3.68 \cdot 10^{-6} \end{bmatrix}$$

$$a \begin{pmatrix} \frac{45}{180} \cdot \pi, \frac{45}{180} \cdot \pi \\ \alpha_2 \cdot a \left( \frac{45}{180} \cdot \pi, \frac{45}{180} \cdot \pi \right) \end{pmatrix}^T = \begin{bmatrix} 5.6 \cdot 10^{-9} & 0 & 0 \\ 0 & 1.32 \cdot 10^{-8} & 7.6 \cdot 10^{-9} \\ 0 & 7.6 \cdot 10^{-9} & 1.32 \cdot 10^{-8} \end{bmatrix}$$

The first order coeff is:  $\alpha_{45\_45\_1} = 3.68 \cdot 10^{-6}$

The second order coeff is:  $\alpha_{45\_45\_2} := 1.32 \cdot 10^{-8}$

The thickness as a function of temperature is:  $t_{45\_45_j} := 200.1 \cdot 10^{-6} \cdot [1 + \alpha_{45\_45\_1} \cdot (10j - 5) + \alpha_{45\_45\_2} \cdot (10j - 5)^2]$

For the (YXw)0,90 orientation:

$$a \begin{pmatrix} 0, \frac{90}{180} \cdot \pi \\ \alpha_1 \cdot a \left( 0, \frac{90}{180} \cdot \pi \right) \end{pmatrix}^T = \begin{bmatrix} 1.11 \cdot 10^{-5} & 0 & 0 \\ 0 & -3.74 \cdot 10^{-6} & 0 \\ 0 & 0 & 1.11 \cdot 10^{-5} \end{bmatrix}$$

$$a \begin{pmatrix} 0, \frac{90}{180} \cdot \pi \\ \alpha_2 \cdot a \left( 0, \frac{90}{180} \cdot \pi \right) \end{pmatrix}^T = \begin{bmatrix} 5.6 \cdot 10^{-9} & 0 & 0 \\ 0 & 2.08 \cdot 10^{-8} & 0 \\ 0 & 0 & 5.6 \cdot 10^{-9} \end{bmatrix}$$

The first order coeff is:  $\alpha_{0\_90\_1} = -3.74 \cdot 10^{-6}$

The second order coeff is:  $\alpha_{0\_90\_2} := 2.08 \cdot 10^{-8}$

The thickness as a function of temperature is:  $t_{0\_90_j} := 201.5 \cdot 10^{-6} \cdot [1 + \alpha_{0\_90\_1} \cdot (10j - 5) + \alpha_{0\_90\_2} \cdot (10j - 5)^2]$

For the (YXw)0,28.2 orientation:

$$a \begin{pmatrix} 28.2 \\ 180 \end{pmatrix} \cdot \pi \cdot \alpha_1 \cdot a \begin{pmatrix} 28.2 \\ 180 \end{pmatrix} \cdot \pi \begin{matrix} 1.11 \cdot 10^{-5} & 0 & 0 \\ 0 & 7.786 \cdot 10^{-6} & -6.18 \cdot 10^{-6} \\ 0 & -6.18 \cdot 10^{-6} & -4.262 \cdot 10^{-7} \end{matrix} = \begin{matrix} 5.6 \cdot 10^{-9} & 0 & 0 \\ 0 & 8.994 \cdot 10^{-9} & 6.33 \cdot 10^{-9} \\ 0 & 6.33 \cdot 10^{-9} & 1.741 \cdot 10^{-8} \end{matrix}$$

The first order coeff is:  $\alpha_{0\_28\_1} := 7.786 \cdot 10^{-6}$

The second order coeff is:  $\alpha_{0\_28\_2} := 8.994 \cdot 10^{-9}$

The thickness as a function of temperature is:  $t_{0\_28\_j} := 196.0 \cdot 10^{-6} \cdot [1 + \alpha_{0\_28\_1} \cdot (10 \cdot j - 5) + \alpha_{0\_28\_2} \cdot (10 \cdot j - 5)^2]$

For the (YXw)45,56.1 orientation:

$$a \begin{pmatrix} 45 \\ 180 \end{pmatrix} \cdot \pi \cdot \alpha_1 \cdot a \begin{pmatrix} 45 \\ 180 \end{pmatrix} \cdot \pi \begin{matrix} 1.11 \cdot 10^{-5} & 0 & 0 \\ 0 & 8.764 \cdot 10^{-7} & -6.87 \cdot 10^{-7} \\ 0 & -6.87 \cdot 10^{-7} & 6.484 \cdot 10^{-6} \end{matrix} = \begin{matrix} 5.6 \cdot 10^{-9} & 0 & 0 \\ 0 & 1.607 \cdot 10^{-8} & 7.037 \cdot 10^{-9} \\ 0 & 7.037 \cdot 10^{-9} & 1.033 \cdot 10^{-8} \end{matrix}$$

The first order coeff is:  $\alpha_{45\_56\_1} := 8.764 \cdot 10^{-7}$

The second order coeff is:  $\alpha_{45\_56\_2} := 1.607 \cdot 10^{-8}$

The thickness as a function of temperature is:  $t_{45\_56\_j} := 203.8 \cdot 10^{-6} \cdot [1 + \alpha_{45\_56\_1} \cdot (10 \cdot j - 5) + \alpha_{45\_56\_2} \cdot (10 \cdot j - 5)^2]$

Dielectric constant varies with temperature and crystal orientation, however, only the unrotated dielectric constants are needed, so no rotations need to be performed:

From Shiosaki, et. al., [10] the dielectric constant and the first and second order temperature coefficients of dielectric constant for  $\text{Li}_2\text{B}_4\text{O}_7$  are:

$$\epsilon_0 := \begin{pmatrix} 78.8 & 0 & 0 \\ 0 & 78.8 & 0 \\ 0 & 0 & 71.5 \end{pmatrix} \cdot 10^{-12}$$

$$\epsilon_1 := \begin{pmatrix} 97.1 & 0 & 0 \\ 0 & 97.1 & 0 \\ 0 & 0 & 545 \end{pmatrix} \cdot 10^{-6}$$

$$\epsilon_2 := \begin{pmatrix} 2800 & 0 & 0 \\ 0 & 2800 & 0 \\ 0 & 0 & 2900 \end{pmatrix} \cdot 10^{-9}$$

All are  
at a reference  
temperature of  
25 degrees C.

The zeroth order coefficient is:  $\epsilon_{S110} := 78.8 \cdot 10^{-12}$

The first order coefficient is:  $\epsilon_{S111} := 97.1 \cdot 10^{-6}$

The second order coefficient is:  $\epsilon_{S112} := 2800 \cdot 10^{-9}$

The unrotated dielectric constant  $\epsilon_{11}^2$  as a function of temperature is:

$$\epsilon_{S11_j} := \epsilon_{S110} \cdot [1 + \epsilon_{S111} \cdot (10 \cdot j - 5) + \epsilon_{S112} \cdot (10 \cdot j - 5)^2]$$

## Calculation of the Stiffness Eigenvalues:

Now that we have all the components calculated over our range of temperatures and at our orientations, we can calculate the stiffness eigenvalues for each crystal over our temperature range using Equation (3.21):

$$\begin{aligned}
 \text{cbar1}_j &:= (2 \cdot t0\_j \cdot \text{Fit1}_j \cdot 10^6)^2 \cdot \rho1_j & \text{cbar18b}_j &:= (2 \cdot t45\_j \cdot 0 \cdot \text{Fit18b}_j \cdot 10^6)^2 \cdot \rho18_j \\
 \text{cbar1b}_j &:= (2 \cdot t0\_j \cdot \text{Fit1b}_j \cdot 10^6)^2 \cdot \rho1_j & \text{cbar20a}_j &:= (2 \cdot t45\_j \cdot 0 \cdot \text{Fit20a}_j \cdot 10^6)^2 \cdot \rho20_j \\
 \text{cbar2}_j &:= (2 \cdot t0\_j \cdot \text{Fit2}_j \cdot 10^6)^2 \cdot \rho2_j & \text{cbar20b}_j &:= (2 \cdot t45\_j \cdot 0 \cdot \text{Fit20b}_j \cdot 10^6)^2 \cdot \rho20_j \\
 \text{cbar2b}_j &:= (2 \cdot t0\_j \cdot \text{Fit2b}_j \cdot 10^6)^2 \cdot \rho2_j & \text{cbar20c}_j &:= (2 \cdot t45\_j \cdot 0 \cdot \text{Fit20c}_j \cdot 10^6)^2 \cdot \rho20_j \\
 \text{cbar3}_j &:= (2 \cdot t0\_j \cdot \text{Fit3}_j \cdot 10^6)^2 \cdot \rho3_j & \text{cbar20d}_j &:= (2 \cdot t45\_j \cdot 0 \cdot \text{Fit20d}_j \cdot 10^6)^2 \cdot \rho20_j \\
 \text{cbar4}_j &:= (2 \cdot t0\_j \cdot \text{Fit4}_j \cdot 10^6)^2 \cdot \rho4_j & \text{cbar21}_j &:= (2 \cdot t45\_j \cdot 0 \cdot \text{Fit21}_j \cdot 10^6)^2 \cdot \rho21_j \\
 \text{cbar5}_j &:= (2 \cdot t0\_j \cdot \text{Fit5}_j \cdot 10^6)^2 \cdot \rho5_j & \text{cbar21b}_j &:= (2 \cdot t45\_j \cdot 0 \cdot \text{Fit21b}_j \cdot 10^6)^2 \cdot \rho21_j \\
 \text{cbar6}_j &:= (2 \cdot t0\_j \cdot \text{Fit6}_j \cdot 10^6)^2 \cdot \rho6_j & \text{cbar22}_j &:= (2 \cdot t45\_j \cdot 0 \cdot \text{Fit22}_j \cdot 10^6)^2 \cdot \rho22_j \\
 \text{cbar7}_j &:= (2 \cdot t0\_j \cdot \text{Fit7}_j \cdot 10^6)^2 \cdot \rho7_j & \text{cbar23}_j &:= (2 \cdot t45\_j \cdot 0 \cdot \text{Fit23}_j \cdot 10^6)^2 \cdot \rho23_j \\
 \text{cbar8}_j &:= (2 \cdot t0\_j \cdot \text{Fit8}_j \cdot 10^6)^2 \cdot \rho8_j & \text{cbar24}_j &:= (2 \cdot t45\_j \cdot 0 \cdot \text{Fit24}_j \cdot 10^6)^2 \cdot \rho24_j \\
 \text{cbar9}_j &:= (2 \cdot t0\_j \cdot \text{Fit9}_j \cdot 10^6)^2 \cdot \rho9_j & \text{cbar25}_j &:= (2 \cdot t45\_j \cdot 0 \cdot \text{Fit25}_j \cdot 10^6)^2 \cdot \rho25_j \\
 \text{cbar10}_j &:= (2 \cdot t0\_j \cdot \text{Fit10}_j \cdot 10^6)^2 \cdot \rho10_j & \text{cbar25b}_j &:= (2 \cdot t45\_j \cdot 0 \cdot \text{Fit25b}_j \cdot 10^6)^2 \cdot \rho25_j \\
 \text{cbar10b}_j &:= (2 \cdot t0\_j \cdot \text{Fit10b}_j \cdot 10^6)^2 \cdot \rho10_j & \text{cbar26}_j &:= (2 \cdot t45\_j \cdot 0 \cdot \text{Fit26}_j \cdot 10^6)^2 \cdot \rho26_j \\
 \text{cbar11}_j &:= (2 \cdot t0\_j \cdot \text{Fit11}_j \cdot 10^6)^2 \cdot \rho11_j & \text{cbar27}_j &:= (2 \cdot t45\_j \cdot 0 \cdot \text{Fit27}_j \cdot 10^6)^2 \cdot \rho27_j \\
 \text{cbar12}_j &:= (2 \cdot t0\_j \cdot \text{Fit12}_j \cdot 10^6)^2 \cdot \rho12_j & \text{cbar28}_j &:= (2 \cdot t45\_j \cdot 0 \cdot \text{Fit28}_j \cdot 10^6)^2 \cdot \rho28_j \\
 \text{cbar18}_j &:= (2 \cdot t45\_j \cdot 0 \cdot \text{Fit18}_j \cdot 10^6)^2 \cdot \rho18_j & \text{cbar37a}_j &:= (2 \cdot t0\_j \cdot 0 \cdot \text{Fit37a}_j \cdot 10^6)^2 \cdot \rho37_j
 \end{aligned}$$

$$\begin{aligned}
 \text{cbar37b}_j &:= (2 \cdot t0\_j \cdot \text{Fit37b}_j \cdot 10^6)^2 \cdot \rho37_j \\
 \text{cbar37c}_j &:= (2 \cdot t0\_j \cdot \text{Fit37c}_j \cdot 10^6)^2 \cdot \rho37_j \\
 \text{cbar38}_j &:= (2 \cdot t0\_j \cdot \text{Fit38}_j \cdot 10^6)^2 \cdot \rho38_j \\
 \text{cbar39}_j &:= (2 \cdot t0\_j \cdot \text{Fit39}_j \cdot 10^6)^2 \cdot \rho39_j \\
 \text{cbar40}_j &:= (2 \cdot t0\_j \cdot \text{Fit40}_j \cdot 10^6)^2 \cdot \rho40_j \\
 \text{cbar49}_j &:= (2 \cdot t0\_j \cdot \text{Fit49}_j \cdot 10^6)^2 \cdot \rho49_j \\
 \text{cbar49b}_j &:= (2 \cdot t0\_j \cdot \text{Fit49b}_j \cdot 10^6)^2 \cdot \rho49_j \\
 \text{cbar50}_j &:= (2 \cdot t0\_j \cdot \text{Fit50}_j \cdot 10^6)^2 \cdot \rho50_j \\
 \text{cbar50b}_j &:= (2 \cdot t0\_j \cdot \text{Fit50b}_j \cdot 10^6)^2 \cdot \rho50_j \\
 \text{cbar51}_j &:= (2 \cdot t0\_j \cdot \text{Fit51}_j \cdot 10^6)^2 \cdot \rho51_j \\
 \text{cbar51b}_j &:= (2 \cdot t0\_j \cdot \text{Fit51b}_j \cdot 10^6)^2 \cdot \rho51_j \\
 \text{cbar52}_j &:= (2 \cdot t0\_j \cdot \text{Fit52}_j \cdot 10^6)^2 \cdot \rho52_j \\
 \text{cbar52b}_j &:= (2 \cdot t0\_j \cdot \text{Fit52b}_j \cdot 10^6)^2 \cdot \rho52_j \\
 \text{cbar61}_j &:= (2 \cdot t45\_j \cdot 0 \cdot \text{Fit61}_j \cdot 10^6)^2 \cdot \rho61_j \\
 \text{cbar61b}_j &:= (2 \cdot t45\_j \cdot 0 \cdot \text{Fit61b}_j \cdot 10^6)^2 \cdot \rho61_j
 \end{aligned}$$

$$\begin{aligned}
 \text{cbar62}_j &:= (2 \cdot t45\_j \cdot \text{Fit62}_j \cdot 10^6)^2 \cdot \rho62_j \\
 \text{cbar62b}_j &:= (2 \cdot t45\_j \cdot \text{Fit62b}_j \cdot 10^6)^2 \cdot \rho62_j \\
 \text{cbar63}_j &:= (2 \cdot t45\_j \cdot \text{Fit63}_j \cdot 10^6)^2 \cdot \rho63_j \\
 \text{cbar63b}_j &:= (2 \cdot t45\_j \cdot \text{Fit63b}_j \cdot 10^6)^2 \cdot \rho63_j \\
 \text{cbar64}_j &:= (2 \cdot t45\_j \cdot \text{Fit64}_j \cdot 10^6)^2 \cdot \rho64_j \\
 \text{cbar64b}_j &:= (2 \cdot t45\_j \cdot \text{Fit64b}_j \cdot 10^6)^2 \cdot \rho64_j
 \end{aligned}$$

Now a third order power fit is performed so the room temperature values of the stiffened elastic constants can be compared to those of Kosinski [2]:

$$\text{Fifunction}(\theta, F) := \begin{bmatrix} F_0 \cdot \left[ 1 + F_1 \cdot (\theta - 25) + F_2 \cdot (\theta - 25)^2 + F_3 \cdot (\theta - 25)^3 \right] \\ \left[ 1 + F_1 \cdot (\theta - 25) + F_2 \cdot (\theta - 25)^2 + F_3 \cdot (\theta - 25)^3 \right] \\ F_0 \cdot \left[ 1 + (\theta - 25) + F_2 \cdot (\theta - 25)^2 + F_3 \cdot (\theta - 25)^3 \right] \\ F_0 \cdot \left[ 1 + F_1 \cdot (\theta - 25) + (\theta - 25)^2 + F_3 \cdot (\theta - 25)^3 \right] \\ F_0 \cdot \left[ 1 + F_1 \cdot (\theta - 25) + F_2 \cdot (\theta - 25)^2 + (\theta - 25)^3 \right] \end{bmatrix}$$

$$\text{guess} := \begin{bmatrix} 10^{10} \\ 10^{-6} \\ 10^{-9} \\ 10^{-12} \end{bmatrix}$$

$$\text{temps}_j := 10 \cdot j + 20$$

The value for the room temperature stiffened elastic constant for Trial #1 is:

$$\text{fitbar1} := \text{genfit}(\text{temps}, \text{cbar1}, \text{guess}, \text{Fifunction})$$

$$\text{roomcbar1} := \text{fitbar1}_0$$

$$\begin{bmatrix} 5.929 \cdot 10^{10} \\ -1.062 \cdot 10^{-4} \\ -1.095 \cdot 10^{-7} \\ 1.033 \cdot 10^{-10} \end{bmatrix}$$

$$\text{roomcbar1} = 5.929 \cdot 10^{10}$$

The value for the room temperature stiffened elastic constant for Trial #1b is:

$$\text{fitbar1b} := \text{genfit}(\text{temps}, \text{cbar1b}, \text{guess}, \text{Fifunction})$$

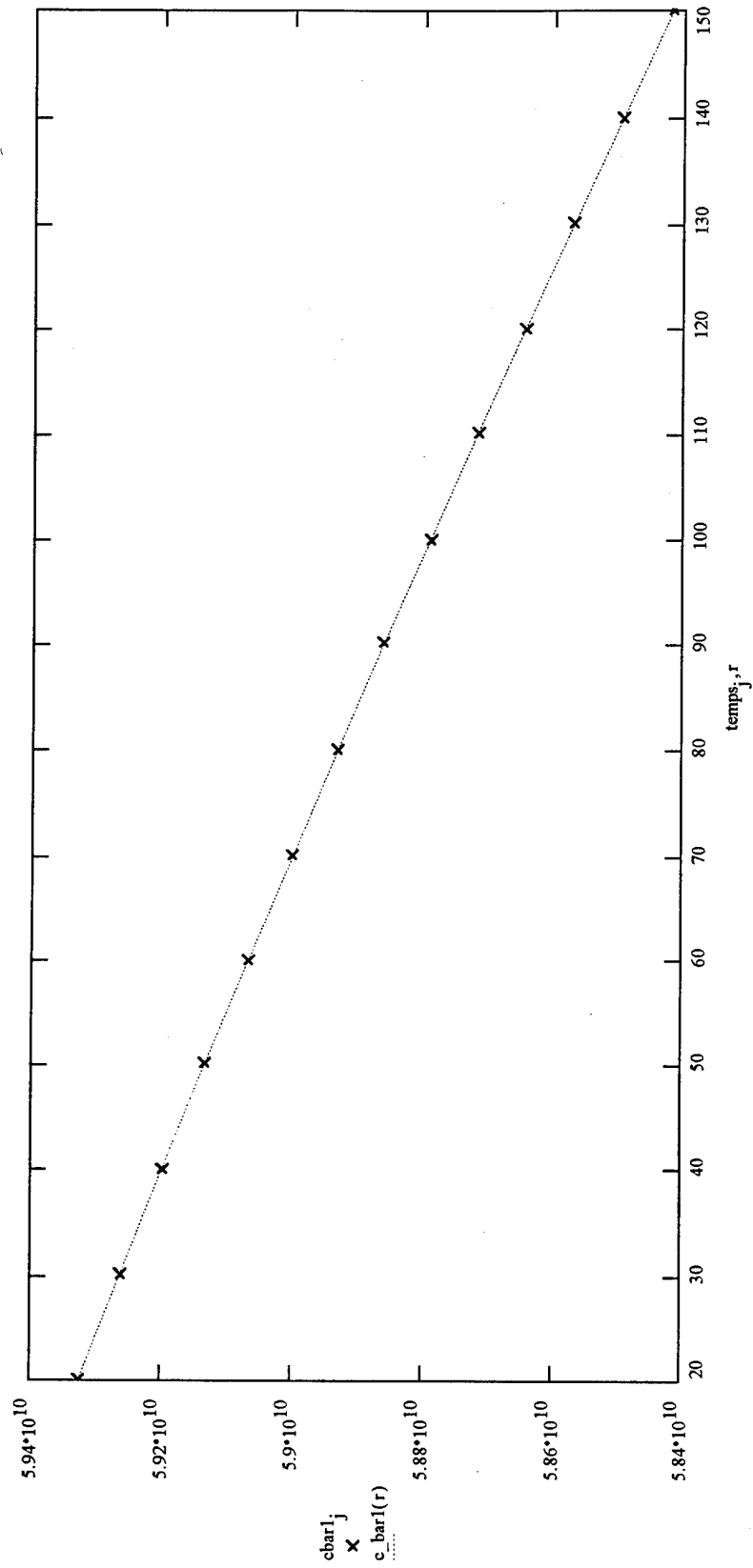
$$\text{roomcbar1b} := \text{fitbar1b}_0$$

$$\begin{bmatrix} 5.929 \cdot 10^{10} \\ -1.081 \cdot 10^{-4} \\ -8.099 \cdot 10^{-8} \\ 1.204 \cdot 10^{-11} \end{bmatrix}$$

$$\text{roomcbar1b} = 5.929 \cdot 10^{10}$$

This is a plot of the cbar1 values and the corresponding power series fit:

$r := 20, 20.1 .. 150$      $c\_bar1(r) := \text{Fitfunction}(r, \text{firebar1})_0$





The value for the room temperature stiffened elastic constant for Trial #2 is:

fitbar2 := genfit(temps, cbar2, guess, Fifunction)

roomcbar2 := fitbar2<sub>0</sub>

$$\text{fitbar2} = \begin{bmatrix} 5.931 \cdot 10^{10} \\ -1.119 \cdot 10^{-4} \\ 1.795 \cdot 10^{-8} \\ -6.012 \cdot 10^{-10} \end{bmatrix}$$

roomcbar2 =  $5.931 \cdot 10^{10}$

The value for the room temperature stiffened elastic constant for Trial #2b is:

fitbar2b := genfit(temps, cbar2b, guess, Fifunction)

roomcbar2b := fitbar2b<sub>0</sub>

$$\text{fitbar2b} = \begin{bmatrix} 5.931 \cdot 10^{10} \\ -1.05 \cdot 10^{-4} \\ -1.373 \cdot 10^{-7} \\ 2.292 \cdot 10^{-10} \end{bmatrix}$$

roomcbar2b =  $5.931 \cdot 10^{10}$

The value for the room temperature stiffened elastic constant for Trial #3 is:

fitbar3 := genfit(temps, cbar3, guess, Fifunction)

roomcbar3 := fitbar3<sub>0</sub>

$$\text{fitbar3} = \begin{bmatrix} 5.883 \cdot 10^{10} \\ -1.094 \cdot 10^{-4} \\ -7.097 \cdot 10^{-8} \\ 3.04 \cdot 10^{-11} \end{bmatrix}$$

roomcbar3 =  $5.883 \cdot 10^{10}$

The value for the room temperature stiffened elastic constant for Trial #4 is:

fitbar4 := genfit(temps, cbar4, guess, Fifunction)

roomcbar4 := fitbar4<sub>0</sub>

$$\text{fitbar4} = \begin{bmatrix} 5.923 \cdot 10^{10} \\ -1.109 \cdot 10^{-4} \\ -1.033 \cdot 10^{-8} \\ -4.303 \cdot 10^{-10} \end{bmatrix}$$

roomcbar4 =  $5.923 \cdot 10^{10}$

The value for the room temperature stiffened elastic constant for Trial #5 is:

$$\text{fitcbar5} = \begin{bmatrix} 1.364 \cdot 10^{11} \\ -7.22 \cdot 10^{-5} \\ -1.978 \cdot 10^{-7} \\ 2.554 \cdot 10^{-10} \end{bmatrix}$$
$$\text{roomcbar5} = 1.364 \cdot 10^{11}$$

The value for the room temperature stiffened elastic constant for Trial #6 is:

$$\text{fitcbar6} = \begin{bmatrix} 1.36 \cdot 10^{11} \\ -7.222 \cdot 10^{-5} \\ -1.978 \cdot 10^{-7} \\ 2.554 \cdot 10^{-10} \end{bmatrix}$$
$$\text{roomcbar6} = 1.36 \cdot 10^{11}$$

The value for the room temperature stiffened elastic constant for Trial #7 is:

$$\text{fitcbar7} = \begin{bmatrix} 1.358 \cdot 10^{11} \\ -7.132 \cdot 10^{-5} \\ -1.952 \cdot 10^{-7} \\ 1.969 \cdot 10^{-10} \end{bmatrix}$$
$$\text{roomcbar7} = 1.358 \cdot 10^{11}$$

The value for the room temperature stiffened elastic constant for Trial #8 is:

$$\text{fitcbar8} = \begin{bmatrix} 1.356 \cdot 10^{11} \\ -7.023 \cdot 10^{-5} \\ -2.42 \cdot 10^{-7} \\ 5.163 \cdot 10^{-10} \end{bmatrix}$$
$$\text{roomcbar8} = 1.356 \cdot 10^{11}$$

The value for the room temperature stiffened elastic constant for Trial #9 is:

$$\begin{aligned} \text{fitcbar9} &:= \text{genfit}(\text{temps}, \text{cbar9}, \text{guess}, \text{Fitfunction}) \\ \text{roomcbar9} &:= \text{fitcbar9}_0 \end{aligned} \quad \text{fitcbar9} = \begin{bmatrix} 5.244 \cdot 10^{10} \\ -1.944 \cdot 10^{-4} \\ -1.019 \cdot 10^{-7} \\ 6.675 \cdot 10^{-10} \end{bmatrix} \quad \text{roomcbar9} = 5.244 \cdot 10^{10}$$

The value for the room temperature stiffened elastic constant for Trial #10 is:

$$\begin{aligned} \text{fitcbar10} &:= \text{genfit}(\text{temps}, \text{cbar10}, \text{guess}, \text{Fitfunction}) \\ \text{roomcbar10} &:= \text{fitcbar10}_0 \end{aligned} \quad \text{fitcbar10} = \begin{bmatrix} 5.255 \cdot 10^{10} \\ -2.006 \cdot 10^{-4} \\ 3.119 \cdot 10^{-8} \\ -1.357 \cdot 10^{-11} \end{bmatrix} \quad \text{roomcbar10} = 5.255 \cdot 10^{10}$$

The value for the room temperature stiffened elastic constant for Trial #10b is:

$$\begin{aligned} \text{fitcbar10b} &:= \text{genfit}(\text{temps}, \text{cbar10b}, \text{guess}, \text{Fitfunction}) \\ \text{roomcbar10b} &:= \text{fitcbar10b}_0 \end{aligned} \quad \text{fitcbar10b} = \begin{bmatrix} 5.255 \cdot 10^{10} \\ -1.993 \cdot 10^{-4} \\ 4.144 \cdot 10^{-8} \\ -1.88 \cdot 10^{-10} \end{bmatrix} \quad \text{roomcbar10b} = 5.255 \cdot 10^{10}$$

The value for the room temperature stiffened elastic constant for Trial #11 is:

$$\begin{aligned} \text{fitcbar11} &:= \text{genfit}(\text{temps}, \text{cbar11}, \text{guess}, \text{Fitfunction}) \\ \text{roomcbar11} &:= \text{fitcbar11}_0 \end{aligned} \quad \text{fitcbar11} = \begin{bmatrix} 5.25 \cdot 10^{10} \\ -1.864 \cdot 10^{-4} \\ -1.437 \cdot 10^{-7} \\ 6.81 \cdot 10^{-10} \end{bmatrix} \quad \text{roomcbar11} = 5.25 \cdot 10^{10}$$

The value for the room temperature stiffened elastic constant for Trial #12 is:

$$\begin{aligned} \text{fitcbar12} &:= \text{genfit}(\text{temps}, \text{cbar12}, \text{guess}, \text{Fitfunction}) \\ \text{roomcbar12} &:= \text{fitcbar12}_0 \end{aligned} \quad \text{fitcbar12} = \begin{bmatrix} 5.223 \cdot 10^{10} \\ -2.03 \cdot 10^{-4} \\ 1.049 \cdot 10^{-7} \\ -5.039 \cdot 10^{-10} \end{bmatrix} \quad \text{roomcbar12} = 5.223 \cdot 10^{10}$$

The value for the room temperature stiffened elastic constant for Trial #18 is:

$$\begin{aligned} \text{fitcbar18} &:= \text{genfit}(\text{temps}, \text{cbar18}, \text{guess}, \text{Fitfunction}) \\ \text{roomcbar18} &:= \text{fitcbar18}_0 \end{aligned} \quad \text{fitcbar18} = \begin{bmatrix} 5.875 \cdot 10^{10} \\ -1.065 \cdot 10^{-4} \\ -9.298 \cdot 10^{-8} \\ -8.679 \cdot 10^{-12} \end{bmatrix} \quad \text{roomcbar18} = 5.875 \cdot 10^{10}$$

The value for the room temperature stiffened elastic constant for Trial #18b is:

$$\begin{aligned} \text{fitcbar18b} &:= \text{genfit}(\text{temps}, \text{cbar18b}, \text{guess}, \text{Fitfunction}) \\ \text{roomcbar18b} &:= \text{fitcbar18b}_0 \end{aligned} \quad \text{fitcbar18b} = \begin{bmatrix} 5.875 \cdot 10^{10} \\ -1.101 \cdot 10^{-4} \\ -6.748 \cdot 10^{-8} \\ -1.346 \cdot 10^{-11} \end{bmatrix} \quad \text{roomcbar18b} = 5.875 \cdot 10^{10}$$

The value for the room temperature stiffened elastic constant for Trial #20a is:

$$\begin{aligned} \text{fitcbar20a} &:= \text{genfit}(\text{temps}, \text{cbar20a}, \text{guess}, \text{Fitfunction}) \\ \text{roomcbar20a} &:= \text{fitcbar20a}_0 \end{aligned} \quad \text{fitcbar20a} = \begin{bmatrix} 5.912 \cdot 10^{10} \\ -1.111 \cdot 10^{-4} \\ -3.408 \cdot 10^{-8} \\ -2.54 \cdot 10^{-10} \end{bmatrix} \quad \text{roomcbar20a} = 5.912 \cdot 10^{10}$$

The value for the room temperature stiffened elastic constant for Trial #20b is:

fitcbar20b := genfit(temps, cbar20b, guess, Fitfunction)

roomcbar20b := fitcbar20b<sub>0</sub>

$$\text{fitcbar20b} = \begin{bmatrix} 5.912 \cdot 10^{10} \\ -1.062 \cdot 10^{-4} \\ -1.046 \cdot 10^{-7} \\ 1.763 \cdot 10^{-11} \end{bmatrix}$$

$$\text{roomcbar20b} = 5.912 \cdot 10^{10}$$

The value for the room temperature stiffened elastic constant for Trial #20c is:

fitcbar20c := genfit(temps, cbar20c, guess, Fitfunction)

roomcbar20c := fitcbar20c<sub>0</sub>

$$\text{fitcbar20c} = \begin{bmatrix} 5.912 \cdot 10^{10} \\ -1.072 \cdot 10^{-4} \\ -1.246 \cdot 10^{-7} \\ 3.057 \cdot 10^{-10} \end{bmatrix}$$

$$\text{roomcbar20c} = 5.912 \cdot 10^{10}$$

The value for the room temperature stiffened elastic constant for Trial #20d is:

fitcbar20d := genfit(temps, cbar20d, guess, Fitfunction)

roomcbar20d := fitcbar20d<sub>0</sub>

$$\text{fitcbar20d} = \begin{bmatrix} 5.912 \cdot 10^{10} \\ -1.084 \cdot 10^{-4} \\ -7.332 \cdot 10^{-8} \\ -5.85 \cdot 10^{-11} \end{bmatrix}$$

$$\text{roomcbar20d} = 5.912 \cdot 10^{10}$$

The value for the room temperature stiffened elastic constant for Trial #21 is:

fitcbar21 := genfit(temps, cbar21, guess, Fitfunction)

roomcbar21 := fitcbar21<sub>0</sub>

$$\text{fitcbar21} = \begin{bmatrix} 1.159 \cdot 10^{11} \\ -1.379 \cdot 10^{-4} \\ 2.845 \cdot 10^{-9} \\ -1.268 \cdot 10^{-10} \end{bmatrix}$$

$$\text{roomcbar21} = 1.159 \cdot 10^{11}$$

The value for the room temperature stiffened elastic constant for Trial #21b is:

$$\begin{aligned} \text{fitcbar21b} &:= \text{genfit}(\text{temps}, \text{cbar21b}, \text{guess}, \text{Fitfunction}) \\ \text{roomcbar21b}_0 &:= \text{fitcbar21b}_0 \end{aligned} \quad \text{fitcbar21b} = \begin{bmatrix} 1.159 \cdot 10^{11} \\ -1.327 \cdot 10^{-4} \\ -6.529 \cdot 10^{-8} \\ 1.558 \cdot 10^{-10} \end{bmatrix} \quad \text{roomcbar21b} = 1.159 \cdot 10^{11}$$

The value for the room temperature stiffened elastic constant for Trial #22 is:

$$\begin{aligned} \text{fitcbar22} &:= \text{genfit}(\text{temps}, \text{cbar22}, \text{guess}, \text{Fitfunction}) \\ \text{roomcbar22}_0 &:= \text{fitcbar22}_0 \end{aligned} \quad \text{fitcbar22} = \begin{bmatrix} 1.153 \cdot 10^{11} \\ -1.098 \cdot 10^{-4} \\ -8.134 \cdot 10^{-8} \\ 4.961 \cdot 10^{-11} \end{bmatrix} \quad \text{roomcbar22} = 1.153 \cdot 10^{11}$$

The value for the room temperature stiffened elastic constant for Trial #23 is:

$$\begin{aligned} \text{fitcbar23} &:= \text{genfit}(\text{temps}, \text{cbar23}, \text{guess}, \text{Fitfunction}) \\ \text{roomcbar23}_0 &:= \text{fitcbar23}_0 \end{aligned} \quad \text{fitcbar23} = \begin{bmatrix} 1.152 \cdot 10^{11} \\ -1.368 \cdot 10^{-4} \\ 9.528 \cdot 10^{-9} \\ -2.72 \cdot 10^{-10} \end{bmatrix} \quad \text{roomcbar23} = 1.152 \cdot 10^{11}$$

The value for the room temperature stiffened elastic constant for Trial #24 is:

$$\begin{aligned} \text{fitcbar24} &:= \text{genfit}(\text{temps}, \text{cbar24}, \text{guess}, \text{Fitfunction}) \\ \text{roomcbar24}_0 &:= \text{fitcbar24}_0 \end{aligned} \quad \text{fitcbar24} = \begin{bmatrix} 1.153 \cdot 10^{11} \\ -1.354 \cdot 10^{-4} \\ -3.879 \cdot 10^{-8} \\ 5.42 \cdot 10^{-11} \end{bmatrix} \quad \text{roomcbar24} = 1.153 \cdot 10^{11}$$

The value for the room temperature stiffened elastic constant for Trial #25 is:

fitcbar25 := genfit(temps, cbar25, guess, Fitfunction)

$$\text{fitcbar25} = \begin{bmatrix} 6.267 \cdot 10^{10} \\ -1.235 \cdot 10^{-4} \\ -1.03 \cdot 10^{-7} \\ -3.962 \cdot 10^{-11} \end{bmatrix}$$

roomcbar25 := fitcbar25<sub>0</sub>

$$\text{roomcbar25} = 6.267 \cdot 10^{10}$$

The value for the room temperature stiffened elastic constant for Trial #25b is:

fitcbar25b := genfit(temps, cbar25b, guess, Fitfunction)

$$\text{fitcbar25b} = \begin{bmatrix} 6.267 \cdot 10^{10} \\ -1.209 \cdot 10^{-4} \\ -1.023 \cdot 10^{-7} \\ -1.941 \cdot 10^{-10} \end{bmatrix}$$

roomcbar25b := fitcbar25b<sub>0</sub>

$$\text{roomcbar25b} = 6.267 \cdot 10^{10}$$

The value for the room temperature stiffened elastic constant for Trial #26 is:

fitcbar26 := genfit(temps, cbar26, guess, Fitfunction)

$$\text{fitcbar26} = \begin{bmatrix} 6.241 \cdot 10^{10} \\ -1.219 \cdot 10^{-4} \\ -1.145 \cdot 10^{-7} \\ -5.395 \cdot 10^{-11} \end{bmatrix}$$

roomcbar26 := fitcbar26<sub>0</sub>

$$\text{roomcbar26} = 6.241 \cdot 10^{10}$$

The value for the room temperature stiffened elastic constant for Trial #27 is:

fitcbar27 := genfit(temps, cbar27, guess, Fitfunction)

$$\text{fitcbar27} = \begin{bmatrix} 6.29 \cdot 10^{10} \\ -1.245 \cdot 10^{-4} \\ -8.726 \cdot 10^{-8} \\ -1.539 \cdot 10^{-10} \end{bmatrix}$$

roomcbar27 := fitcbar27<sub>0</sub>

$$\text{roomcbar27} = 6.29 \cdot 10^{10}$$

The value for the room temperature stiffened elastic constant for Trial #28 is:

$$\text{fitbar28} := \text{genfit}(\text{temps}, \text{cbar28}, \text{guess}, \text{Fitfunction})$$

$$\text{roomcbar28} := \text{fitbar28}_0$$

$$\text{fitbar28} = \begin{bmatrix} 6.241 \cdot 10^{10} \\ -1.215 \cdot 10^{-4} \\ -1.184 \cdot 10^{-7} \\ -7.234 \cdot 10^{-11} \end{bmatrix}$$

$$\text{roomcbar28} = 6.241 \cdot 10^{10}$$

The value for the room temperature stiffened elastic constant for Trial #37a is:

$$\text{fitbar37a} := \text{genfit}(\text{temps}, \text{cbar37a}, \text{guess}, \text{Fitfunction})$$

$$\text{roomcbar37a} := \text{fitbar37a}_0$$

$$\text{fitbar37a} = \begin{bmatrix} 5.722 \cdot 10^{10} \\ -1.463 \cdot 10^{-5} \\ -4.074 \cdot 10^{-7} \\ 9.305 \cdot 10^{-10} \end{bmatrix}$$

$$\text{roomcbar37a} = 5.722 \cdot 10^{10}$$

The value for the room temperature stiffened elastic constant for Trial #37b is:

$$\text{fitbar37b} := \text{genfit}(\text{temps}, \text{cbar37b}, \text{guess}, \text{Fitfunction})$$

$$\text{roomcbar37b} := \text{fitbar37b}_0$$

$$\text{fitbar37b} = \begin{bmatrix} 5.722 \cdot 10^{10} \\ -1.439 \cdot 10^{-5} \\ -3.839 \cdot 10^{-7} \\ 6.867 \cdot 10^{-10} \end{bmatrix}$$

$$\text{roomcbar37b} = 5.722 \cdot 10^{10}$$

The value for the room temperature stiffened elastic constant for Trial #37c is:

$$\text{fitbar37c} := \text{genfit}(\text{temps}, \text{cbar37c}, \text{guess}, \text{Fitfunction})$$

$$\text{roomcbar37c} := \text{fitbar37c}_0$$

$$\text{fitbar37c} = \begin{bmatrix} 5.722 \cdot 10^{10} \\ -2.088 \cdot 10^{-5} \\ -2.584 \cdot 10^{-7} \\ 9.369 \cdot 10^{-11} \end{bmatrix}$$

$$\text{roomcbar37c} = 5.722 \cdot 10^{10}$$



The value for the room temperature stiffened elastic constant for Trial #38 is:

$$\text{fitcbar38} := \text{genfit}(\text{temps}, \text{cbar38}, \text{guess}, \text{Fitfunction})$$

$$\text{roomcbar38}_0 := \text{fitcbar38}$$

$$\text{fitcbar38} = \begin{bmatrix} 5.707 \cdot 10^{10} \\ -1.832 \cdot 10^{-5} \\ -3.649 \cdot 10^{-7} \\ 8.144 \cdot 10^{-10} \end{bmatrix}$$

$$\text{roomcbar38} = 5.707 \cdot 10^{10}$$

The value for the room temperature stiffened elastic constant for Trial #39 is:

$$\text{fitcbar39} := \text{genfit}(\text{temps}, \text{cbar39}, \text{guess}, \text{Fitfunction})$$

$$\text{roomcbar39}_0 := \text{fitcbar39}$$

$$\text{fitcbar39} = \begin{bmatrix} 5.686 \cdot 10^{10} \\ -5.052 \cdot 10^{-6} \\ -7.541 \cdot 10^{-7} \\ 2.903 \cdot 10^{-9} \end{bmatrix}$$

$$\text{roomcbar39} = 5.686 \cdot 10^{10}$$

The value for the room temperature stiffened elastic constant for Trial #40 is:

$$\text{fitcbar40} := \text{genfit}(\text{temps}, \text{cbar40}, \text{guess}, \text{Fitfunction})$$

$$\text{roomcbar40}_0 := \text{fitcbar40}$$

$$\text{fitcbar40} = \begin{bmatrix} 5.667 \cdot 10^{10} \\ -1.941 \cdot 10^{-5} \\ -2.927 \cdot 10^{-7} \\ 4.551 \cdot 10^{-10} \end{bmatrix}$$

$$\text{roomcbar40} = 5.667 \cdot 10^{10}$$

The value for the room temperature stiffened elastic constant for Trial #49 is:

$$\text{fitcbar49} := \text{genfit}(\text{temps}, \text{cbar49}, \text{guess}, \text{Fitfunction})$$

$$\text{roomcbar49}_0 := \text{fitcbar49}$$

$$\text{fitcbar49} = \begin{bmatrix} 4.989 \cdot 10^{10} \\ -3.14 \cdot 10^{-4} \\ 2.085 \cdot 10^{-7} \\ -1.535 \cdot 10^{-10} \end{bmatrix}$$

$$\text{roomcbar49} = 4.989 \cdot 10^{10}$$

The value for the room temperature stiffened elastic constant for Trial #49b is:

fitcbar49b := genfit(temps, cbar49b, guess, Fitfunction)

roomcbar49b := fitcbar49b<sub>0</sub>

$$\text{fitcbar49b} = \begin{bmatrix} 4.989 \cdot 10^{10} \\ -3.157 \cdot 10^{-4} \\ 2.482 \cdot 10^{-7} \\ -3.171 \cdot 10^{-10} \end{bmatrix}$$

roomcbar49b =  $4.989 \cdot 10^{10}$

The value for the room temperature stiffened elastic constant for Trial #50 is:

fitcbar50 := genfit(temps, cbar50, guess, Fitfunction)

roomcbar50 := fitcbar50<sub>0</sub>

$$\text{fitcbar50} = \begin{bmatrix} 4.972 \cdot 10^{10} \\ -3.195 \cdot 10^{-4} \\ 3.045 \cdot 10^{-7} \\ -6.224 \cdot 10^{-10} \end{bmatrix}$$

roomcbar50 =  $4.972 \cdot 10^{10}$

The value for the room temperature stiffened elastic constant for Trial #50b is:

fitcbar50b := genfit(temps, cbar50b, guess, Fitfunction)

roomcbar50b := fitcbar50b<sub>0</sub>

$$\text{fitcbar50b} = \begin{bmatrix} 4.972 \cdot 10^{10} \\ -3.187 \cdot 10^{-4} \\ 3.048 \cdot 10^{-7} \\ -6.695 \cdot 10^{-10} \end{bmatrix}$$

roomcbar50b =  $4.972 \cdot 10^{10}$

The value for the room temperature stiffened elastic constant for Trial #51 is:

fitcbar51 := genfit(temps, cbar51, guess, Fitfunction)

roomcbar51 := fitcbar51<sub>0</sub>

$$\text{fitcbar51} = \begin{bmatrix} 4.955 \cdot 10^{10} \\ -3.192 \cdot 10^{-4} \\ 3.14 \cdot 10^{-7} \\ -6.719 \cdot 10^{-10} \end{bmatrix}$$

roomcbar51 =  $4.955 \cdot 10^{10}$

The value for the room temperature stiffened elastic constant for Trial #51b is:

$$\begin{aligned} \text{fitcbar51b} &:= \text{genfit}(\text{temps}, \text{cbar51b}, \text{guess}, \text{Fitfunction}) \\ \text{roomcbar51b}_0 &:= \text{fitcbar51b}_0 \end{aligned} \quad \text{fitcbar51b} = \begin{bmatrix} 4.955 \cdot 10^{10} \\ -3.176 \cdot 10^{-4} \\ 2.969 \cdot 10^{-7} \\ -6.153 \cdot 10^{-10} \end{bmatrix} \quad \text{roomcbar51b} = 4.955 \cdot 10^{10}$$

The value for the room temperature stiffened elastic constant for Trial #52 is:

$$\begin{aligned} \text{fitcbar52} &:= \text{genfit}(\text{temps}, \text{cbar52}, \text{guess}, \text{Fitfunction}) \\ \text{roomcbar52}_0 &:= \text{fitcbar52}_0 \end{aligned} \quad \text{fitcbar52} = \begin{bmatrix} 4.987 \cdot 10^{10} \\ -3.127 \cdot 10^{-4} \\ 1.676 \cdot 10^{-7} \\ 4.376 \cdot 10^{-11} \end{bmatrix} \quad \text{roomcbar52} = 4.987 \cdot 10^{10}$$

The value for the room temperature stiffened elastic constant for Trial #52b is:

$$\begin{aligned} \text{fitcbar52b} &:= \text{genfit}(\text{temps}, \text{cbar52b}, \text{guess}, \text{Fitfunction}) \\ \text{roomcbar52b}_0 &:= \text{fitcbar52b}_0 \end{aligned} \quad \text{fitcbar52b} = \begin{bmatrix} 4.987 \cdot 10^{10} \\ -3.14 \cdot 10^{-4} \\ 2.231 \cdot 10^{-7} \\ -2.841 \cdot 10^{-10} \end{bmatrix} \quad \text{roomcbar52b} = 4.987 \cdot 10^{10}$$

The value for the room temperature stiffened elastic constant for Trial #61 is:

$$\begin{aligned} \text{fitcbar61} &:= \text{genfit}(\text{temps}, \text{cbar61}, \text{guess}, \text{Fitfunction}) \\ \text{roomcbar61}_0 &:= \text{fitcbar61}_0 \end{aligned} \quad \text{fitcbar61} = \begin{bmatrix} 6.045 \cdot 10^{10} \\ -7.97 \cdot 10^{-5} \\ -3.168 \cdot 10^{-7} \\ 8.366 \cdot 10^{-10} \end{bmatrix} \quad \text{roomcbar61} = 6.045 \cdot 10^{10}$$

The value for the room temperature stiffened elastic constant for Trial #61b is:

$$\begin{aligned} \text{fitcbar61b} &:= \text{genfit}(\text{temps}, \text{cbar61b}, \text{guess}, \text{Fifunction}) \\ \text{roomcbar61b}_0 &:= \text{fitcbar61b}_0 \end{aligned}$$
$$\text{fitcbar61b} = \begin{bmatrix} 6.045 \cdot 10^{10} \\ -8.601 \cdot 10^{-5} \\ -1.952 \cdot 10^{-7} \\ 2.196 \cdot 10^{-10} \end{bmatrix}$$
$$\text{roomcbar61b} = 6.045 \cdot 10^{10}$$

The value for the room temperature stiffened elastic constant for Trial #62 is:

$$\begin{aligned} \text{fitcbar62} &:= \text{genfit}(\text{temps}, \text{cbar62}, \text{guess}, \text{Fifunction}) \\ \text{roomcbar62}_0 &:= \text{fitcbar62}_0 \end{aligned}$$
$$\text{fitcbar62} = \begin{bmatrix} 6.044 \cdot 10^{10} \\ -8.334 \cdot 10^{-5} \\ -2.542 \cdot 10^{-7} \\ 5.545 \cdot 10^{-10} \end{bmatrix}$$
$$\text{roomcbar62} = 6.044 \cdot 10^{10}$$

The value for the room temperature stiffened elastic constant for Trial #62b is:

$$\begin{aligned} \text{fitcbar62b} &:= \text{genfit}(\text{temps}, \text{cbar62b}, \text{guess}, \text{Fifunction}) \\ \text{roomcbar62b}_0 &:= \text{fitcbar62b}_0 \end{aligned}$$
$$\text{fitcbar62b} = \begin{bmatrix} 6.044 \cdot 10^{10} \\ -8.787 \cdot 10^{-5} \\ -1.698 \cdot 10^{-7} \\ 1.214 \cdot 10^{-10} \end{bmatrix}$$
$$\text{roomcbar62b} = 6.044 \cdot 10^{10}$$

The value for the room temperature stiffened elastic constant for Trial #63 is:

$$\begin{aligned} \text{fitcbar63} &:= \text{genfit}(\text{temps}, \text{cbar63}, \text{guess}, \text{Fifunction}) \\ \text{roomcbar63}_0 &:= \text{fitcbar63}_0 \end{aligned}$$
$$\text{fitcbar63} = \begin{bmatrix} 6.031 \cdot 10^{10} \\ -8.525 \cdot 10^{-5} \\ -1.927 \cdot 10^{-7} \\ 9.679 \cdot 10^{-11} \end{bmatrix}$$
$$\text{roomcbar63} = 6.031 \cdot 10^{10}$$

The value for the room temperature stiffened elastic constant for Trial #63b is:

`fitcbar63b := genfit(temps, cbar63b, guess, Fitfunction)`

`roomcbar63b := fitcbar63b0`

$$\text{fitcbar63b} = \begin{bmatrix} 6.031 \cdot 10^{10} \\ -8.553 \cdot 10^{-5} \\ -1.958 \cdot 10^{-7} \\ 2.144 \cdot 10^{-10} \end{bmatrix}$$

$$\text{roomcbar63b} = 6.031 \cdot 10^{10}$$

The value for the room temperature stiffened elastic constant for Trial #64 is:

`fitcbar64 := genfit(temps, cbar64, guess, Fitfunction)`

`roomcbar64 := fitcbar640`

$$\text{fitcbar64} = \begin{bmatrix} 6.072 \cdot 10^{10} \\ -7.976 \cdot 10^{-5} \\ -3.171 \cdot 10^{-7} \\ 8.374 \cdot 10^{-10} \end{bmatrix}$$

$$\text{roomcbar64} = 6.072 \cdot 10^{10}$$

The value for the room temperature stiffened elastic constant for Trial #64b is:

`fitcbar64b := genfit(temps, cbar64b, guess, Fitfunction)`

`roomcbar64b := fitcbar64b0`

$$\text{fitcbar64b} = \begin{bmatrix} 6.072 \cdot 10^{10} \\ -8.304 \cdot 10^{-5} \\ -2.562 \cdot 10^{-7} \\ 5.199 \cdot 10^{-10} \end{bmatrix}$$

$$\text{roomcbar64b} = 6.072 \cdot 10^{10}$$

Now we can calculate the average room temperature values for stiffness eigenvalues for each crystal orientation:

$$\text{roomcbar0\_OTE} := \text{mean} \left[ \begin{array}{l} \text{roomcbar1} \\ \text{roomcbar2} \\ \text{roomcbar3} \\ \text{roomcbar4} \\ \text{roomcbar1b} \\ \text{roomcbar2b} \end{array} \right]$$

$$\text{roomcbar0\_OLE90} = \text{mean} \left[ \begin{array}{l} \text{roomcbar5} \\ \text{roomcbar6} \\ \text{roomcbar7} \\ \text{roomcbar8} \end{array} \right]$$

$$\text{roomcbar0\_45LE0} := \text{mean} \left[ \begin{array}{l} \text{roomcbar9} \\ \text{roomcbar10} \\ \text{roomcbar11} \\ \text{roomcbar12} \\ \text{roomcbar10b} \end{array} \right]$$

$$\text{roomcbar45\_OTE} := \text{mean} \left[ \begin{array}{l} \text{roomcbar18} \\ \text{roomcbar20a} \\ \text{roomcbar20b} \\ \text{roomcbar18b} \\ \text{roomcbar20c} \\ \text{roomcbar20d} \end{array} \right]$$

$$\text{sd0\_OTE} := \frac{\text{stdev} \left[ \begin{array}{l} \text{roomcbar1} \\ \text{roomcbar2} \\ \text{roomcbar3} \\ \text{roomcbar4} \\ \text{roomcbar1b} \\ \text{roomcbar2b} \end{array} \right] \cdot 100}{\text{roomcbar0\_OTE}}$$

$$\text{sd0\_OLE90} = \frac{\text{stdev} \left[ \begin{array}{l} \text{roomcbar5} \\ \text{roomcbar6} \\ \text{roomcbar7} \\ \text{roomcbar8} \end{array} \right] \cdot 100}{\text{roomcbar0\_OLE90}}$$

$$\text{sd0\_45LE0} := \frac{\text{stdev} \left[ \begin{array}{l} \text{roomcbar9} \\ \text{roomcbar10} \\ \text{roomcbar11} \\ \text{roomcbar12} \\ \text{roomcbar10b} \end{array} \right] \cdot 100}{\text{roomcbar0\_45LE0}}$$

$$\text{sd45\_OTE} := \frac{\text{stdev} \left[ \begin{array}{l} \text{roomcbar18} \\ \text{roomcbar20a} \\ \text{roomcbar20b} \\ \text{roomcbar18b} \\ \text{roomcbar20c} \\ \text{roomcbar20d} \end{array} \right] \cdot 100}{\text{roomcbar45\_OTE}}$$

$$\text{roomcbar45\_OLE90} = \text{mean} \left[ \begin{array}{l} \text{roomcbar21} \\ \text{roomcbar22} \\ \text{roomcbar23} \\ \text{roomcbar24} \\ \text{roomcbar21b} \end{array} \right]$$

$$\text{sd45\_OLE90} := \frac{\text{stdev} \left[ \begin{array}{l} \text{roomcbar21} \\ \text{roomcbar22} \\ \text{roomcbar23} \\ \text{roomcbar24} \\ \text{roomcbar21b} \end{array} \right] \cdot 100}{\text{roomcbar45\_OLE90}}$$

```

roomcbar25
roomcbar26
roomcbar27
roomcbar28
roomcbar25b

```

roomcbar45\_45LE0 := mean

roomcbar0\_90LE90 := mean

```

roomcbar37a
roomcbar37b
roomcbar37c
roomcbar38
roomcbar39
roomcbar40

```

roomcbar0\_28LE0 := mean

```

roomcbar49
roomcbar50
roomcbar51
roomcbar52
roomcbar49b
roomcbar50b
roomcbar51b
roomcbar52b

```

roomcbar45\_56LE0 := mean

```

roomcbar61
roomcbar62
roomcbar63
roomcbar64
roomcbar61b
roomcbar62b
roomcbar63b
roomcbar64b

```

roomcbar45\_56LE0 := mean

```

roomcbar25
roomcbar26
roomcbar27
roomcbar28
roomcbar25b

```

sidev

.100

sd45\_45LE0 := roomcbar45\_45LE0

```

roomcbar37a
roomcbar37b
roomcbar37c
roomcbar38
roomcbar39
roomcbar40

```

sidev

.100

sd0\_90LE90 := roomcbar0\_90LE90

```

roomcbar49
roomcbar50
roomcbar51
roomcbar52
roomcbar49b
roomcbar50b
roomcbar51b
roomcbar52b

```

sidev

.100

sd0\_28LE0 :=

roomcbar0\_28LE0

```

roomcbar61
roomcbar62
roomcbar63
roomcbar64
roomcbar61b
roomcbar62b
roomcbar63b
roomcbar64b

```

sidev

.100

sd45\_56LE0 :=

roomcbar45\_56LE0

Now compare the calculated values of stiffness eigenvalues to those of Kosinski [2]:

Stiffness eigenvalues calculated in this thesis:

In GigaPascals:	Standard Deviations (%):	From Kosinski [2]:	Error (%):
$\text{roomcbar0\_OTE} \cdot 10^{-9} = 59.212$	$\text{sd0\_OTE} = 0.294$	$\text{Kroomcbar0\_OTE} := 59.12$	$\frac{\text{roomcbar0\_OTE} \cdot 10^{-9} - \text{Kroomcbar0\_OTE}}{\text{Kroomcbar0\_OTE}} \cdot 100 = 0.155$
$\text{roomcbar0\_OLE90} \cdot 10^{-9} = 135.952$	$\text{sd0\_OLE90} = 0.228$	$\text{Kroomcbar0\_OLE90} := 135.9$	$\frac{\text{roomcbar0\_OLE90} \cdot 10^{-9} - \text{Kroomcbar0\_OLE90}}{\text{Kroomcbar0\_OLE90}} \cdot 100 = 0.038$
$\text{roomcbar0\_45LE0} \cdot 10^{-9} = 52.455$	$\text{sd0\_45LE0} = 0.23$	$\text{Kroomcbar0\_45LE0} := 52.49$	$\frac{\text{roomcbar0\_45LE0} \cdot 10^{-9} - \text{Kroomcbar0\_45LE0}}{\text{Kroomcbar0\_45LE0}} \cdot 100 = 0.067$
$\text{roomcbar45\_OTE} \cdot 10^{-9} = 58.997$	$\text{sd45\_OTE} = 0.291$	$\text{Kroomcbar45\_OTE} := 58.95$	$\frac{\text{roomcbar45\_OTE} \cdot 10^{-9} - \text{Kroomcbar45\_OTE}}{\text{Kroomcbar45\_OTE}} \cdot 100 = 0.079$
$\text{roomcbar45\_OLE90} \cdot 10^{-9} = 115.535$	$\text{sd45\_OLE90} = 0.278$	$\text{Kroomcbar45\_OLE90} := 115.4$	$\frac{\text{roomcbar45\_OLE90} \cdot 10^{-9} - \text{Kroomcbar45\_OLE90}}{\text{Kroomcbar45\_OLE90}} \cdot 100 = 0.117$
$\text{roomcbar45\_45LE0} \cdot 10^{-9} = 62.612$	$\text{sd45\_45LE0} = 0.296$	$\text{Kroomcbar45\_45LE0} := 62.49$	$\frac{\text{roomcbar45\_45LE0} \cdot 10^{-9} - \text{Kroomcbar45\_45LE0}}{\text{Kroomcbar45\_45LE0}} \cdot 100 = 0.194$
$\text{roomcbar0\_90LE90} \cdot 10^{-9} = 57.042$	$\text{sd0\_90LE90} = 0.369$	$\text{Kroomcbar0\_90LE90} := 57.06$	$\frac{\text{roomcbar0\_90LE90} \cdot 10^{-9} - \text{Kroomcbar0\_90LE90}}{\text{Kroomcbar0\_90LE90}} \cdot 100 = 0.031$
$\text{roomcbar0\_28LE0} \cdot 10^{-9} = 49.757$	$\text{sd0\_28LE0} = 0.27$	$\text{Kroomcbar0\_26LE0} := 49.76$	$\frac{\text{roomcbar0\_28LE0} \cdot 10^{-9} - \text{Kroomcbar0\_26LE0}}{\text{Kroomcbar0\_26LE0}} \cdot 100 = 0.006$
$\text{roomcbar45\_56LE0} \cdot 10^{-9} = 60.48$	$\text{sd45\_56LE0} = 0.245$	$\text{Kroomcbar45\_56LE0} := 60.49$	$\frac{\text{roomcbar45\_56LE0} \cdot 10^{-9} - \text{Kroomcbar45\_56LE0}}{\text{Kroomcbar45\_56LE0}} \cdot 100 = 0.016$



## Linear Least Squares Material Constants Extraction:

Now we have 32 temperature curves for the stiffness eigenvalues of 8 crystal orientation/excitations. The next step is to derive the matrix used to extract the material constants from the various sets of stiffness eigenvalue data.

For each Trial, there is one row in the Linear Least Squares (LLS) matrix (reference Chapter 5):

$$\begin{matrix}
 a0\_OTE := \begin{bmatrix} 0 & 0 & 1 & 0 & 1 \\ 0 & 0 & 1 & 0 & 1 \\ 0 & 0 & 1 & 0 & 1 \\ 0 & 0 & 1 & 0 & 1 \\ 0 & 0 & 1 & 0 & 1 \\ 0 & 0 & 1 & 0 & 1 \end{bmatrix} &
 a0\_OLE90 := \begin{bmatrix} 1 & 0 & 0 & 0 & 0 \\ 1 & 0 & 0 & 0 & 0 \\ 1 & 0 & 0 & 0 & 0 \\ 1 & 0 & 0 & 0 & 0 \end{bmatrix} &
 a0\_45LE0 := \begin{bmatrix} 0 & 0 & .5 & .5 & 0 \\ 0 & 0 & .5 & .5 & 0 \\ 0 & 0 & .5 & .5 & 0 \\ 0 & 0 & .5 & .5 & 0 \end{bmatrix} &
 a45\_OTE := \begin{bmatrix} 0 & 0 & 1 & 0 & 1 \\ 0 & 0 & 1 & 0 & 1 \\ 0 & 0 & 1 & 0 & 1 \\ 0 & 0 & 1 & 0 & 1 \\ 0 & 0 & 1 & 0 & 1 \\ 0 & 0 & 1 & 0 & 1 \end{bmatrix} &
 a45\_OLE90 := \begin{bmatrix} .5 & .5 & 0 & 1 & 0 \\ .5 & .5 & 0 & 1 & 0 \\ .5 & .5 & 0 & 1 & 0 \\ .5 & .5 & 0 & 1 & 0 \\ .5 & .5 & 0 & 1 & 0 \\ .5 & .5 & 0 & 1 & 0 \end{bmatrix}
 \end{matrix}$$

$$\begin{matrix}
 a45\_45LE0 := \begin{bmatrix} .25 & -.25 & .5 & 0 & 0 \\ .25 & -.25 & .5 & 0 & 0 \\ .25 & -.25 & .5 & 0 & 0 \\ .25 & -.25 & .5 & 0 & 0 \end{bmatrix} &
 a0\_90LE90 := \begin{bmatrix} 0 & 0 & 1 & 0 & 0 \\ 0 & 0 & 1 & 0 & 0 \\ 0 & 0 & 1 & 0 & 0 \\ 0 & 0 & 1 & 0 & 0 \end{bmatrix} &
 a0\_28LE0 := \begin{bmatrix} 0 & 0 & .22330423 & .77669577 & 0 \\ 0 & 0 & .22330423 & .77669577 & 0 \\ 0 & 0 & .22330423 & .77669577 & 0 \\ 0 & 0 & .22330423 & .77669577 & 0 \end{bmatrix} &
 a45\_56LE0 := \begin{bmatrix} .1555398 & -.1555398 & .6889204 & 0 & 0 \\ .1555398 & -.1555398 & .6889204 & 0 & 0 \\ .1555398 & -.1555398 & .6889204 & 0 & 0 \\ .1555398 & -.1555398 & .6889204 & 0 & 0 \\ .1555398 & -.1555398 & .6889204 & 0 & 0 \\ .1555398 & -.1555398 & .6889204 & 0 & 0 \end{bmatrix}
 \end{matrix}$$

$$\begin{matrix}
 Tempa1 := stack(a0\_OTE, a0\_OLE90) & Tempa2 = stack(Tempa1, a0\_45LE0) & Tempa3 := stack(Tempa2, a45\_OTE) & Tempa4 := stack(Tempa3, a45\_OLE90) \\
 Tempa5 := stack(Tempa4, a45_45LE0) & Tempa6 = stack(Tempa5, a0_90LE90) & Tempa7 := stack(Tempa6, a0_28LE0) &
 \end{matrix}$$

$$a := stack(Tempa7, a45_56LE0)$$

Our linear least squares extraction matrix (LLS) is:

$$LLS := (a^T \cdot a)^{-1} \cdot a^T$$

Now a matrix is formed that contains the values for the stiffness eigenvalues for each Trial at each temperature point:

```

TempMatrix1 := augment(cbar1, cbar1b)
TempMatrix2 := augment(TempMatrix1, cbar2)
TempMatrix3 := augment(TempMatrix2, cbar2b)
TempMatrix4 := augment(TempMatrix3, cbar3)
TempMatrix5 := augment(TempMatrix4, cbar4)
TempMatrix6 := augment(TempMatrix5, cbar5)
TempMatrix7 := augment(TempMatrix6, cbar6)
TempMatrix8 := augment(TempMatrix7, cbar7)
TempMatrix9 := augment(TempMatrix8, cbar8)
TempMatrix10 := augment(TempMatrix9, cbar9)
TempMatrix11 := augment(TempMatrix10, cbar10)
TempMatrix12 := augment(TempMatrix11, cbar10b)
TempMatrix13 := augment(TempMatrix12, cbar11)
TempMatrix14 := augment(TempMatrix13, cbar12)
TempMatrix15 := augment(TempMatrix14, cbar18)
TempMatrix16 := augment(TempMatrix15, cbar18b)
TempMatrix17 := augment(TempMatrix16, cbar20a)
TempMatrix18 := augment(TempMatrix17, cbar20b)
TempMatrix19 := augment(TempMatrix18, cbar20c)
TempMatrix20 := augment(TempMatrix19, cbar20d)
TempMatrix21 := augment(TempMatrix20, cbar21)
TempMatrix22 := augment(TempMatrix21, cbar21b)
TempMatrix23 := augment(TempMatrix22, cbar22)
TempMatrix24 := augment(TempMatrix23, cbar23)
TempMatrix25 := augment(TempMatrix24, cbar24)
TempMatrix26 := augment(TempMatrix25, cbar25)
TempMatrix27 := augment(TempMatrix26, cbar25b)
TempMatrix28 := augment(TempMatrix27, cbar26)
TempMatrix29 := augment(TempMatrix28, cbar27)
TempMatrix30 := augment(TempMatrix29, cbar27b)
TempMatrix31 := augment(TempMatrix30, cbar37a)
TempMatrix32 := augment(TempMatrix31, cbar37b)
TempMatrix33 := augment(TempMatrix32, cbar37c)
TempMatrix34 := augment(TempMatrix33, cbar38)
TempMatrix35 := augment(TempMatrix34, cbar39)
TempMatrix36 := augment(TempMatrix35, cbar40)
TempMatrix37 := augment(TempMatrix36, cbar49)
TempMatrix38 := augment(TempMatrix37, cbar49b)
TempMatrix39 := augment(TempMatrix38, cbar50b)
TempMatrix40 := augment(TempMatrix39, cbar52)
TempMatrix41 := augment(TempMatrix40, cbar51)
TempMatrix42 := augment(TempMatrix41, cbar51b)
TempMatrix43 := augment(TempMatrix42, cbar52)
TempMatrix44 := augment(TempMatrix43, cbar52b)
TempMatrix45 := augment(TempMatrix44, cbar61)
TempMatrix46 := augment(TempMatrix45, cbar61b)
TempMatrix47 := augment(TempMatrix46, cbar62)
TempMatrix48 := augment(TempMatrix47, cbar62b)
TempMatrix49 := augment(TempMatrix48, cbar63)
TempMatrix50 := augment(TempMatrix49, cbar63b)
TempMatrix51 := augment(TempMatrix50, cbar64)
TempMatrix52 := augment(TempMatrix51, cbar64b)

```

Matrix := TempMatrix52<sup>T</sup> "Matrix" is an 53 by 14 matrix of stiffness eigenvalue data from all 53 Trials.

Perform the linear least squares matrix operation:

$$\text{Cnsts} \leftarrow \text{LLS}(\text{Matrix})$$

Yielding a matrix of the material constants in which Row 1 is  $c^{E_{11}}$  (GPa) at the 14 temperature points (20C, 30C, ..., 150C), row 2 is  $c^{E_{12}}$ , row 3 is  $c^{E_{44}}$ , row 4 is  $c^{E_{66}}$ , and row 5 is  $e^{-15/\varepsilon_{11}}$ :

$1.36 \cdot 10^{11}$	$1.36 \cdot 10^{11}$	$1.36 \cdot 10^{11}$	$1.36 \cdot 10^{11}$	$1.35 \cdot 10^{11}$	$1.35 \cdot 10^{11}$	$1.35 \cdot 10^{11}$	$1.35 \cdot 10^{11}$	$1.35 \cdot 10^{11}$	$1.35 \cdot 10^{11}$	$1.35 \cdot 10^{11}$	$1.35 \cdot 10^{11}$	$1.35 \cdot 10^{11}$	$1.35 \cdot 10^{11}$	$1.35 \cdot 10^{11}$	$1.35 \cdot 10^{11}$	$1.35 \cdot 10^{11}$	$1.35 \cdot 10^{11}$	$1.35 \cdot 10^{11}$	$1.35 \cdot 10^{11}$
$-3.86 \cdot 10^8$	$-1.92 \cdot 10^8$	$-4.4 \cdot 10^6$	$1.77 \cdot 10^8$	$3.54 \cdot 10^8$	$5.25 \cdot 10^8$	$6.92 \cdot 10^8$	$8.56 \cdot 10^8$	$1.02 \cdot 10^9$	$1.17 \cdot 10^9$	$1.33 \cdot 10^9$	$1.48 \cdot 10^9$	$1.63 \cdot 10^9$	$1.78 \cdot 10^9$	$1.93 \cdot 10^9$	$2.08 \cdot 10^9$	$2.23 \cdot 10^9$	$2.38 \cdot 10^9$	$2.53 \cdot 10^9$	$2.68 \cdot 10^9$
$5.71 \cdot 10^{10}$	$5.71 \cdot 10^{10}$	$5.7 \cdot 10^{10}$	$5.7 \cdot 10^{10}$	$5.7 \cdot 10^{10}$	$5.7 \cdot 10^{10}$	$5.7 \cdot 10^{10}$	$5.69 \cdot 10^{10}$	$5.69 \cdot 10^{10}$	$5.69 \cdot 10^{10}$	$5.68 \cdot 10^{10}$	$5.68 \cdot 10^{10}$	$5.67 \cdot 10^{10}$	$5.67 \cdot 10^{10}$	$5.67 \cdot 10^{10}$	$5.67 \cdot 10^{10}$	$5.67 \cdot 10^{10}$	$5.67 \cdot 10^{10}$	$5.67 \cdot 10^{10}$	$5.67 \cdot 10^{10}$
$4.78 \cdot 10^{10}$	$4.76 \cdot 10^{10}$	$4.74 \cdot 10^{10}$	$4.72 \cdot 10^{10}$	$4.7 \cdot 10^{10}$	$4.68 \cdot 10^{10}$	$4.67 \cdot 10^{10}$	$4.65 \cdot 10^{10}$	$4.63 \cdot 10^{10}$	$4.61 \cdot 10^{10}$	$4.6 \cdot 10^{10}$	$4.58 \cdot 10^{10}$	$4.56 \cdot 10^{10}$	$4.55 \cdot 10^{10}$	$4.54 \cdot 10^{10}$	$4.53 \cdot 10^{10}$	$4.52 \cdot 10^{10}$	$4.51 \cdot 10^{10}$	$4.5 \cdot 10^{10}$	$4.5 \cdot 10^{10}$
$2.08 \cdot 10^9$	$2.02 \cdot 10^9$	$1.97 \cdot 10^9$	$1.92 \cdot 10^9$	$1.87 \cdot 10^9$	$1.83 \cdot 10^9$	$1.79 \cdot 10^9$	$1.75 \cdot 10^9$	$1.71 \cdot 10^9$	$1.67 \cdot 10^9$	$1.64 \cdot 10^9$	$1.6 \cdot 10^9$	$1.57 \cdot 10^9$	$1.53 \cdot 10^9$	$1.5 \cdot 10^9$	$1.47 \cdot 10^9$	$1.44 \cdot 10^9$	$1.41 \cdot 10^9$	$1.38 \cdot 10^9$	$1.35 \cdot 10^9$

The error (v) associated with the stiffened elastic constant calculations is calculated as follows:

$$\text{ErrorMatrix} := a \cdot \begin{pmatrix} T \\ a \end{pmatrix}^{-1} \cdot a^T - \text{identity}(53) \quad i := 0..31$$

$$\text{Error} \leftarrow \text{ErrorMatrix} \cdot \text{Matrix} \leftarrow \left| \frac{\text{Error}}{\text{Matrix}} \cdot 100 \right| \quad \text{PercentError} :=$$

$$\text{MaximumError} := \max(\text{PercentError})$$

The maximum percent error of the calculated stiffened eigenvalues: MaximumError = 0.687

In order to calculate  $e_{15}$  from the fifth row data in the  $Cnsts$  matrix, it is necessary to perform addition operations:

$$\text{square\_e15overe} := (Cnsts^T)^{<4>} \quad \text{square\_e15}_j := \text{square\_e15overe}_j \cdot eS11_j$$

So the material constants over the temperature range are:

$$c11 := (Cnsts^T)^{<0>} \quad c12 := (Cnsts^T)^{<1>} \quad c44 := (Cnsts^T)^{<2>} \quad c66 := (Cnsts^T)^{<3>} \quad e15 := \sqrt{\text{square\_e15}}$$

All that remains is to calculate the temperature coefficients of the material constants.

## The Temperature Coefficients of the Material Constants of Dilithium Tetraborate:

The temperature coefficients of  $c_{11}^E$ :

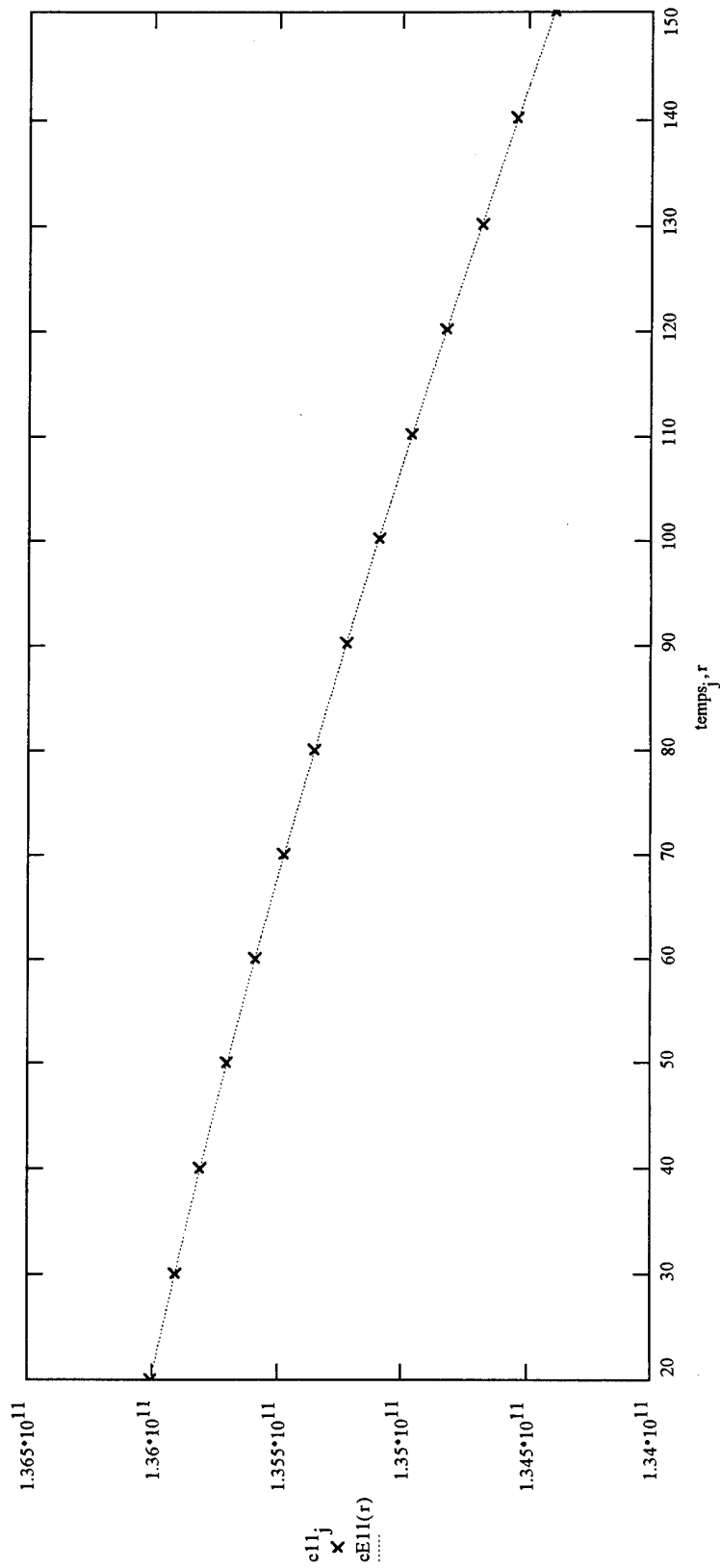
```
fitc11 := genfit(temp, c11, guess, Fitfunction)
```

$$\text{fitc11} = \begin{bmatrix} 1.36 \cdot 10^{11} \\ -7.126 \cdot 10^{-5} \\ -1.931 \cdot 10^{-7} \\ 2.138 \cdot 10^{-10} \end{bmatrix}$$

```
roomc11 := fitc11_0
```

$$\text{roomc11} = 1.35955 \cdot 10^{11}$$

```
r := 20, 20.1 .. 150   cE11(r) := Fitfunction(r, fitc11)_0
```



The standard deviation for the  $c_{11}^E$  power series fit and corresponding Chauvenet's criteria:

$$N := 14 \quad i := 0..N-1$$

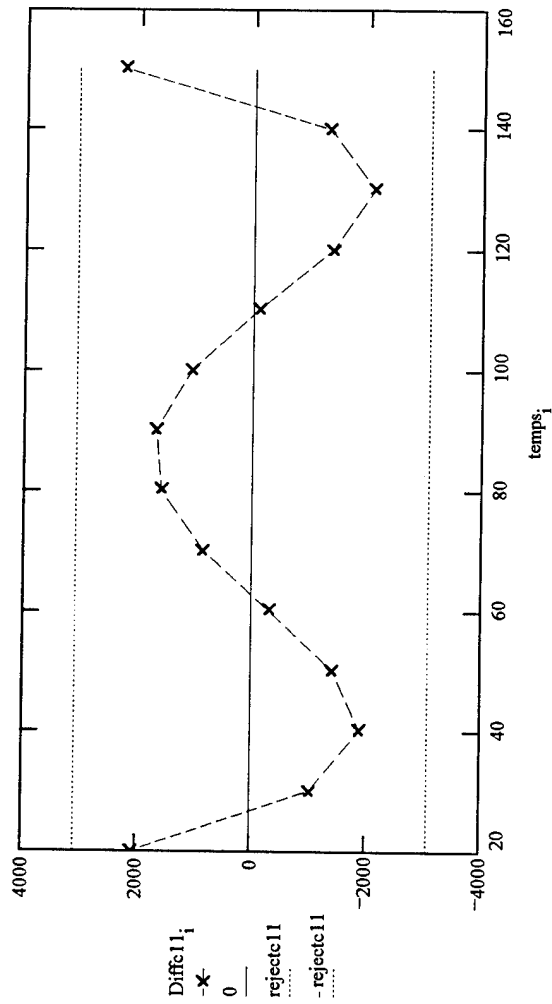
$$\text{Powfitc11}_i := \text{fitc11}_0 \cdot [1 + \text{fitc11}_1 \cdot (\text{temps}_i - 25) + \text{fitc11}_2 \cdot (\text{temps}_i - 25)^2 + \text{fitc11}_3 \cdot (\text{temps}_i - 25)^3]$$

$$\text{Diffc11}_i := (\text{Powfitc11}_i - c11_i)$$

$$\text{standevc11} := \frac{1}{N-1} \cdot \sum_i \sqrt{(\text{Diffc11}_i)^2}$$

$$\text{standevc11} = 1467.5709$$

$$\text{rejectc11} := 2.1 \cdot \text{standevc11}$$



The temperature coefficients of  $cE_{12}$ :

`fitc12 := genfit(temps, c12, guess, Fitfunction)`

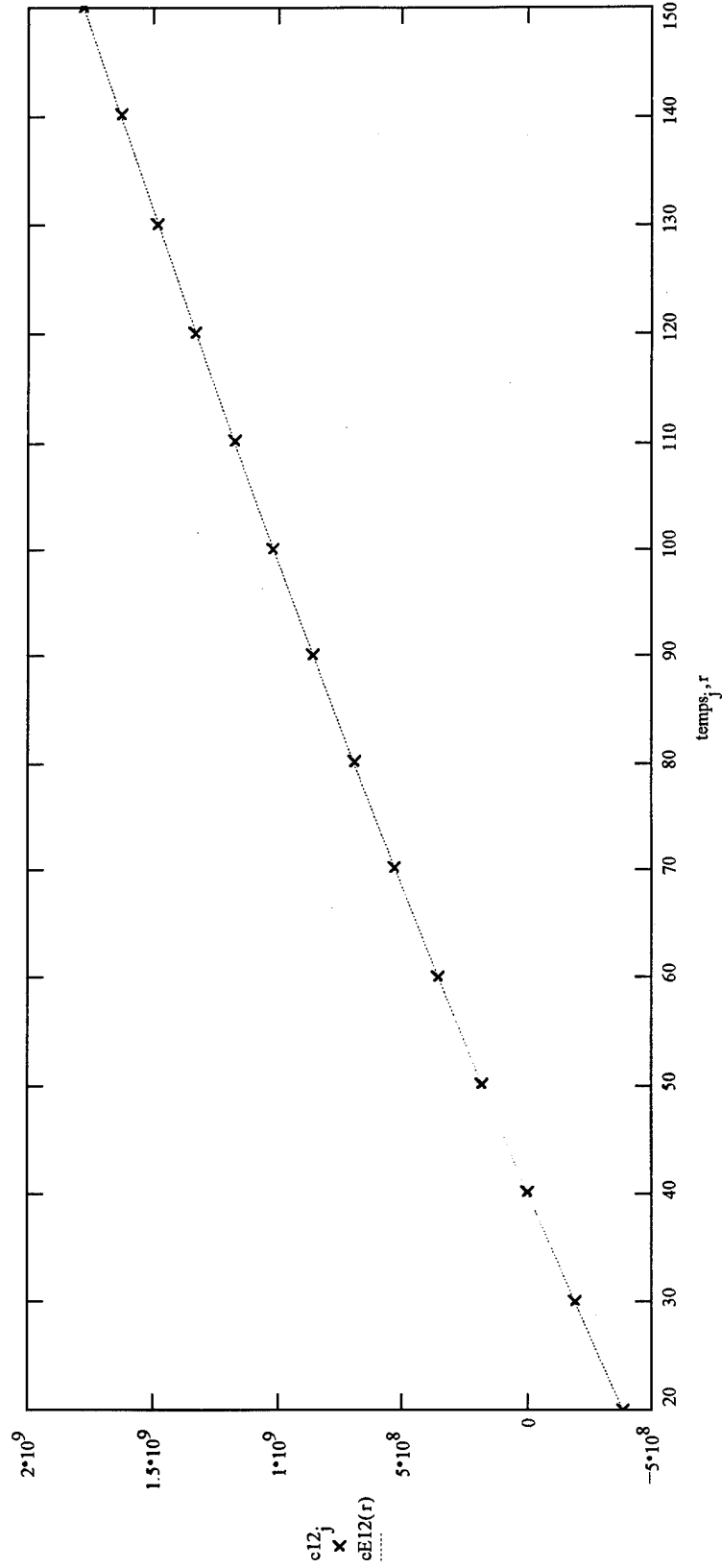
`roomc12 := fitc12_0`

`fitc12 =`

$-2.884 \cdot 10^8$
$-0.06731$
$1.14939 \cdot 10^{-4}$
$-2.82568 \cdot 10^{-7}$

`roomc12 =  $-2.884 \cdot 10^8$`

`cE12(r) := Fitfunction(r, fitc12)_0`



The standard deviation for the  $c_{12}^E$  power series fit and corresponding Chauvenet's criteria:

$$N := 14 \quad i := 0..N - 1$$

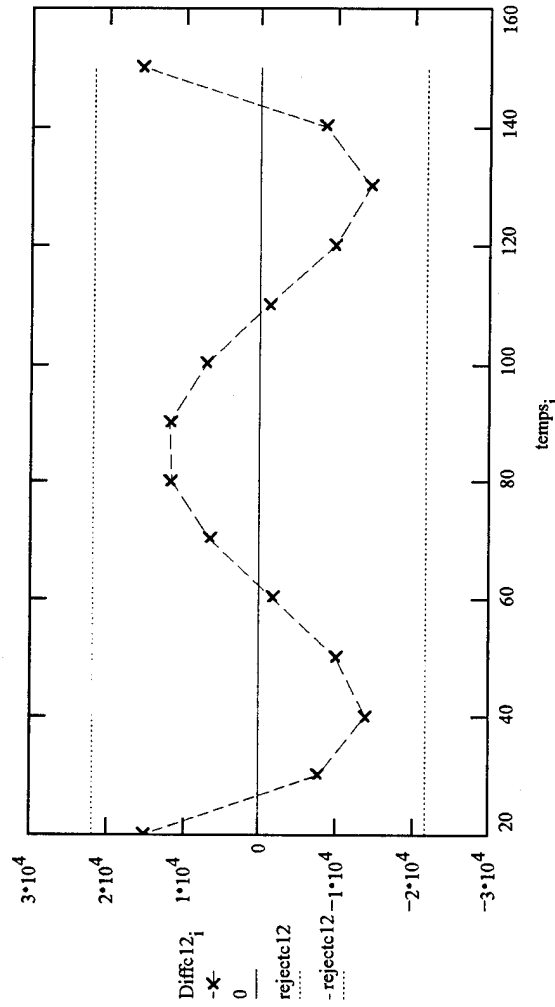
$$\text{Powfitc12}_i := \text{fitc12}_0 \cdot [1 + \text{fitc12}_1 \cdot (\text{temps}_i - 25) + \text{fitc12}_2 \cdot (\text{temps}_i - 25)^2 + \text{fitc12}_3 \cdot (\text{temps}_i - 25)^3]$$

$$\text{Diffc12}_i := (\text{Powfitc12}_i - c12_i)$$

$$\text{standevc12} := \frac{1}{N - 1} \cdot \sum_i \sqrt{(\text{Diffc12}_i)^2}$$

$$\text{standevc12} = 10380.02972$$

$$\text{rejectc12} := 2.1 \cdot \text{standevc12}$$





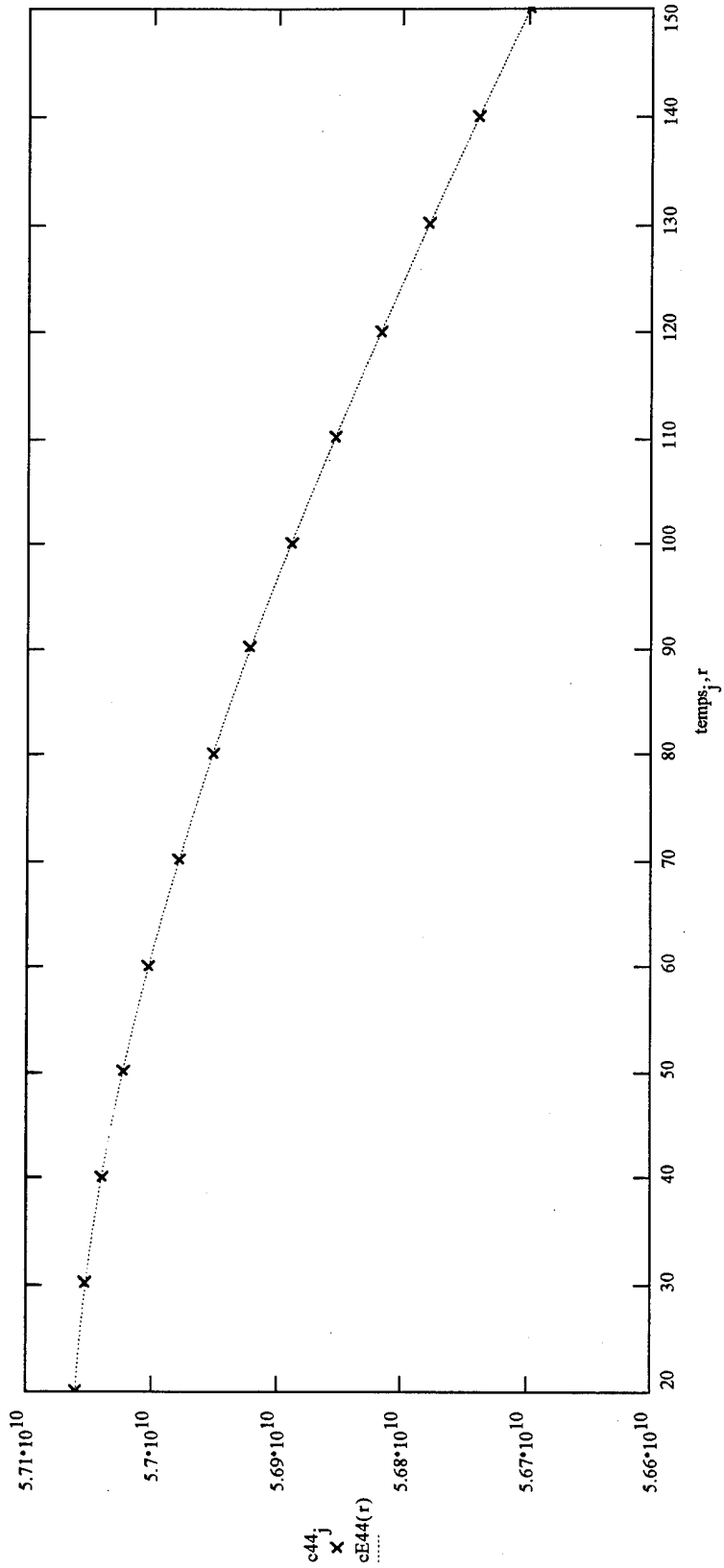
The temperature coefficients of  $cE_{44}$ :

```

fitc44 := genfit(temp, c44, guess, Fitfunction)
roomc44 := fitc44_0
fitc44 = [ 5.706·1010
          -1.453·10-5
          -3.981·10-7
          8.931·10-10 ]
roomc44 = 5.7057·1010

```

$r = 20, 20.1 \dots 150$      $cE44(r) := \text{Fitfunction}(r, \text{fitc44})_0$



The standard deviation for the  $c_{44}^E$  power series fit and corresponding Chauvenet's criteria:

$$N := 14 \quad i := 0..N - 1$$

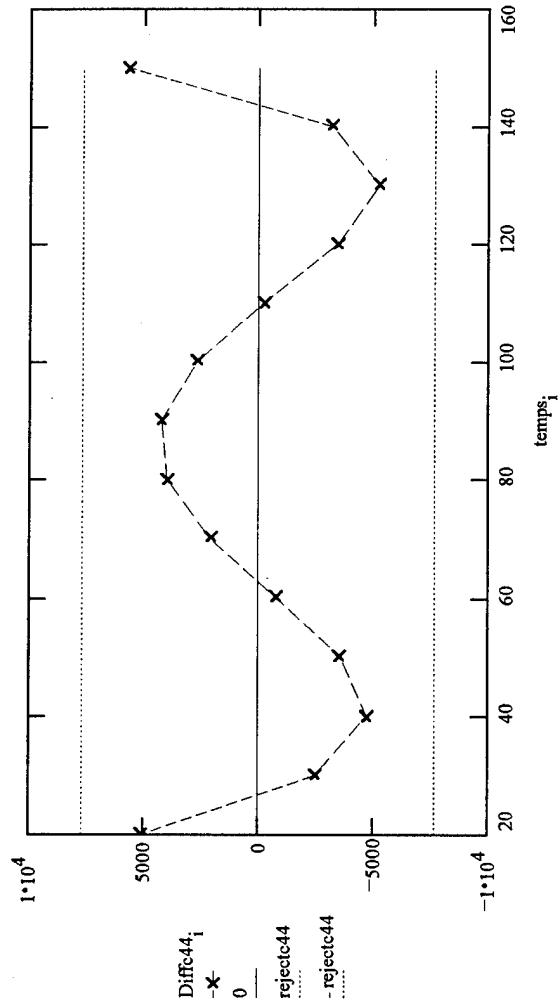
$$\text{Powfitc44}_i := \text{fitc44}_0 \cdot [1 + \text{fitc44}_1 \cdot (\text{temps}_i - 25) + \text{fitc44}_2 \cdot (\text{temps}_i - 25)^2 + \text{fitc44}_3 \cdot (\text{temps}_i - 25)^3]$$

$$\text{Diffc44}_i := (\text{Powfitc44}_i - c44_i)$$

$$\text{standevc44} := \frac{1}{N - 1} \cdot \sum_i \sqrt{(\text{Diffc44}_i)^2}$$

$$\text{standevc44} = 3652.42955$$

$$\text{rejectc44} := 2.1 \cdot \text{standevc44}$$



The temperature coefficients of  $cE_{66}$ :

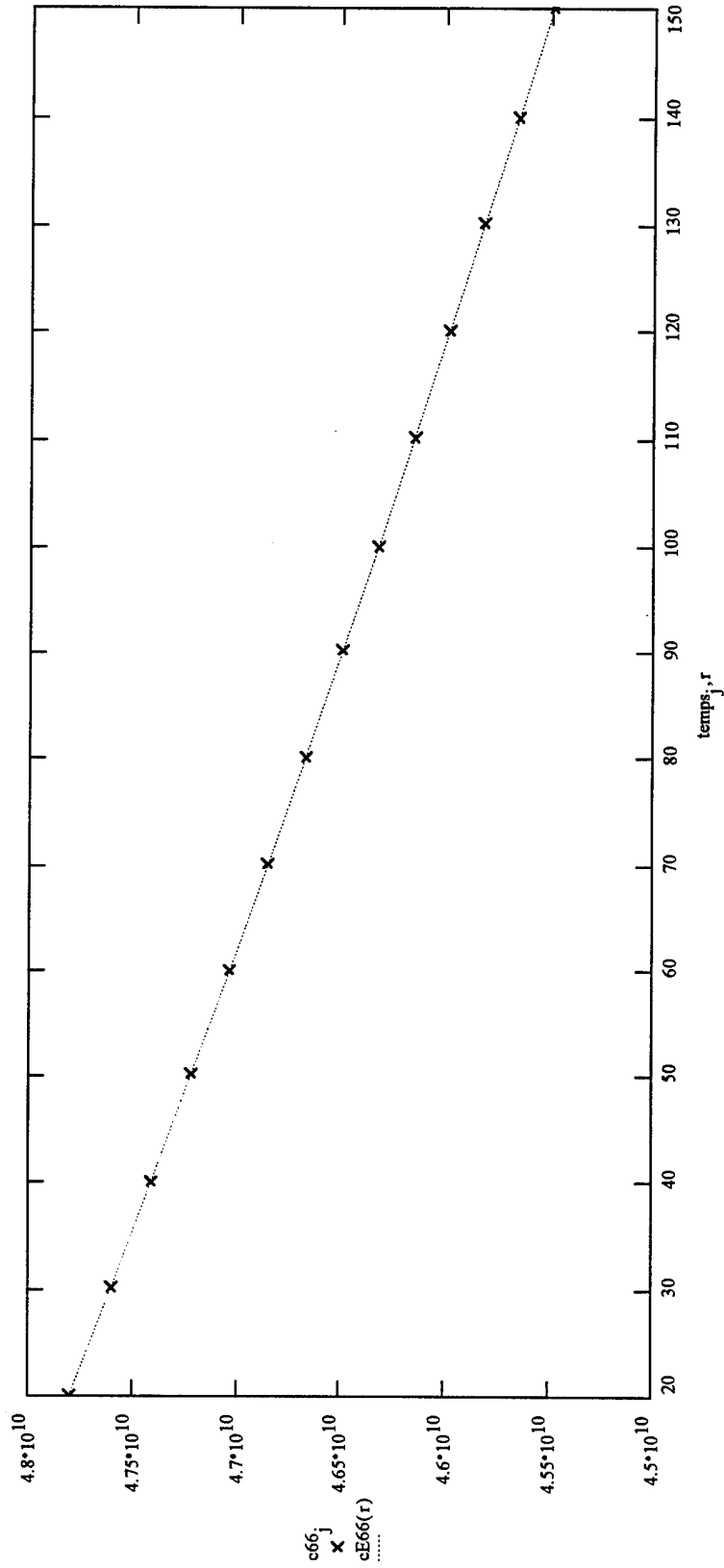
`fitc66 := genfit(temp6, c66, guess, Fitfunction)`

`roomc66 := fitc66_0`

`fitc66 =` 
$$\begin{bmatrix} 4.77 \cdot 10^{10} \\ -4.186 \cdot 10^{-4} \\ 5.044 \cdot 10^{-7} \\ -1.016 \cdot 10^{-9} \end{bmatrix}$$

`roomc66 =  $4.76998 \cdot 10^{10}$`

`cE66(r) := Fitfunction(r, fitc66)_0`



The standard deviation for the  $cE_{66}$  power series fit and corresponding Chauvenet's criteria:

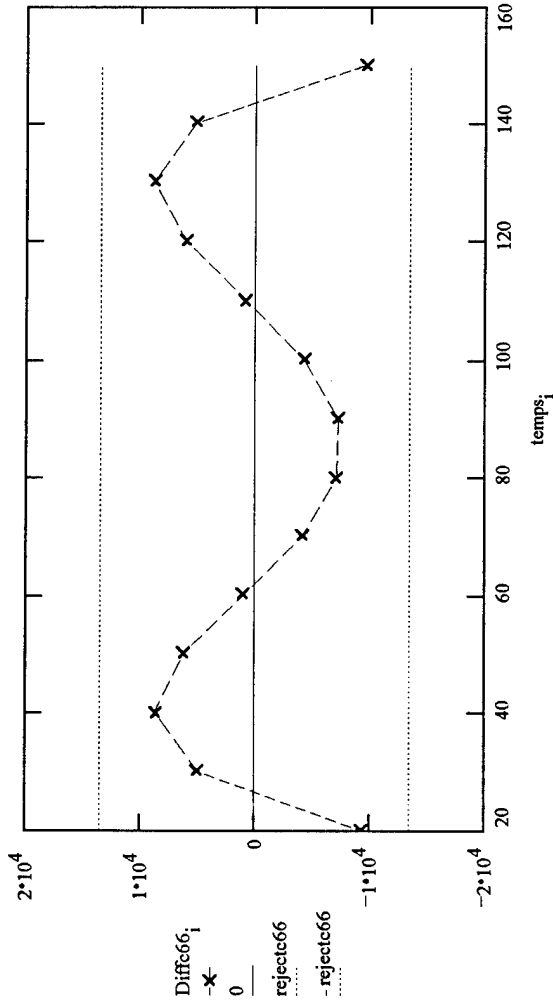
$$N := 14 \quad i := 0..N-1$$

$$\text{Powfitc66}_i := \text{fitc66}_0 \cdot [1 + \text{fitc66}_1 \cdot (\text{temps}_i - 25) + \text{fitc66}_2 \cdot (\text{temps}_i - 25)^2 + \text{fitc66}_3 \cdot (\text{temps}_i - 25)^3]$$

$$\text{Diffc66}_i := (\text{Powfitc66}_i - c66_i)$$

$$\text{standevc66} := \frac{1}{N-1} \cdot \sum_i \sqrt{(\text{Diffc66}_i)^2}$$

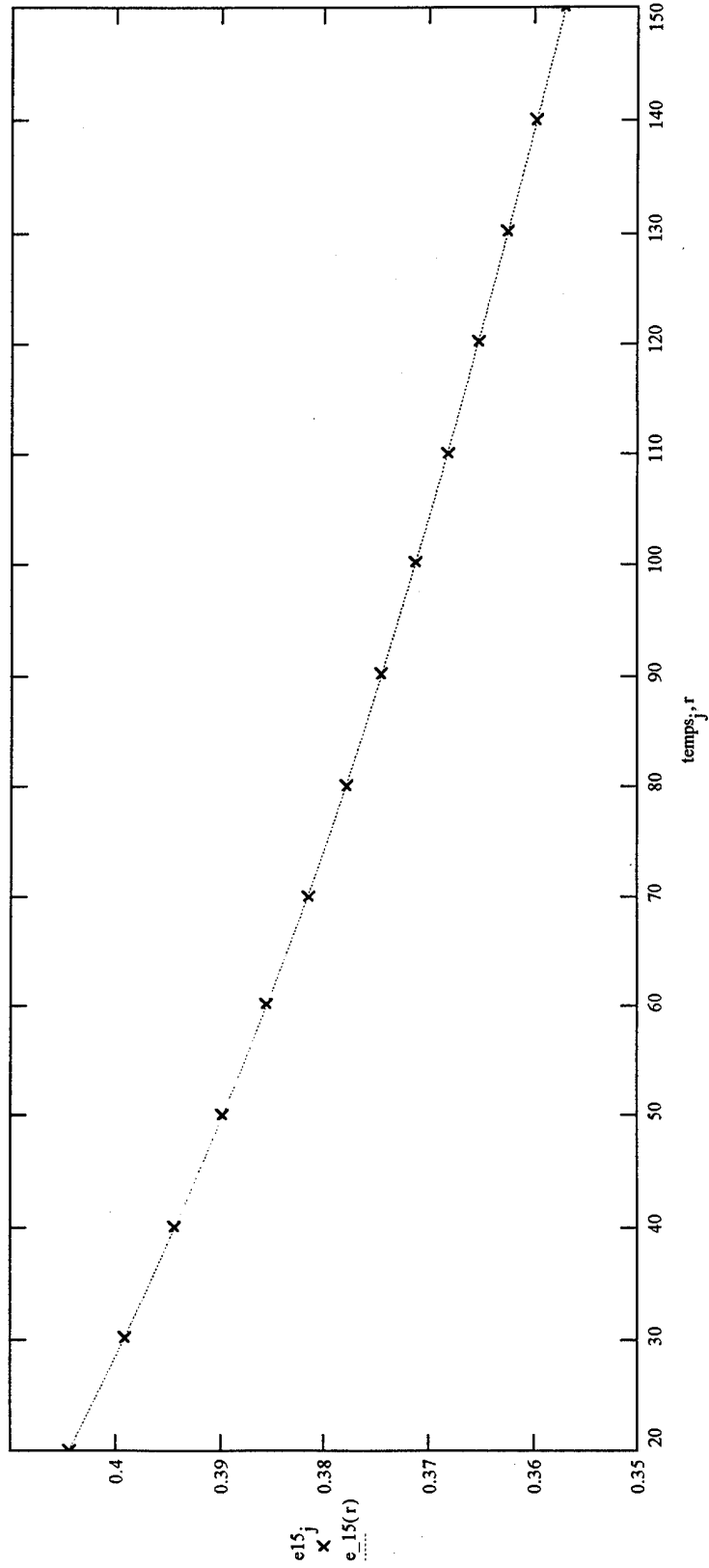
$$\text{standevc66} = 6423.57895 \quad \text{rejectc66} := 2.1 \cdot \text{standevc66}$$



The temperature coefficients of  $e_{15}$ :

```
fit15 := genfit(temps, e15, guess, Fitfunction)
room15 := fit15_0
room15 = 0.401668
-0.00132
5.162702·10-6
-1.390147·10-8
```

$e_{15}(r) := \text{Fitfunction}(r, \text{fit15})_0$



The standard deviation for the  $e_{15}$  power series fit and corresponding Chauvenet's criteria:

$$N := 14 \quad i := 0..N - 1$$

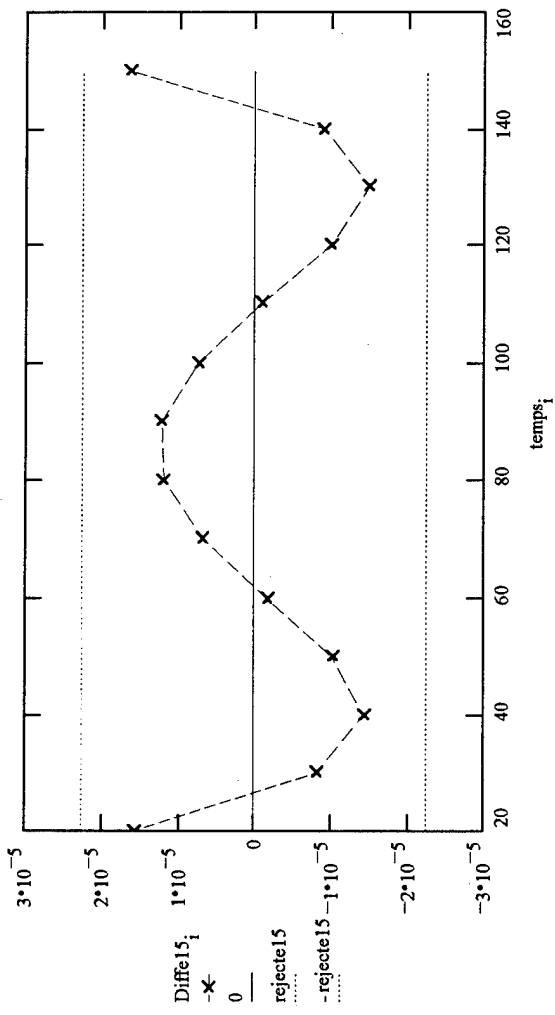
$$\text{Powfite15}_i := \text{fite15}_0 \cdot [1 + \text{fite15}_1 \cdot (\text{temps}_i - 25) + \text{fite15}_2 \cdot (\text{temps}_i - 25)^2 + \text{fite15}_3 \cdot (\text{temps}_i - 25)^3]$$

$$\text{Diffe15}_i := (\text{Powfite15}_i - e_{15}_i)$$

$$\text{standeve15} := \frac{1}{N - 1} \cdot \sum_i \sqrt{(\text{Diffe15}_i)^2}$$

$$\text{standeve15} = 0.00001$$

$$\text{rejecte15} := 2.1 \cdot \text{standeve15}$$



# Prediction of Measured Antiresonant Frequencies Using Calculated Temperature Coefficients of Selected Material Constants:

For Trial #1, crystal #1, (YXw)0,0 TE:

$$th0\_0(temp) := 206.6 \cdot 10^{-6} \cdot (1 + \alpha0\_0 \cdot temp + \alpha0\_0 \cdot temp^2)$$

$$es11(temp) := es110 \cdot (1 + es111 \cdot temp + es112 \cdot temp^2)$$

$$\rho\_1(temp) := 2436 \cdot (1 + \rho\_1 \cdot temp + \rho\_2 \cdot temp^2)$$

Using the eigenvalue expression for (YXw)0,0 TE and Equation (2.4) to find the antiresonant frequencies:

$$fA0\_1\_j := \frac{1}{2 \cdot th0\_0(temp1\_j)} \cdot \sqrt{\frac{cE44(temp1\_j) + \frac{e\_15(temp1\_j)^2}{es11(temp1\_j)}}{\rho\_1(temp1\_j)}}$$

Measured Data:

22.0	11.796
30.7	11.790
40.3	11.784
49.7	11.778
59.2	11.771
68.7	11.765
78.3	11.758
87.6	11.751
101.0	11.742
110.3	11.735
120.1	11.728
129.6	11.721
140.9	11.713
150.5	11.705

temps1 :=

freqs1 :=

The percent error in the prediction of the antiresonant frequencies of Trial #1 crystal #1 (YXw)0,0 TE is:

1.065
1.066
1.061
1.056
1.06
1.054
1.056
1.059
1.053
1.054
1.052
1.051
1.047
1.053

$$errorfA0\_1\_j := \frac{fA0\_1\_j \cdot 10^{-6} - freqs1\_j}{freqs1\_j} \cdot 100$$

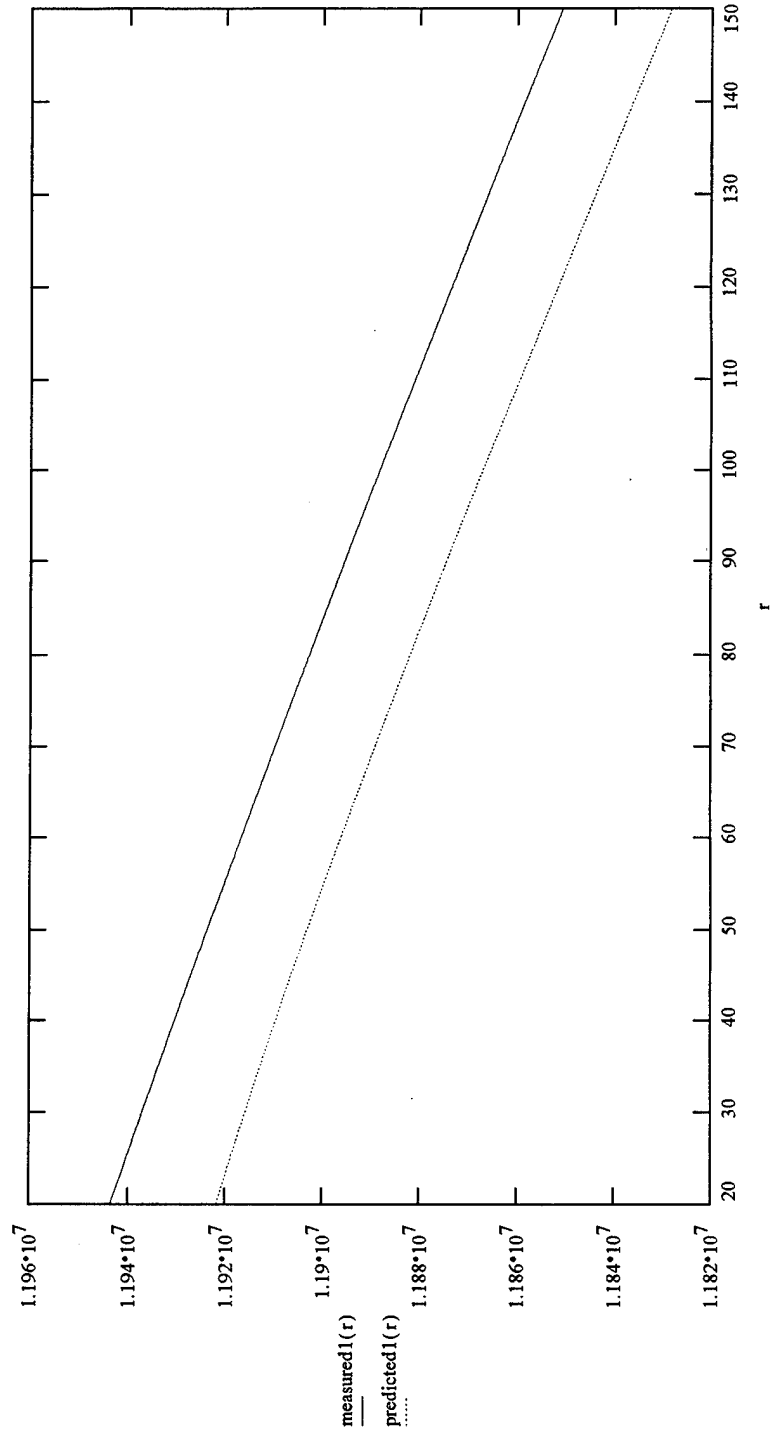
errorfA0\_1 =

The following is a plot of the measured frequency curve and the predicted frequency curve for Trial #1, crystal #1:

```

meas1 := [
  11.94·106
  Coef1 1·10-6
  Coef1 2·10-9
  Coef1 3·10-12
]
measured1(r) := Fitfunction(r, meas1)_0
pred1 := genfit(temps, fA0_1, guess, Fitfunction)
pred1 = [
  1.191858·107
  -5.015282·10-5
  -1.351724·10-7
  4.086448·10-10
]
predicted1(r) := Fitfunction(r, pred1)_0

```





Measured Data:

28.5
33.6
43.2
51.7
61.4
70.9
80.5
90.0
100.5
110.1
120.7
130.2
139.8
150.2

11.792
11.788
11.782
11.776
11.770
11.763
11.756
11.750
11.742
11.735
11.728
11.721
11.713
11.706

$$th0\_0(temp) := 206.6 \cdot 10^{-6} \cdot (1 + \alpha0\_0 \cdot temp + \alpha0\_0^2 \cdot temp^2)$$

$$es11(temp) := es110 \cdot (1 + es111 \cdot temp + es112 \cdot temp^2)$$

$$\rho\_1(temp) := 2436 \cdot (1 + \rho\_1 \cdot temp + \rho\_2 \cdot temp^2)$$

temps1b :=

freqs1b :=

The percent error in the prediction of the antiresonant frequencies of Trial #1b crystal #1 (YXw)0,0 TE is:

Using the eigenvalue expression for (YXw)0,0 TE and Equation (2.4) to find the antiresonant frequencies:

$$fA0\_1b\_j := \frac{1}{2 \cdot th0\_0(temp1b\_j)} \sqrt{\frac{cE44(temp1b\_j) + \frac{e\_15(temp1b\_j)^2}{es11(temp1b\_j)}}{\rho\_1(temp1b\_j)}}$$

$$errorfA0\_1b\_j := \frac{fA0\_1b\_j \cdot 10^{-6} - freqs1b\_j}{freqs1b\_j} \cdot 100 \quad errorfA0\_1b =$$

1.062
1.066
1.061
1.062
1.055
1.058
1.059
1.052
1.056
1.056
1.048
1.048
1.054
1.047

For Trial #2, crystal #2, (YXw)0,0 TE:

$$th0\_0(temp) := 206.6 \cdot 10^{-6} \cdot (1 + \alpha0\_0 \cdot 1 \cdot temp + \alpha0\_0 \cdot 2 \cdot temp^2)$$

$$es11(temp) := \epsilon S110 \cdot (1 + \epsilon S111 \cdot temp + \epsilon S112 \cdot temp^2)$$

$$\rho\_2(temp) := 2453.2 \cdot (1 + \rho \_1 \cdot temp + \rho \_2 \cdot temp^2)$$

Using the eigenvalue expression for (YXw)0,0 TE and Equation (2.4) to find the antiresonant frequencies:

$$fA0\_2_j = \frac{1}{2 \cdot th0\_0(temp2_j)} \sqrt{\frac{cE44(temp2_j) + \frac{e\_15(temp2_j)^2}{\epsilon S11(temp2_j)}}{\rho\_2(temp2_j)}}$$

Measured Data:

22.0	11.761
30.7	11.755
40.3	11.748
49.7	11.742
59.2	11.736
68.7	11.729
78.3	11.723
87.6	11.716
101.0	11.707
110.3	11.700
120.1	11.693
129.6	11.686
140.9	11.677
150.5	11.670

temps2 :=

freqs2 :=

The percent error in the prediction of the antiresonant frequencies of Trial #2 crystal #2 (YXw)0,0 TE is:

1.01
1.011
1.014
1.01
1.005
1.008
1.001
1.005
0.999
1.001
0.999
0.998
1.003
1

$$errorfA0\_2_j := \frac{fA0\_2_j \cdot 10^{-6} - freqs2_j}{freqs2_j} \cdot 100$$

errorfA0\_2 =

For Trial #2b, crystal #2, (YXw)0,0 TE:

$$th0\_0(temp) := 206.6 \cdot 10^{-6} \cdot (1 + \alpha0\_0 \cdot 1 \cdot temp + \alpha0\_0 \cdot 2 \cdot temp^2)$$

$$es11(temp) := sS110 \cdot (1 + sS111 \cdot temp + sS112 \cdot temp^2)$$

$$\rho\_2(temp) := 2453.2 \cdot (1 + \rho \cdot 1 \cdot temp + \rho \cdot 2 \cdot temp^2)$$

Using the eigenvalue expression for (YXw)0,0 TE and Equation (2.4) to find the antiresonant frequencies:

$$fA0\_2b\_j := \frac{1}{2 \cdot th0\_0(temp2b\_j) \cdot \sqrt{\frac{cE44(temp2b\_j) + \frac{e\_15(temp2b\_j)^2}{es11(temp2b\_j)}}{\rho\_2(temp2b\_j)}}$$

Measured Data:

28.5	11.756
33.6	11.753
43.2	11.747
51.7	11.741
61.4	11.734
70.9	11.728
80.5	11.721
90.0	11.714
100.5	11.707
110.1	11.700
120.7	11.692
130.2	11.685
139.8	11.678
150.2	11.670

temps2b :=

freqs2b :=

The percent error in the prediction of the antiresonant frequencies of Trial #2b crystal #2 (YXw)0,0 TE is:

$$errorfA0\_2b\_j := \frac{fA0\_2b \cdot 10^{-6} - freqs2b\_j}{freqs2b\_j} \cdot 100$$

1.015
1.011
1.006
1.007
1.009
1.003
1.005
1.007
1.002
1.002
1.004
1.003
1.001
1.002

For Trial #3, crystal #3, (YXw)0,0 TE:

$$th0\_0(temp) := 206.6 \cdot 10^{-6} \cdot (1 + \alpha0\_0 \cdot temp + \alpha0\_0 \cdot temp^2)$$

$$es11(temp) := es110 \cdot (1 + es111 \cdot temp + es112 \cdot temp^2)$$

$$\rho\_3(temp) := 2437.2 \cdot (1 + \rho\_1 \cdot temp + \rho\_2 \cdot temp^2)$$

Using the eigenvalue expression for (YXw)0,0 TE and Equation (2.4) to find the antiresonant frequencies:

$$fA0\_j := \frac{1}{2 \cdot th0\_0(temp3_j)} \sqrt{\frac{cE44(temp3_j) + \frac{e_{15}(temp3_j)^2}{es11(temp3_j)}}{\rho\_3(temp3_j)}}$$

Measured Data:

22.0	11.751
30.7	11.745
40.3	11.739
49.7	11.732
59.2	11.726
68.7	11.719
78.3	11.713
87.6	11.706
101.0	11.697
110.3	11.690
120.1	11.683
129.6	11.676
140.9	11.668
150.5	11.661

temps3 :=

freqs3 :=

The percent error in the prediction of the antiresonant frequencies of Trial #3 crystal #3 (YXw)0,0 TE is:

$$errorfA0\_j := \frac{fA0\_j \cdot 10^{-6} - freqs3_j}{freqs3_j} \cdot 100$$

$$errorfA0\_3 =$$

1.427
1.428
1.423
1.428
1.422
1.426
1.419
1.422
1.416
1.418
1.416
1.416
1.412
1.41

For Trial #4, crystal #4, (YXwl)0,0 TE:

$$th0\_0(temp) := 206.6 \cdot 10^{-6} \cdot (1 + \alpha0\_0 \cdot 1 \cdot temp + \alpha0\_0 \cdot 2 \cdot temp^2)$$

$$es11(temp) := \epsilon S110 \cdot (1 + \epsilon S111 \cdot temp + \epsilon S112 \cdot temp^2)$$

$$\rho\_4(temp) := 2437.5 \cdot (1 + \rho \cdot 1 \cdot temp + \rho \cdot 2 \cdot temp^2)$$

Using the eigenvalue expression for (YXwl)0,0 TE and Equation (2.4) to find the antiresonant frequencies:

$$fA0\_j := \frac{1}{2 \cdot th0\_0(temp4_j)} \sqrt{\frac{cE44(temp4_j) + \frac{e\_15(temp4_j)^2}{\epsilon S11(temp4_j)}}{\rho\_4(temp4_j)}}$$

Measured Data:

22.0	11.790
30.7	11.784
40.3	11.778
49.7	11.771
59.2	11.765
68.7	11.758
78.3	11.752
87.6	11.745
101.0	11.736
110.3	11.729
120.1	11.722
129.6	11.715
140.9	11.706
150.5	11.699

temps4 :=

freqs4 :=

The percent error in the prediction of the antiresonant frequencies of Trial #4 crystal #4 (YXwl)0,0 TE is:

$$errorfA0\_j := \frac{fA0\_j \cdot 10^{-6} - freqs4_j}{freqs4_j} \cdot 100$$

1.086	1.083
1.086	1.076
1.081	1.079
1.085	1.073
1.08	1.075
1.083	1.073
1.076	1.072
1.079	1.076
1.073	1.074

For Trial #5, crystal #5, (YXwl)0,0 TE:

$$th0\_0(temp) := 206.6 \cdot 10^{-6} \cdot (1 + \alpha0\_0 \cdot 1 \cdot temp + \alpha0\_0 \cdot 2 \cdot temp^2)$$

$$es11(temp) := \epsilon S110 \cdot (1 + \epsilon S111 \cdot temp + \epsilon S112 \cdot temp^2)$$

$$\rho\_5(temp) := 2450.1 \cdot (1 + \rho \_1 \cdot temp + \rho \_2 \cdot temp^2)$$

Using the eigenvalue expression for (YXwl)0,0 LE90 and Equation (2.4) to find the antiresonant frequencies:

$$fA0\_5\_j := \frac{1}{2 \cdot th0\_0(tempS5\_j)} \cdot \sqrt{\frac{cE11(tempS5\_j)}{\rho\_5(tempS5\_j)}}$$

Measured Data:

23.1	17.963
30.8	17.958
40.4	17.951
49.9	17.944
60.4	17.936
70.3	17.928
79.6	17.920
90.0	17.911
100.6	17.902
110.2	17.894
119.7	17.885
130.2	17.875
139.6	17.866
150.0	17.856

temps5 :=

freqs5 :=

The percent error in the prediction of the antiresonant frequencies of Trial #5 crystal #5 (YXwl)0,0 LE90 is:

$$errorfA0\_5\_j := \frac{fA0\_5 \cdot 10^{-6} - freqs5\_j}{freqs5\_j} \cdot 100$$

errorfA0_5 =	0.364
	0.363
	0.365
	0.366
	0.366
	0.368
	0.371
	0.373
	0.372
	0.37
	0.373
	0.375
	0.376
	0.376

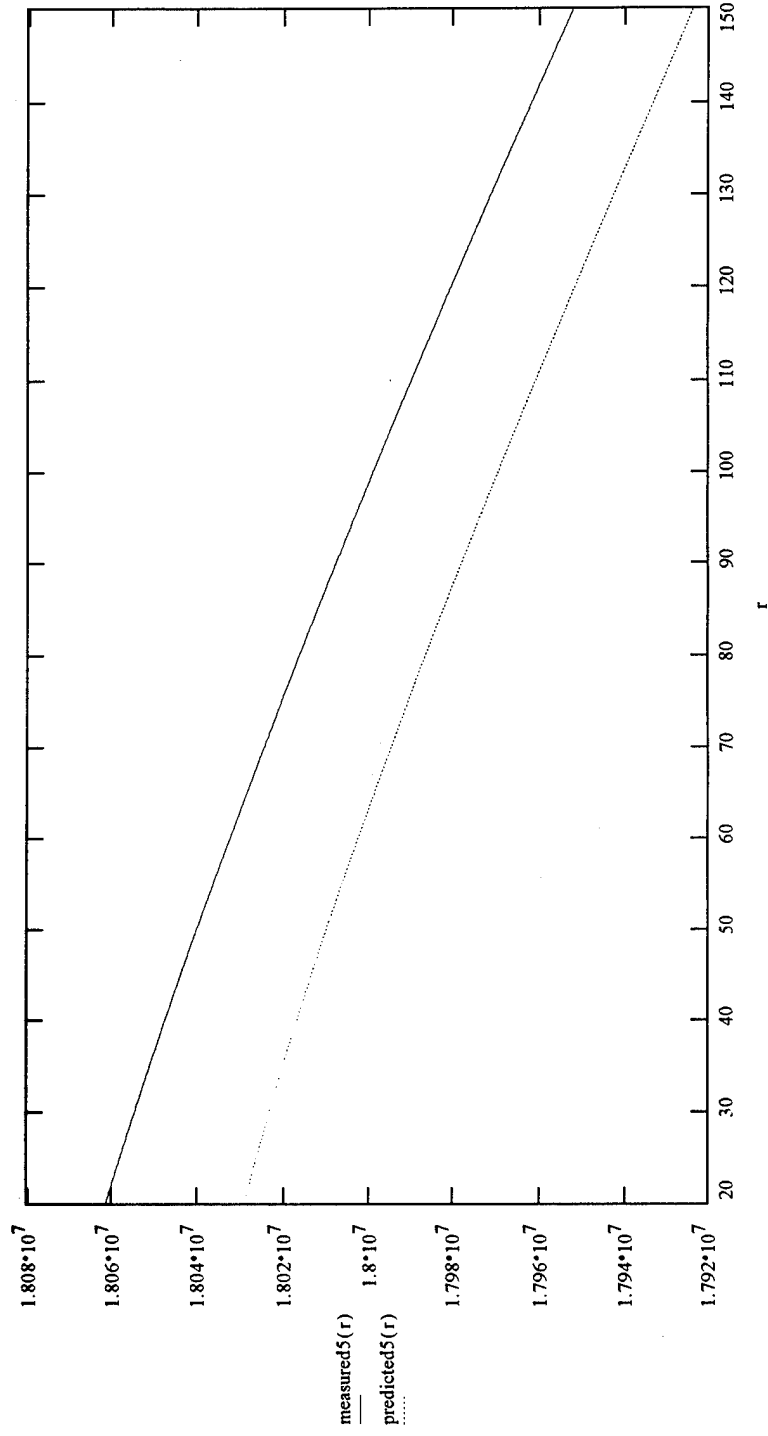
The following is a plot of the measured frequency curve and the predicted frequency curve for Trial #5, crystal #5:

$$\text{meas5} := \begin{bmatrix} 18.058 \cdot 10^6 \\ \text{Coef5}_1 \cdot 10^{-6} \\ \text{Coef5}_2 \cdot 10^{-9} \\ \text{Coef5}_3 \cdot 10^{-12} \end{bmatrix}$$

$$\text{pred5} = \begin{bmatrix} 1.80259 \cdot 10^7 \\ -3.3232229 \cdot 10^{-5} \\ -1.452558 \cdot 10^{-7} \\ 3.786382 \cdot 10^{-10} \end{bmatrix}$$

$$\text{measured5}(r) = \text{Fitfunction}(r, \text{meas5})_0 \quad \text{pred5} := \text{genfit}(\text{temps}, \text{fA0}_5, \text{guess}, \text{Fitfunction})$$

$$\text{predicted5}(r) := \text{Fitfunction}(r, \text{pred5})_0$$



For Trial #6, crystal #6, (YXwl)0,0 LE90:

$$th0\_0(temp) := 206.6 \cdot 10^{-6} \cdot (1 + \alpha0\_0 \cdot 1 \cdot temp + \alpha0\_0 \cdot 2 \cdot temp^2)$$

$$es11(temp) := \epsilon S110 \cdot (1 + \epsilon S111 \cdot temp + \epsilon S112 \cdot temp^2)$$

$$\rho\_6(temp) := 2442.7 \cdot (1 + \rho \_1 \cdot temp + \rho \_2 \cdot temp^2)$$

Using the eigenvalue expression for (YXwl)0,0 LE90 and Equation (2.4) to find the antiresonant frequencies:

$$fA0\_6\_j := \frac{1}{2 \cdot th0\_0(temp6\_j)} \sqrt{\frac{cE11(temp6\_j)}{\rho\_6(temp6\_j)}}$$

Measured Data:

23.1	17.961
30.8	17.956
40.4	17.949
49.9	17.942
60.4	17.934
70.3	17.926
79.6	17.918
90.0	17.909
100.6	17.900
110.2	17.892
119.7	17.883
130.2	17.873
139.6	17.864
150.0	17.854

temp6 :=

freqs6 :=

The percent error in the prediction of the antiresonant frequencies of Trial #6 crystal #6 (YXwl)0,0 LE90 is:

$$errorfA0\_6\_j := \frac{fA0\_6 \cdot 10^{-6} - freqs6\_j}{freqs6\_j} \cdot 100$$

0.527	errorfA0_6 =
0.526	
0.528	
0.529	
0.529	
0.531	
0.534	
0.536	
0.536	
0.533	
0.536	
0.538	
0.539	
0.539	



For Trial #7, crystal #7, (YXw)0,0 LE90:

$$\text{th0}_0(\text{temp}) := 206.6 \cdot 10^{-6} \cdot (1 + \alpha_{0_0_1} \cdot \text{temp} + \alpha_{0_0_2} \cdot \text{temp}^2)$$

$$\text{es11}(\text{temp}) := \text{es110} \cdot (1 + \text{es111} \cdot \text{temp} + \text{es112} \cdot \text{temp}^2)$$

$$\rho_7(\text{temp}) := 2446.0 \cdot (1 + \rho_1 \cdot \text{temp} + \rho_2 \cdot \text{temp}^2)$$

Using the eigenvalue expression for (YXw)0,0 LE90 and Equation (2.4) to find the antiresonant frequencies:

$$f_{A0\_j} := \frac{1}{2 \cdot \text{th0}_0(\text{temps7}_j)} \cdot \sqrt{\frac{cE11(\text{temps7}_j)}{\rho_7(\text{temps7}_j)}}$$

Measured Data:

23.1	17.944
30.8	17.938
40.4	17.931
49.9	17.925
60.4	17.917
70.3	17.909
79.6	17.901
90.0	17.892
100.6	17.883
110.2	17.875
119.7	17.866
130.2	17.856
139.6	17.847
150.0	17.837

temps7 :=

freqs7 :=

The percent error in the prediction of the antiresonant frequencies of Trial #7 crystal #7 (YXw)0,0 LE90 is:

$$\text{errorfA0\_j} := \frac{f_{A0\_j} \cdot 10^{-6} - \text{freqs7}_j}{\text{freqs7}_j} \cdot 100$$

0.555
0.559
0.561
0.556
0.557
0.559
0.561
0.564
0.563
0.561
0.564
0.566
0.567
0.567

For Trial #8, crystal #8, (YXwl)0,0 LE90:

$$th0\_0(temp) := 206.6 \cdot 10^{-6} \cdot (1 + \alpha0\_0 \cdot temp + \alpha0\_0^2 \cdot temp^2)$$

$$es11(temp) := es110 \cdot (1 + \epsilon s111 \cdot temp + \epsilon s112 \cdot temp^2)$$

$$\rho\_8(temp) := 2440.4 \cdot (1 + \rho\_1 \cdot temp + \rho\_2 \cdot temp^2)$$

Using the eigenvalue expression for (YXwl)0,0 LE90 and Equation (2.4) to find the antiresonant frequencies:

$$fA0\_8\_j := \frac{1}{2 \cdot th0\_0(temp8\_j)} \sqrt{\frac{cE11(temp8\_j)}{\rho\_8(temp8\_j)}}$$

Measured Data:

23.1	17.943
30.8	17.938
40.4	17.931
49.9	17.924
60.4	17.916
70.3	17.908
79.6	17.900
90.0	17.892
100.6	17.882
110.2	17.874
119.7	17.865
130.2	17.855
139.6	17.846
150.0	17.837

temps8 :=

freqs8 :=

The percent error in the prediction of the antiresonant frequencies of Trial #8 crystal #8 (YXwl)0,0 LE90 is:

$$errorfA0\_8\_j := \frac{fA0\_8 \cdot 10^{-6} - freqs8\_j}{freqs8\_j} \cdot 100$$

0.676
0.675
0.677
0.677
0.678
0.679
0.682
0.679
0.684
0.682
0.685
0.687
0.688
0.682

For Trial #9, crystal #9, (YXwl)0,45 LEO:

$$th0\_45(temp) := 202.1 \cdot 10^{-6} \cdot (1 + \alpha0\_45 \cdot 1 \cdot temp + \alpha0\_45 \cdot 2 \cdot temp^2)$$

$$\rho\_9(temp) := 2437.5 \cdot (1 + \rho\_1 \cdot temp + \rho\_2 \cdot temp^2)$$

temps9 :=

24.5	11.471
30.8	11.464
40.3	11.454
49.8	11.444
59.3	11.434
69.9	11.422
80.5	11.411
90.0	11.400
99.7	11.390
111.2	11.378
120.9	11.367
130.5	11.357
139.3	11.348
148.8	11.338

Using the eigenvalue expression for (YXwl)0,45 LEO and Equation (2.4) to find the antiresonant frequencies:

$$fA0\_9\_j := \frac{1}{2 \cdot th0\_45(temp9\_j)} \cdot \sqrt{\frac{0.5 \cdot cE66(temp9\_j) + 0.5 \cdot cE44(temp9\_j)}{\rho\_9(temp9\_j)}}$$

The percent error in the prediction of the antiresonant frequencies of Trial #9 crystal #9 (YXwl)0,45 LEO is:

$$errorfA0\_9\_j := \frac{fA0\_9\_j \cdot 10^{-6} - freqs9\_j}{freqs9\_j} \cdot 100$$

-0.003
-8.496 · 10 <sup>-4</sup>
-0.002
-0.004
-0.005
3.971 · 10 <sup>-4</sup>
-0.002
0.005
0.002
3.843 · 10 <sup>-4</sup>
0.007
0.005
0.002
0.002

For Trial #10, crystal #10, (YXwl)0,45 LE90:

$$th0\_45(temp) := 202.1 \cdot 10^{-6} \cdot (1 + \alpha0\_45 \cdot 1 \cdot temp + \alpha0\_45 \cdot 2 \cdot temp^2)$$

$$p\_10(temp) := 2441.2 \cdot (1 + \rho \cdot 1 \cdot temp + \rho \cdot 2 \cdot temp^2)$$

Using the eigenvalue expression for (YXwl)0,45 LE90 and Equation (2.4) to find the antiresonant frequencies:

$$fA0\_10\_j := \frac{1}{2 \cdot th0\_45(temp10\_j)} \sqrt{\frac{0.5 \cdot cE66(temp10\_j) + 0.5 \cdot cE44(temp10\_j)}{\rho\_10(temp10\_j)}}$$

Measured Data:

24.5	11.477
30.8	11.470
40.3	11.460
49.8	11.449
59.3	11.439
69.9	11.428
80.5	11.417
90.0	11.406
99.7	11.396
111.2	11.384
120.9	11.373
130.5	11.363
139.3	11.354
148.8	11.344

temps10 :=

freqs10 :=

The percent error in the prediction of the antiresonant frequencies of Trial #10 crystal #10 (YXwl)0,45 LE90 is:

$$errorfA0\_10\_j := \frac{fA0\_10\_j \cdot 10^{-6} - freqs10\_j}{freqs10\_j} \cdot 100$$

-0.131
-0.129
-0.131
-0.123
-0.125
-0.128
-0.131
-0.123
-0.126
-0.128
-0.122
-0.124
-0.126
-0.127

For Trial #10b, crystal #10, (YXwl)0,45 LE90:

$$th0\_45(temp) := 202.1 \cdot 10^{-6} \cdot (1 + \alpha0\_45 \cdot 1 \cdot temp + \alpha0\_45 \cdot 2 \cdot temp^2)$$

$$\rho\_10(temp) := 2441.2 \cdot (1 + \rho \cdot 1 \cdot temp + \rho \cdot 2 \cdot temp^2)$$

Using the eigenvalue expression for (YXwl)0,45 LE90 and Equation (2.4) to find the antiresonant frequencies:

$$fA0\_10b\_j := \frac{1}{2 \cdot th0\_45(temp10b\_j)} \cdot \sqrt{\frac{0.5 \cdot cE66(temp10b\_j) + 0.5 \cdot cE44(temp10b\_j)}{\rho\_10(temp10b\_j)}}$$

Measured Data:

28.5	11.472
33.6	11.467
43.2	11.457
51.7	11.447
61.4	11.437
70.9	11.427
80.5	11.417
90.0	11.406
100.5	11.395
110.1	11.385
120.7	11.374
130.2	11.364
139.8	11.353
150.2	11.342

freqs10b :=

The percent error in the prediction of the antiresonant frequencies of Trial #10b crystal #10 (YXwl)0,45 LE90 is:

$$errorfA0\_10b\_j := \frac{fA0\_10b\_j \cdot 10^{-6} - freqs10b\_j}{freqs10b\_j} \cdot 100$$

-0.125
-0.129
-0.132
-0.124
-0.127
-0.128
-0.131
-0.123
-0.125
-0.127
-0.129
-0.13
-0.122
-0.122

For Trial #11 crystal #11 (YXw)0,45 LE90:

$$\text{th0\_45}(\text{temp}) := 202.1 \cdot 10^{-6} \cdot (1 + \alpha_{0\_45} \cdot \text{temp} + \alpha_{0\_45}^2 \cdot \text{temp}^2)$$

$$\rho_{11}(\text{temp}) := 2437.2 \cdot (1 + \rho_1 \cdot \text{temp} + \rho_2 \cdot \text{temp}^2)$$

Using the eigenvalue expression for (YXw)0,45 LE90 and Equation (2.4) to find the antiresonant frequencies:

$$f_{A0\_11,j} := \frac{1}{2 \cdot \text{th0\_45}(\text{temps11}_j)} \sqrt{\frac{0.5 \cdot cE66(\text{temps11}_j) + 0.5 \cdot cE44(\text{temps11}_j)}{\rho_{11}(\text{temps11}_j)}}$$

Measured Data:

24.5	11.477
30.8	11.470
40.3	11.460
49.8	11.451
59.3	11.441
69.9	11.430
80.5	11.418
90.0	11.408
99.7	11.398
111.2	11.386
120.9	11.375
130.5	11.365
139.3	11.356
148.8	11.346

temps11 :=

freqs11 :=

The percent error in the prediction of the antiresonant frequencies of Trial #11 crystal #11 (YXw)0,45 LE90 is:

$$\text{errorfA0\_11}_j := \frac{f_{A0\_11,j} \cdot 10^{-6} - \text{freqs11}_j}{\text{freqs11}_j} \cdot 100 \quad \text{errorfA0\_11} =$$

-0.049
-0.047
-0.049
-0.059
-0.06
-0.063
-0.058
-0.059
-0.062
-0.064
-0.058
-0.059
-0.062
-0.062

For Trial #12, crystal #12, (YXwl)0,45 LE90:

$$th0\_45(temp) := 202.1 \cdot 10^{-6} \cdot (1 + \alpha0\_45 \cdot 1 \cdot temp + \alpha0\_45 \cdot 2 \cdot temp^2)$$

$$\rho\_12(temp) := 2417.7 \cdot (1 + \rho \cdot 1 \cdot temp + \rho \cdot 2 \cdot temp^2)$$

Using the eigenvalue expression for (YXwl)0,45 LE90 and Equation (2.4) to find the antiresonant frequencies:

$$fA0\_12\_j := \frac{1}{2 \cdot th0\_45(temp12\_j)} \sqrt{\frac{0.5 \cdot cE66(temp12\_j) + 0.5 \cdot cE44(temp12\_j)}{\rho\_12(temp12\_j)}}$$

Measured Data:

24.5	11.493
30.8	11.486
40.3	11.476
49.8	11.465
59.3	11.455
69.9	11.444
80.5	11.433
90.0	11.422
99.7	11.412
111.2	11.400
120.9	11.389
130.5	11.379
139.3	11.370
148.8	11.359

temps12 :=

The percent error in the prediction of the antiresonant frequencies of Trial #12 crystal #12 (YXwl)0,45 LE90 is:

$$errorfA0\_12\_j := \frac{fA0\_12\_j \cdot 10^{-6} - freqs12\_j}{freqs12\_j} \cdot 100$$

0.213
0.215
0.214
0.221
0.219
0.216
0.213
0.221
0.217
0.215
0.221
0.22
0.217
0.225

For Trial #18, crystal #18, (YXwl)45,0 TE:

$$th45\_0(temp) := 206.9 \cdot 10^{-6} \cdot (1 + \alpha45\_0 \cdot temp + \alpha45\_0^2 \cdot temp^2)$$

$$es11(temp) := es110 \cdot (1 + es111 \cdot temp + es112 \cdot temp^2)$$

$$\rho\_18(temp) := 2435.3 \cdot (1 + \rho\_1 \cdot temp + \rho\_2 \cdot temp^2)$$

Using the eigenvalue expression for (YXwl)45,0 TE and Equation (2.4) to find the antiresonant frequencies:

$$fA0\_18\_j := \frac{1}{2 \cdot th45\_0(temp18\_j)} \sqrt{\frac{cE44(temp18\_j) + \frac{e\_15(temp18\_j)^2}{es11(temp18\_j)}}{\rho\_18(temp18\_j)}}$$

Measured Data:

22.1	11.728
30.8	11.723
40.3	11.717
49.7	11.710
59.2	11.704
68.7	11.697
78.3	11.691
87.6	11.684
101.0	11.675
110.3	11.668
120.1	11.661
129.6	11.654
140.9	11.646
150.5	11.638

temps18 :=

freqs18 :=

The percent error in the prediction of the antiresonant frequencies of Trial #18 crystal #18 (YXwl)45,0 TE is:

$$errorfA0\_18\_j := \frac{fA0\_18\_j \cdot 10^{-6} - freqs18\_j}{freqs18\_j} \cdot 100$$

errorfA0_18 =	1.518
	1.51
	1.506
	1.51
	1.505
	1.509
	1.502
	1.505
	1.5
	1.502
	1.5
	1.5
	1.496
	1.502



For Trial #18b, crystal #18, (YXwl)45,0 TE:

$$th45_0(temp) := 206.9 \cdot 10^{-6} \cdot (1 + \alpha45_0 \cdot 1 \cdot temp + \alpha45_0 \cdot 2 \cdot temp^2)$$

$$es11(temp) := \epsilon S110 \cdot (1 + \epsilon S111 \cdot temp + \epsilon S112 \cdot temp^2)$$

$$\rho_{18}(temp) := 2435.3 \cdot (1 + \rho_1 \cdot temp + \rho_2 \cdot temp^2)$$

Using the eigenvalue expression for (YXwl)45,0 TE and Equation (2.4) to find the antiresonant frequencies:

$$fA0_{18b_j} := \frac{1}{2 \cdot th45_0(temp_{18b_j})} \sqrt{\frac{cE44(temp_{18b_j}) + \frac{e_{15}(temp_{18b_j})^2}{\epsilon S11(temp_{18b_j})}}{\rho_{18}(temp_{18b_j})}}$$

Measured Data:

28.5	11.724
33.6	11.721
43.2	11.714
51.7	11.708
61.4	11.702
70.9	11.695
80.5	11.689
90.0	11.682
100.5	11.674
110.1	11.667
120.7	11.660
130.2	11.653
139.8	11.646
150.2	11.638

temp<sub>18b</sub> :=

freqs<sub>18b</sub> :=

The percent error in the prediction of the antiresonant frequencies of Trial #18b crystal #18 (YXwl)45,0 TE is:

$$errorfA0_{18b_j} := \frac{fA0_{18b_j} \cdot 10^{-6} - freqs18b_j}{freqs18b_j} \cdot 100$$

1.515
1.511
1.514
1.516
1.509
1.512
1.506
1.508
1.512
1.512
1.505
1.504
1.503
1.504

For Trial #20a, crystal #20, (YXwl)45,0 TE:

$$th45\_0(temp) := 206.9 \cdot 10^{-6} \cdot (1 + \alpha45\_0 \cdot 1 \cdot temp + \alpha45\_0 \cdot 2 \cdot temp^2)$$

$$es11(temp) := \epsilon S110 \cdot (1 + \epsilon S111 \cdot temp + \epsilon S112 \cdot temp^2)$$

$$\rho\_20(temp) := 2423.8 \cdot (1 + \rho \cdot 1 \cdot temp + \rho \cdot 2 \cdot temp^2)$$

Using the eigenvalue expression for (YXwl)45,0 TE and Equation (2.4) to find the antiresonant frequencies:

$$fAO\_20a\_j := \frac{1}{2 \cdot th45\_0(temp20a\_j)} \cdot \sqrt{\frac{cE44(temp20a\_j) + \frac{e\_15(temp20a\_j)^2}{\epsilon s11(temp20a\_j)}}{\rho\_20(temp20a\_j)}}$$

Measured Data:

22.1	11.794
30.8	11.789
40.3	11.782
49.7	11.776
59.2	11.769
68.7	11.762
78.3	11.756
87.6	11.749
101.0	11.740
110.3	11.733
120.1	11.726
129.6	11.719
140.9	11.710
150.5	11.703

temps20a :=

freqs20a :=

The percent error in the prediction of the antiresonant frequencies of Trial #20a crystal #20 (YXwl)45,0 TE is:

$$errorfAO\_20a\_j := \frac{fAO\_20a\_j \cdot 10^{-6} - freqs20a\_j}{freqs20a\_j} \cdot 100$$

1.189
1.181
1.185
1.181
1.184
1.187
1.18
1.183
1.177
1.179
1.177
1.176
1.18
1.178

For Trial #20b, crystal #20, (YXwl)45,0 TE:

$$th45\_0(temp) := 206.9 \cdot 10^{-6} \cdot (1 + \alpha45\_0 \cdot temp + \alpha45\_0^2 \cdot temp^2)$$

$$es11(temp) := es110 \cdot (1 + \epsilon s111 \cdot temp + \epsilon s112 \cdot temp^2)$$

$$\rho\_20(temp) := 2423.8 \cdot (1 + \rho\_1 \cdot temp + \rho\_2 \cdot temp^2)$$

$$temps20b :=$$

$$freqs20b :=$$

24.4	11.792
30.8	11.789
40.2	11.782
49.8	11.776
59.4	11.769
69.9	11.762
79.5	11.755
90.0	11.748
99.7	11.741
110.1	11.733
119.8	11.726
130.2	11.719
139.7	11.711
150.2	11.703

Using the eigenvalue expression for (YXwl)45,0 TE and Equation (2.4) to find the antiresonant frequencies:

$$fA0\_20b\_j := \frac{1}{2 \cdot th45\_0(temps20b\_j)} \sqrt{\frac{cE44(temps20b\_j) + \frac{e\_15(temps20b\_j)^2}{es11(temps20b\_j)}}{\rho\_20(temps20b\_j)}}$$

The percent error in the prediction of the antiresonant frequencies of Trial #20b crystal #20 (YXwl)45,0 TE is:

$$errorfA0\_20b\_j := \frac{fA0\_20b\_j \cdot 10^{-6} - freqs20b\_j}{freqs20b\_j} \cdot 100$$

1.193
1.181
1.186
1.18
1.183
1.179
1.181
1.177
1.176
1.18
1.178
1.172
1.179
1.18

For Trial #20c, crystal #20, (YXwl)45,0 TE:

$$th45\_0(temp) := 206.9 \cdot 10^{-6} \cdot (1 + \alpha45\_0 \cdot temp + \alpha45\_0^2 \cdot temp^2)$$

$$es11(temp) := \epsilon S110 \cdot (1 + \epsilon S111 \cdot temp + \epsilon S112 \cdot temp^2)$$

$$\rho\_20(temp) := 2423.8 \cdot (1 + \rho\_1 \cdot temp + \rho\_2 \cdot temp^2)$$

Using the eigenvalue expression for (YXwl)45,0 TE and Equation (2.4) to find the antiresonant frequencies:

$$fA0\_20c\_j := \frac{1}{2 \cdot th45\_0(temp20c\_j)} \sqrt{\frac{cE44(temp20c\_j) + \frac{e\_15(temp20c\_j)^2}{es11(temp20c\_j)}}{\rho\_20(temp20c\_j)}}$$

Measured Data:

23.3	11.793
30.8	11.789
40.3	11.782
49.8	11.776
59.4	11.769
69.0	11.762
79.5	11.755
90.1	11.748
100.6	11.740
110.1	11.733
119.6	11.726
130.1	11.719
139.6	11.712
150.0	11.704

temps20c :=

freqs20c :=

The percent error in the prediction of the antiresonant frequencies of Trial #20c crystal #20 (YXwl)45,0 TE is:

$$errorfA0\_20c\_j := \frac{fA0\_20c\_j \cdot 10^{-6} - freqs20c\_j}{freqs20c\_j} \cdot 100$$

1.191
1.181
1.185
1.18
1.183
1.185
1.181
1.176
1.179
1.18
1.18
1.173
1.171
1.172

For Trial #20d, crystal #20, (YXwl)45.0 TE:

$$th45\_0(temp) := 206.9 \cdot 10^{-6} \cdot (1 + \alpha45\_0 \cdot temp + \alpha45\_0 \cdot temp^2)$$

$$es11(temp) := es110 \cdot (1 + es111 \cdot temp + es112 \cdot temp^2)$$

$$\rho\_20(temp) := 2423.8 \cdot (1 + \rho\_1 \cdot temp + \rho\_2 \cdot temp^2)$$

temps20d :=

28.5
33.6
43.2
51.7
61.4
70.9
80.5
90.0
100.5
110.1
120.7
130.2
139.8
150.2

freqs20d :=

11.789
11.786
11.780
11.774
11.767
11.760
11.754
11.747
11.740
11.733
11.725
11.718
11.711
11.703

Using the eigenvalue expression for (YXwl)45.0 TE and Equation (2.4) to find the antiresonant frequencies:

$$fA0\_20d\_j := \frac{1}{2 \cdot th45\_0(temps20d\_j)} \cdot \sqrt{\frac{cE44(temps20d\_j) + \frac{e\_15(temps20d\_j)^2}{es11(temps20d\_j)}}{\rho\_20(temps20d\_j)}}$$

The percent error in the prediction of the antiresonant frequencies of Trial #20d crystal #20 (YXwl)45.0 TE is:

$$errorfA0\_20d\_j := \frac{fA0\_20d\_j \cdot 10^{-6} - freqs20d\_j}{freqs20d\_j} \cdot 100$$

1.194
1.19
1.185
1.186
1.188
1.191
1.184
1.185
1.18
1.18
1.181
1.181
1.179
1.18

For Trial #21, crystal #21, (YXwl)45,0 LE90:

$$th45\_0(temp) := 206.9 \cdot 10^{-6} \cdot (1 + \alpha45\_0 \cdot temp + \alpha45\_0 \cdot temp^2)$$

$$\rho\_21(temp) := 2436.3 \cdot (1 + \rho\_1 \cdot temp + \rho\_2 \cdot temp^2)$$

Using the eigenvalue expression for (YXwl)45,0 LE90 and Equation (2.4) to find the antiresonant frequencies:

$$fA0\_21\_j := \frac{1}{2 \cdot th45\_0(temp21\_j)} \cdot \sqrt{\frac{\rho\_21(temp21\_j)}{0.5 \cdot cE11(temp21\_j) + 0.5 \cdot cE12(temp21\_j) + cE66(temp21\_j)}}$$

Measured Data:

22.1	16.652
30.8	16.642
40.3	16.631
49.7	16.620
59.2	16.609
68.7	16.597
78.3	16.586
87.6	16.575
101.0	16.560
110.3	16.549
120.1	16.537
129.6	16.526
140.9	16.513
150.5	16.501

temps21 :=

freqs21 :=

The percent error in the prediction of the antiresonant frequencies of Trial #21 crystal #21 (YXwl)45,0 LE90 is:

$$errorfA0\_21\_j := \frac{fA0\_21\_j \cdot 10^{-6} - freqs21\_j}{freqs21\_j} \cdot 100$$

-0.047
-0.045
-0.042
-0.039
-0.038
-0.03
-0.029
-0.027
-0.028
-0.026
-0.021
-0.021
-0.021
-0.015

For Trial #21b, crystal #21, (YXwl)45,0 LE90:

$$th45\_0(temp) := 206.9 \cdot 10^{-6} \cdot (1 + \alpha45\_0 \cdot temp + \alpha45\_0\_2 \cdot temp^2)$$

$$\rho\_21(temp) := 2436.3 \cdot (1 + \rho\_1 \cdot temp + \rho\_2 \cdot temp^2)$$

Using the eigenvalue expression for (YXwl)45,0 LE90 and Equation (2.4) to find the antiresonant frequencies:

$$fA0\_21b\_j := \frac{1}{2 \cdot th45\_0(temp21b\_j)} \sqrt{\frac{0.5 \cdot cE11(temp21b\_j) + 0.5 \cdot cE12(temp21b\_j) + cE66(temp21b\_j)}{\rho\_21(temp21b\_j)}}$$

Measured Data:

28.5	16.644
33.6	16.638
43.2	16.627
51.7	16.617
61.4	16.606
70.9	16.595
80.5	16.584
90.0	16.573
100.5	16.560
110.1	16.549
120.7	16.537
130.2	16.525
139.8	16.514
150.2	16.502

The percent error in the prediction of the antiresonant frequencies of Trial #21b crystal #21 (YXwl)45,0 LE90 is:

$$errorfA0\_21b\_j := \frac{fA0\_21b\_j \cdot 10^{-6} - freqs21b\_j}{freqs21b\_j} \cdot 100$$

-0.041
-0.039
-0.038
-0.035
-0.034
-0.033
-0.032
-0.031
-0.025
-0.025
-0.026
-0.019
-0.019
-0.019

For Trial #22, crystal #22, (YXwl)45,0 LE90:

$$th45\_0(temp) := 206.9 \cdot 10^{-6} \cdot (1 + \alpha45\_0 \cdot 1 \cdot temp + \alpha45\_0 \cdot 2 \cdot temp^2)$$

$$\rho\_22(temp) := 2437 \cdot (1 + \rho \cdot 1 \cdot temp + \rho \cdot 2 \cdot temp^2)$$

Using the eigenvalue expression for (YXwl)45,0 LE90 and Equation (2.4) to find the antiresonant frequencies:

$$fA0\_22\_j := \frac{1}{2 \cdot th45\_0(temp22\_j)} \sqrt{\frac{0.5 \cdot cE11(temp22\_j) + 0.5 \cdot cE12(temp22\_j) + cE66(temp22\_j)}{\rho\_22(temp22\_j)}}$$

Measured Data:

24.5	16.537
30.8	16.531
40.3	16.522
49.8	16.513
59.3	16.504
69.9	16.493
80.5	16.483
90.0	16.473
99.7	16.464
111.2	16.452
120.9	16.442
130.5	16.432
139.3	16.423
148.8	16.413

temps22 :=

freqs22 :=

The percent error in the prediction of the antiresonant frequencies of Trial #22 crystal #22 (YXwl)45,0 LE90 is:

0.618
0.612
0.603
0.593
0.583
0.578
0.566
0.561
0.549
0.543
0.536
0.53
0.524
0.518

$$errorfA0\_22\_j := \frac{fA0\_22\_j \cdot 10^{-6} - freqs22\_j}{freqs22\_j} \cdot 100$$

errorfA0\_22 =



For Trial #23, crystal #23, (YXwl)0,0 TE:

$$th45\_0(temp) := 206.9 \cdot 10^{-6} \cdot (1 + \alpha45\_0 \cdot temp + \alpha45\_0^2 \cdot temp^2)$$

$$\rho\_23(temp) := 2425.2 \cdot (1 + \rho\_1 \cdot temp + \rho\_2 \cdot temp^2)$$

Using the eigenvalue expression for (YXwl)45,0 LE90 and Equation (2.4) to find the antiresonant frequencies:

$$fA0\_23\_j := \frac{1}{2 \cdot th45\_0(temp23\_j)} \cdot \sqrt{\frac{0.5 \cdot cE11(temp23\_j) + 0.5 \cdot cE12(temp23\_j) + cE66(temp23\_j)}{\rho\_23(temp23\_j)}}$$

Measured Data:

23.4	16.631
30.8	16.622
40.2	16.611
49.8	16.600
59.3	16.589
69.8	16.577
79.4	16.566
89.9	16.553
101.4	16.540
110.9	16.529
120.5	16.517
129.9	16.506
139.4	16.495
149.0	16.483

temps23 :=

freqs23 :=

The percent error in the prediction of the antiresonant frequencies of Trial #23 crystal #23 (YXwl)45,0 LE90 is:

0.3
0.304
0.308
0.309
0.311
0.312
0.313
0.319
0.319
0.32
0.326
0.327
0.327
0.333

$$errorfA0\_23\_j := \frac{fA0\_23\_j \cdot 10^{-6} - freqs23\_j}{freqs23\_j} \cdot 100$$

errorfA0\_23 =

For Trial #24, crystal #24, (YXwl)45,0 LE90:

$$th45\_0(temp) := 206.9 \cdot 10^{-6} \cdot (1 + \alpha45\_0 \cdot 1 \cdot temp + \alpha45\_0 \cdot 2 \cdot temp^2)$$

$$\rho\_24(temp) := 2436.2 \cdot (1 + \rho \cdot 1 \cdot temp + \rho \cdot 2 \cdot temp^2)$$

Using the eigenvalue expression for (YXwl)45,0 LE90 and Equation (2.4) to find the antiresonant frequencies:

$$fA0\_24\_j := \frac{1}{2 \cdot th45\_0(temp24\_j)} \cdot \sqrt{\frac{0.5 \cdot cE11(temp24\_j) + 0.5 \cdot cE12(temp24\_j) + cE66(temp24\_j)}{\rho\_24(temp24\_j)}}$$

Measured Data:

23.4	16.594
30.8	16.585
40.2	16.574
49.8	16.563
59.3	16.552
69.8	16.540
79.4	16.529
89.9	16.516
101.4	16.503
110.9	16.492
120.5	16.480
129.9	16.469
139.4	16.458
149.0	16.447

temps24 :=

freqs24 :=

The percent error in the prediction of the antiresonant frequencies of Trial #24 crystal #24 (YXwl)45,0 LE90 is:

$$errorfA0\_24\_j := \frac{fA0\_24\_j \cdot 10^{-6} - freqs24\_j}{freqs24\_j} \cdot 100$$

0.296
0.301
0.304
0.306
0.308
0.309
0.31
0.317
0.316
0.317
0.324
0.325
0.326
0.325

For Trial #25, crystal #25, (YXwl)45,45 LE0:

$$th_{45\_45}(temp) := 200.1 \cdot 10^{-6} \cdot (1 + \alpha_{45\_45} \cdot temp + \alpha_{45\_45}^2 \cdot temp^2)$$

$$\rho_{25}(temp) := 2437.5 \cdot (1 + \rho_1 \cdot temp + \rho_2 \cdot temp^2)$$

Using the eigenvalue expression for (YXwl)45,45 LE0 and Equation (2.4) to find the antiresonant frequencies:

$$f_{A0\_25_j} := \frac{1}{2 \cdot th_{45\_45}(temps25_j)} \cdot \sqrt{\frac{2.5 \cdot cE_{11}(temps25_j) - 2.5 \cdot cE_{12}(temps25_j) + .5 \cdot cE_{44}(temps25_j)}{\rho_{25}(temps25_j)}}$$

Measured Data:

22.1	12.671
30.8	12.665
40.3	12.658
49.7	12.651
59.2	12.644
68.7	12.637
78.3	12.629
87.6	12.622
101.0	12.611
110.3	12.603
120.1	12.595
129.6	12.587
140.9	12.579
150.5	12.568

temps25 :=

freqs25 :=

The percent error in the prediction of the antiresonant frequencies of Trial #25 crystal #25 (YXwl)45,45 LE0 is:

$$errorf_{A0\_25_j} := \frac{f_{A0\_25_j} \cdot 10^{-6} - freqs25_j}{freqs25_j} \cdot 100$$

-0.041
-0.043
-0.042
-0.042
-0.043
-0.046
-0.043
-0.047
-0.047
-0.046
-0.048
-0.05
-0.065
-0.045

For Trial #25b, crystal #25, (YXwl)45,45 LEO:

$$th_{45\_45}(temp) := 200.1 \cdot 10^{-6} \cdot (1 + \alpha_{45\_45} \cdot temp + \alpha_{45\_45}^2 \cdot temp^2)$$

$$\rho_{25}(temp) := 2437.5 \cdot (1 + \rho_1 \cdot temp + \rho_2 \cdot temp^2)$$

Using the eigenvalue expression for (YXwl)45,45 LEO and Equation (2.4) to find the antiresonant frequencies:

$$f_{A0\_25b\_j} := \frac{1}{2 \cdot th_{45\_45}(temps_{25b\_j})} \sqrt{\frac{.25 \cdot cE11(temps_{25b\_j}) - .25 \cdot cE12(temps_{25b\_j}) + .5 \cdot cE44(temps_{25b\_j})}{\rho_{25}(temps_{25b\_j})}}$$

Measured Data:

28.5	12.666
33.6	12.663
43.2	12.656
51.7	12.649
61.4	12.644
70.9	12.635
80.5	12.627
90.0	12.620
100.5	12.614
110.1	12.603
120.7	12.594
130.2	12.589
139.8	12.578
150.2	12.569

$$temps_{25b} :=$$

$$freqs_{25b} :=$$

The percent error in the prediction of the antiresonant frequencies of Trial #25b crystal #25 (YXwl)45,45 LEO is:

-0.038
-0.043
-0.043
-0.038
-0.057
-0.044
-0.041
-0.047
-0.068
-0.044
-0.045
-0.07
-0.049
-0.051

$$errorf_{A0\_25b\_j} := \frac{f_{A0\_25b\_j} \cdot 10^{-6} - freqs_{25b\_j}}{freqs_{25b\_j}} \cdot 100$$

For Trial #26, crystal #26, (YXwl)45,45 LE0:

$$th45\_45(temp) := 200.1 \cdot 10^{-6} \cdot (1 + \alpha45\_45 \cdot temp + \alpha45\_45^2 \cdot temp^2)$$

$$\rho\_26(temp) := 2428.1 \cdot (1 + \rho\_1 \cdot temp + \rho\_2 \cdot temp^2)$$

Using the eigenvalue expression for (YXwl)45,45 LE0 and Equation (2.4) to find the antiresonant frequencies:

$$fA0\_26\_j := \frac{1}{2 \cdot th45\_45(temp26\_j)} \cdot \sqrt{\frac{.25 \cdot cE11(temp26\_j) - .25 \cdot cE12(temp26\_j) + .5 \cdot cE44(temp26\_j)}{\rho\_26(temp26\_j)}}$$

Measured Data:

23.4	12.668
30.8	12.663
40.2	12.656
49.8	12.649
59.3	12.642
69.8	12.634
79.4	12.627
89.9	12.618
101.4	12.609
110.9	12.601
120.5	12.593
129.9	12.585
139.4	12.577
149.0	12.568

temps26 :=

freqs26 :=

The percent error in the prediction of the antiresonant frequencies of Trial #26 crystal #26 (YXwl)45,45 LE0 is:

$$errorfA0\_26\_j := \frac{fA0\_26\_j \cdot 10^{-6} - freqs26\_j}{freqs26\_j} \cdot 100$$

0.168
0.166
0.168
0.167
0.165
0.164
0.159
0.163
0.159
0.158
0.157
0.155
0.159

For Trial #27, crystal #27, (YXwl)45,45 LEO:

$$th_{45\_45}(temp) := 200.1 \cdot 10^{-6} \cdot (1 + \alpha_{45\_45} \cdot temp + \alpha_{45\_45}^2 \cdot temp^2)$$

$$\rho_{27}(temp) := 2444.6 \cdot (1 + \rho_1 \cdot temp + \rho_2 \cdot temp^2)$$

Using the eigenvalue expression for (YXwl)45,45 LEO and Equation (2.4) to find the antiresonant frequencies:

$$f_{A0\_27_j} := \frac{1}{2 \cdot th_{45\_45}(temp_{27_j})} \sqrt{\frac{.25 \cdot cE11(temp_{27_j}) - .25 \cdot cE12(temp_{27_j}) + .5 \cdot cE44(temp_{27_j})}{\rho_{27}(temp_{27_j})}}$$

Measured Data:

23.4	12.598
30.8	12.593
40.2	12.586
49.8	12.579
59.3	12.572
69.8	12.564
79.4	12.556
89.9	12.548
101.4	12.539
110.9	12.531
120.5	12.523
129.9	12.515
139.4	12.507
149.0	12.498

temps27 :=

freqs27 :=

The percent error in the prediction of the antiresonant frequencies of Trial #27 crystal #27 (YXwl)45,45 LEO is:

$$errorf_{A0\_27_j} := \frac{f_{A0\_27_j} \cdot 10^{-6} - freqs27_j}{freqs27_j} \cdot 100$$

0.385
0.383
0.384
0.384
0.382
0.381
0.385
0.381
0.378
0.378
0.377
0.377
0.375
0.379

For Trial #28, crystal #28, (YXwl)45,45 LEO:

$$th45\_45(temp) := 200.1 \cdot 10^{-6} \cdot (1 + \alpha45\_45 \cdot temp + \alpha45\_45^2 \cdot temp^2)$$

$$\rho\_28(temp) := 2424.8 \cdot (1 + \rho\_1 \cdot temp + \rho\_2 \cdot temp^2)$$

Using the eigenvalue expression for (YXwl)45,45 LEO and Equation (2.4) to find the antiresonant frequencies:

$$fA0\_28\_j := \frac{1}{2 \cdot th45\_45(temp28\_j)} \sqrt{\frac{.25 \cdot cE11(temp28\_j) - .25 \cdot cE12(temp28\_j) + .5 \cdot cE44(temp28\_j)}{\rho\_28(temp28\_j)}}$$

Measured Data:

23.4	12.676
30.8	12.671
40.2	12.664
49.8	12.657
59.3	12.650
69.8	12.642
79.4	12.635
89.9	12.626
101.3	12.617
110.9	12.609
120.5	12.601
129.9	12.593
139.4	12.584
149.0	12.576

temps28 :=

freqs28 :=

The percent error in the prediction of the antiresonant frequencies of Trial #28 crystal #28 (YXwl)45,45 LEO is:

0.173
0.171
0.173
0.172
0.17
0.169
0.164
0.168
0.164
0.164
0.162
0.162
0.167
0.163

$$errorfA0\_28\_j := \frac{fA0\_28\_j \cdot 10^{-6} - freqs28\_j}{freqs28\_j} \cdot 100$$

For Trial #37a, crystal #37, (YXwl)0,90 LE90:

$$th0\_90(temp) := 201.5 \cdot 10^{-6} \cdot (1 + \alpha0\_90 \cdot 1 \cdot temp + \alpha0\_90 \cdot 2 \cdot temp^2)$$

$$\rho\_37(temp) := 2437.7 \cdot (1 + \rho \cdot 1 \cdot temp + \rho \cdot 2 \cdot temp^2)$$

Using the eigenvalue expression for (YXwl)0,90 LE90 and Equation (2.4) to find the antiresonant frequencies:

$$fA0\_37a\_j := \frac{1}{2 \cdot th0\_90(temp37a\_j)} \cdot \sqrt{\frac{cE44(temp37a\_j)}{\rho\_37(temp37a\_j)}}$$

Measured Data:

22.1	12.044
30.8	12.044
40.3	12.045
49.7	12.044
59.2	12.044
68.7	12.043
78.3	12.041
87.6	12.040
101.0	12.037
110.3	12.035
120.1	12.033
129.6	12.030
140.9	12.027
150.5	12.024

temps37a :=

freqs37a :=

The percent error in the prediction of the antiresonant frequencies of Trial #37a crystal #37 (YXwl)0,90 LE90 is:

$$errorfA0\_37a\_j := \frac{fA0\_37a \cdot 10^{-6} - freqs37a\_j}{freqs37a\_j} \cdot 100$$

errorfA0_37a =	-0.294
	-0.29
	-0.297
	-0.291
	-0.296
	-0.296
	-0.29
	-0.294
	-0.291
	-0.292
	-0.295
	-0.291
	-0.293
	-0.291



For Trial #37b, crystal #37, (YXwl)0,90 LE90:

$$th0\_90(temp) := 201.5 \cdot 10^{-6} \cdot (1 + \alpha0\_90 \cdot 1 \cdot temp + \alpha0\_90\_2 \cdot temp^2)$$

$$\rho\_37(temp) := 2437.7 \cdot (1 + \rho \cdot 1 \cdot temp + \rho \cdot 2 \cdot temp^2)$$

Using the eigenvalue expression for (YXwl)0,90 LE90 and Equation (2.4) to find the antiresonant frequencies:

$$fA0\_37b\_j := \frac{1}{2 \cdot th0\_90(temp37b\_j)} \cdot \sqrt{\frac{cE44(temp37b\_j)}{\rho\_37(temp37b\_j)}}$$

Measured Data:

23.4	12.044
30.8	12.044
40.2	12.045
49.8	12.044
59.3	12.044
69.8	12.043
79.4	12.041
89.9	12.040
101.3	12.037
110.9	12.035
120.5	12.033
129.9	12.030
139.4	12.027
149.0	12.024

temps37b :=

freqs37b :=

The percent error in the prediction of the antiresonant frequencies of Trial #37b crystal #37 (YXwl)0,90 LE90 is:

$$errorfA0\_37b\_j := \frac{fA0\_37b\_j \cdot 10^{-6} - freqs37b\_j}{freqs37b\_j} \cdot 100$$

-0.294
-0.29
-0.297
-0.291
-0.296
-0.297
-0.291
-0.298
-0.292
-0.293
-0.296
-0.292
-0.289
-0.288

For Trial #37c, crystal #37, (YXwl)0,90 LE90:

$$th0\_90(temp) := 201.5 \cdot 10^{-6} \cdot (1 + \alpha0\_90 \cdot temp + \alpha0\_90 \cdot temp^2)$$

$$\rho\_37(temp) := 2437.7 \cdot (1 + \rho \cdot temp + \rho \cdot temp^2)$$

Using the eigenvalue expression for (YXwl)0,90 LE90 and Equation (2.4) to find the antiresonant frequencies:

$$fA0\_37c_j := \frac{1}{2 \cdot th0\_90(temp37c_j)} \cdot \sqrt{\frac{cE44(temp37c_j)}{\rho\_37(temp37c_j)}}$$

Measured Data:

28.5	12.044
33.6	12.045
43.2	12.044
51.7	12.044
61.4	12.043
70.9	12.042
80.5	12.041
90.0	12.040
100.5	12.038
110.1	12.035
120.7	12.033
130.2	12.030
139.8	12.027
150.2	12.024

temps37c :=

freqs37c :=

The percent error in the prediction of the antiresonant frequencies of Trial #37c crystal #37 (YXwl)0,90 LE90 is:

$$errorfA0\_37c_j := \frac{fA0\_37c_j \cdot 10^{-6} - freqs37c_j}{freqs37c_j} \cdot 100$$

-0.291
-0.298
-0.289
-0.292
-0.289
-0.29
-0.293
-0.298
-0.299
-0.292
-0.297
-0.293
-0.29
-0.291

For Trial #38, crystal #38, (YXw)0,90 LE90:  $i = 0..12$

$$th0\_90(temp) := 201.5 \cdot 10^{-6} \cdot (1 + \alpha0\_90 \cdot temp + \alpha0\_90^2 \cdot temp^2)$$

$$\rho\_38(temp) := 2436.4 \cdot (1 + \rho\_1 \cdot temp + \rho\_2 \cdot temp^2)$$

Using the eigenvalue expression for (YXw)0,90 LE90 and Equation (2.4) to find the antiresonant frequencies:

$$fA0\_38_i := \frac{1}{2 \cdot th0\_90(temp38_i)} \cdot \sqrt{\frac{cE44(temp38_i)}{\rho\_38(temp38_i)}}$$

Measured Data:

30.8	12.017
40.2	12.017
49.8	12.016
59.3	12.016
69.8	12.015
79.4	12.013
89.9	12.012
101.3	12.009
110.9	12.007
120.5	12.005
129.9	12.002
139.4	12.000
149.0	11.997

temps38 :=

freqs38 :=

The percent error in the prediction of the antiresonant frequencies of Trial #38 crystal #38 (YXw)0,90 LE90 is:

$$errorfA0\_38_i := \frac{fA0\_38_i \cdot 10^{-6} - freqs38_i}{freqs38_i} \cdot 100$$

-0.039
-0.038
-0.032
-0.037
-0.038
-0.032
-0.039
-0.033
-0.034
-0.037
-0.033
-0.038
-0.037

For Trial #39, crystal #39, (YXwl)0,90 LE90:

$$th0\_90(temp) := 201.5 \cdot 10^{-6} \cdot (1 + \alpha0\_90 \cdot temp + \alpha0\_90^2 \cdot temp^2)$$

$$\rho\_39(temp) := 2431.6 \cdot (1 + \rho\_1 \cdot temp + \rho\_2 \cdot temp^2)$$

Using the eigenvalue expression for (YXwl)0,90 LE90 and Equation (2.4) to find the antiresonant frequencies:

$$fA0\_39\_j := \frac{1}{2 \cdot th0\_90(temp39\_i)} \cdot \sqrt{\frac{cE44(temp39\_i)}{\rho\_39(temp39\_i)}}$$

Measured Data:

30.8	12.019
40.2	12.019
49.8	12.018
59.3	12.018
69.8	12.017
79.4	12.015
89.9	12.011
101.3	12.008
110.9	12.006
120.5	12.004
129.9	12.001
139.4	11.999
149.0	11.996

temps39 :=

freqs39 :=

The percent error in the prediction of the antiresonant frequencies of Trial #39 crystal #39 (YXwl)0,90 LE90 is:

-0.121
-0.121
-0.113
-0.113
-0.105
-0.088
-0.055
-0.03
-0.013
0.004
0.029
0.045
0.07

$$errorfA0\_39\_i := \frac{fA0\_39\_i \cdot 10^{-6} - freqs39\_i}{freqs39\_i} \cdot 100 \quad errorfA0\_39 =$$

For Trial #40, crystal #40, (YXw)0,90 LE90:

$$th0\_90(temp) := 201.5 \cdot 10^{-6} \cdot (1 + \alpha0\_90 \cdot temp + \alpha0\_90^2 \cdot temp^2)$$

$$\rho\_40(temp) := 2422.8 \cdot (1 + \rho\_1 \cdot temp + \rho\_2 \cdot temp^2)$$

Using the eigenvalue expression for (YXw)0,90 LE90 and Equation (2.4) to find the antiresonant frequencies:

$$fA0\_40\_j := \frac{1}{2 \cdot th0\_90(temp40\_j)} \cdot \sqrt{\frac{cE44(temp40\_j)}{\rho\_40(temp40\_j)}}$$

Measured Data:

21.4	12.041
40.2	12.041
49.8	12.041
59.3	12.040
69.8	12.040
79.4	12.039
89.9	12.036
101.3	12.034
110.9	12.033
120.5	12.031
129.9	12.028
139.4	12.026
149.0	12.023

temps40 :=

freqs40 :=

The percent error in the prediction of the antiresonant frequencies of Trial #40 crystal #40 (YXw)0,90 LE90 is:

$$errorfA0\_40\_i := \frac{fA0\_40\_i \cdot 10^{-6} - freqs40\_i}{freqs40\_i} \cdot 100$$

-0.123
-0.123
-0.123
-0.114
-0.114
-0.106
-0.081
-0.065
-0.056
-0.04
-0.015
0.002
0.027

For Trial #49, crystal #49, (YXw)0,28.2 LEO:

$$th0\_28(temp) := 196 \cdot 10^{-6} \cdot (1 + \alpha0\_28 \cdot 1 \cdot temp + \alpha0\_28\_2 \cdot temp^2)$$

$$\rho\_49(temp) := 2438.6 \cdot (1 + \rho\_1 \cdot temp + \rho\_2 \cdot temp^2)$$

Using the eigenvalue expression for (YXw)0,28.2 LEO and Equation (2.4) to find the antiresonant frequencies:

$$fA0\_49_j := \frac{1}{2 \cdot th0\_28(temp49_j)} \cdot \sqrt{\frac{\cos\left(\frac{28.2 \cdot \pi}{189}\right)^2 \cdot cE66(temp49_j) + \sin\left(\frac{28.2 \cdot \pi}{189}\right)^2 \cdot cE44(temp49_j)}{\rho\_49(temp49_j)}}$$

Measured Data:

24.4	11.494
30.8	11.482
40.2	11.466
49.8	11.449
59.4	11.432
69.9	11.415
79.5	11.399
90.0	11.381
99.7	11.365
110.1	11.348
119.8	11.333
130.2	11.316
139.7	11.302
150.2	11.285

temps49 :=

freqs49 :=

The percent error in the prediction of the antiresonant frequencies of Trial #49 crystal #49 (YXw)0,28.2 LEO is:

$$errorfA0\_49_j := \frac{fA0\_49_j \cdot 10^{-6} - freqs49_j}{freqs49_j} \cdot 100$$

0.118
0.121
0.112
0.112
0.113
0.103
0.1
0.103
0.102
0.102
0.095
0.097
0.087
0.09

For Trial #49b, crystal #49, (YXwl)0,28.2 LEO:

$$\text{th0\_28}(\text{temp}) := 196 \cdot 10^{-6} \cdot (1 + \alpha 0\_28 \cdot \text{temp} + \alpha 0\_28 \cdot \text{temp}^2)$$

$$\rho\_49(\text{temp}) := 2438.6 \cdot (1 + \rho 1 \cdot \text{temp} + \rho 2 \cdot \text{temp}^2)$$

Using the eigenvalue expression for (YXwl)0,28.2 LEO and Equation (2.4) to find the antiresonant frequencies:

$$f_{A0\_49b_j} = \frac{1}{2 \cdot \text{th0\_28}(\text{temps49b}_j)} \cdot \sqrt{\cos\left(\frac{28.2 \cdot \pi}{189}\right)^2 \cdot cE66(\text{temps49b}_j) + \sin\left(\frac{28.2 \cdot \pi}{189}\right)^2 \cdot cE44(\text{temps49b}_j) - \rho\_49(\text{temps49b}_j)}$$

Measured Data:

23.3	11.496
30.8	11.482
40.3	11.465
49.8	11.449
59.4	11.432
69.0	11.416
79.5	11.399
90.1	11.381
100.6	11.364
110.1	11.348
119.6	11.333
130.1	11.317
139.6	11.302
150.0	11.286

temps49b :=

freqs49b :=

The percent error in the prediction of the antiresonant frequencies of Trial #49b crystal #49 (YXwl)0,28.2 LEO is:

0.119
0.121
0.12
0.112
0.113
0.108
0.1
0.102
0.098
0.102
0.098
0.09
0.088
0.084

$$\text{errorfA0\_49b}_j := \frac{f_{A0\_49b_j} \cdot 10^{-6} - \text{freqs49b}_j}{\text{freqs49b}_j} \cdot 100$$

For Trial #50, crystal #50, (YXwl)0,28.2 LEO:

$$\text{th0\_28}(\text{temp}) := 196 \cdot 10^{-6} \cdot (1 + \alpha_0 \cdot 28_1 \cdot \text{temp} + \alpha_0 \cdot 28_2 \cdot \text{temp}^2)$$

$$\rho\_50(\text{temp}) := 2433.7 \cdot (1 + \rho_1 \cdot \text{temp} + \rho_2 \cdot \text{temp}^2)$$

Using the eigenvalue expression for (YXwl)0,28.2 LEO and Equation (2.4) to find the antiresonant frequencies:

$$fA0\_50_j := \frac{1}{2 \cdot \text{th0\_28}(\text{temps50}_i)} \sqrt{\frac{\cos\left(\frac{28.2 \cdot \pi}{189}\right)^2 \cdot cE66(\text{temps50}_i) + \sin\left(\frac{28.2 \cdot \pi}{189}\right)^2 \cdot cE44(\text{temps50}_i)}{\rho\_50(\text{temps50}_i)}}$$

Measured Data:

24.4	11.486
30.8	11.474
49.8	11.441
59.4	11.424
69.9	11.406
79.5	11.390
90.0	11.373
99.7	11.357
110.1	11.340
119.8	11.325
130.2	11.308
139.7	11.293
150.2	11.277

temps50 :=

The percent error in the prediction of the antiresonant frequencies of Trial #50 crystal #50 (YXwl)0,28.2 LEO is:

-1.563
-1.46
-1.176
-1.029
-0.873
-0.733
-0.585
-0.445
-0.296
-0.164
-0.013
0.119
0.261

$$\text{errorfA0\_50}_i := \frac{fA0\_50_i \cdot 10^{-6} - \text{freqs50}_i}{\text{freqs50}_i} \cdot 100$$



For Trial #50b, crystal #50, (YXwl)0,28.2 LEO:

$$th0\_28(temp) := 196 \cdot 10^{-6} \cdot (1 + \alpha0\_28 \cdot temp + \alpha0\_28 \cdot temp^2)$$

$$\rho\_50(temp) := 2433.7 \cdot (1 + \rho\_1 \cdot temp + \rho\_2 \cdot temp^2)$$

Using the eigenvalue expression for (YXwl)0,28.2 LEO and Equation (2.4) to find the antiresonant frequencies:

$$fA0\_50b\_j := \frac{1}{2 \cdot th0\_28(temp50b\_i)} \sqrt{\frac{\cos\left(\frac{28.2 \cdot \pi}{189}\right)^2 \cdot cE66(temp50b\_i) + \sin\left(\frac{28.2 \cdot \pi}{189}\right)^2 \cdot cE44(temp50b\_i)}{\rho\_50(temp50b\_i)}}$$

Measured Data:

23.3	11.488
30.8	11.474
40.3	11.457
49.8	11.441
59.4	11.424
69.0	11.408
79.5	11.390
90.1	11.373
100.6	11.356
110.1	11.340
119.6	11.325
130.1	11.308
139.6	11.294
150.0	11.277

The percent error in the prediction of the antiresonant frequencies of Trial #50b crystal #50 (YXwl)0,28.2 LEO is:

-1.433
-1.313
-1.167
-1.028
-0.881
-0.742
-0.585
-0.437
-0.288
-0.147
-0.015
0.136
0.26

$$errorfA0\_50b\_i := \frac{fA0\_50b\_i \cdot 10^{-6} - freqs50b\_i}{freqs50b\_i} \cdot 100$$

For Trial #51, crystal #51, (YXwl)0,28.2 LE0:

$$th0\_28(temp) := 196 \cdot 10^{-6} \cdot (1 + \alpha0\_28 \cdot temp + \alpha0\_28^2 \cdot temp^2)$$

$$\rho\_51(temp) := 2428.3 \cdot (1 + \rho\_1 \cdot temp + \rho\_2 \cdot temp^2)$$

Using the eigenvalue expression for (YXwl)0,28.2 LE0 and Equation (2.4) to find the antiresonant frequencies:

$$fA0\_51_j := \frac{1}{2 \cdot th0\_28(temp51_j)} \sqrt{\frac{\cos\left(\frac{28.2 \cdot \pi}{189}\right)^2 \cdot cE66(temp51_j) + \sin\left(\frac{28.2 \cdot \pi}{189}\right)^2 \cdot cE44(temp51_j)}{\rho\_51(temp51_j)}}$$

Measured Data:

24.4	11.482
30.8	11.470
40.2	11.453
49.8	11.437
59.4	11.420
69.9	11.403
79.5	11.386
90.0	11.369
99.7	11.353
110.1	11.336
119.8	11.321
130.2	11.305
139.7	11.290
150.2	11.273

temps51 :=

freqs51 :=

The percent error in the prediction of the antiresonant frequencies of Trial #51 crystal #51 (YXwl)0,28.2 LE0 is:

0.435
0.438
0.438
0.429
0.431
0.421
0.427
0.421
0.421
0.42
0.413
0.407
0.405
0.408

$$errorfA0\_51_j := \frac{fA0\_51_j \cdot 10^{-6} - freqs51_j}{freqs51_j} \cdot 100$$

errorfA0\_51 =

For Trial #51b, crystal #51, (YXwl)0,28.2 LEO:

$$th0\_28(temp) := 196 \cdot 10^{-6} \cdot (1 + \alpha0\_28 \cdot temp + \alpha0\_28^2 \cdot temp^2)$$

$$p\_51(temp) := 2428.3 \cdot (1 + \rho \cdot temp + \rho^2 \cdot temp^2)$$

Using the eigenvalue expression for (YXwl)0,28.2 LEO and Equation (2.4) to find the antiresonant frequencies:

$$fA0\_51b_j := \frac{1}{2 \cdot th0\_28(temp51b_j)} \cdot \sqrt{\frac{\cos\left(\frac{28.2 \cdot \pi}{189}\right)^2 \cdot cE66(temp51b_j) + \sin\left(\frac{28.2 \cdot \pi}{189}\right)^2 \cdot cE44(temp51b_j)}{p\_51(temp51b_j)}}$$

Measured Data:

23.3	11.484
30.8	11.470
40.3	11.453
49.8	11.437
59.4	11.420
69.0	11.404
79.5	11.387
90.1	11.369
100.6	11.352
110.1	11.337
119.6	11.321
130.1	11.305
139.6	11.290
150.0	11.274

temps51b :=

freqs51b :=

The percent error in the prediction of the antiresonant frequencies of Trial #51b crystal #51 (YXwl)0,28.2 LEO is:

$$errorfA0\_51b_j := \frac{fA0\_51b_j \cdot 10^{-6} - freqs51b_j}{freqs51b_j} \cdot 100$$

0.436
0.438
0.437
0.429
0.431
0.426
0.418
0.42
0.416
0.411
0.416
0.408
0.407
0.402

For Trial #52, crystal #52, (YXw)0,28.2 LEO:

$$th0\_28(temp) := 196 \cdot 10^{-6} \cdot (1 + \alpha0\_28 \cdot temp + \alpha0\_28 \cdot temp^2)$$

$$p\_52(temp) := 2435.4 \cdot (1 + \rho \cdot temp + \rho \cdot temp^2)$$

Using the eigenvalue expression for (YXw)0,28.2 LEO and Equation (2.4) to find the antiresonant frequencies:

$$fA0\_52\_j := \frac{1}{2 \cdot th0\_28(temp52\_j)} \sqrt{\frac{\cos\left(\frac{28.2 \cdot \pi}{189}\right)^2 \cdot cE66(temp52\_j) + \sin\left(\frac{28.2 \cdot \pi}{189}\right)^2 \cdot cE44(temp52\_j)}{\rho\_52(temp52\_j)}}$$

Measured Data:

24.4	11.498
30.8	11.487
40.2	11.470
49.8	11.453
59.4	11.437
69.9	11.419
79.5	11.403
90.0	11.385
99.7	11.369
110.1	11.352
119.8	11.337
130.2	11.320
139.7	11.305
150.2	11.289

The percent error in the prediction of the antiresonant frequencies of Trial #52 crystal #52 (YXw)0,28.2 LEO is:

$$errorfA0\_52\_j := \frac{fA0\_52\_j \cdot 10^{-6} - freqs52\_j}{freqs52\_j} \cdot 100$$

0.149
0.143
0.143
0.142
0.135
0.134
0.131
0.134
0.133
0.132
0.125
0.128
0.126
0.12

For Trial #52b, crystal #52, (YXwl)0,28.2 LEO:

$$\text{th0\_28}(\text{temp}) := 196 \cdot 10^{-6} \cdot (1 + \alpha_0 \cdot 28 \cdot \rho_1 \cdot \text{temp} + \alpha_0 \cdot 28 \cdot 2 \cdot \text{temp}^2)$$

$$\rho\_52(\text{temp}) := 2435.4 \cdot (1 + \rho_1 \cdot \text{temp} + \rho_2 \cdot \text{temp}^2)$$

Using the eigenvalue expression for (YXwl)0,28.2 LEO and Equation (2.4) to find the antiresonant frequencies:

$$fA0\_52b_j := \frac{1}{2 \cdot \text{th0\_28}(\text{temps52b}_j)} \sqrt{\frac{\cos\left(\frac{28.2 \cdot \pi}{189}\right)^2 \cdot cE66(\text{temps52b}_j) + \sin\left(\frac{28.2 \cdot \pi}{189}\right)^2 \cdot cE44(\text{temps52b}_j)}{\rho\_52(\text{temps52b}_j)}}$$

temps52b :=

Measured Data:

23.3	11.500
30.8	11.486
40.3	11.470
49.8	11.453
59.4	11.437
69.0	11.420
79.5	11.403
90.1	11.385
100.6	11.368
110.1	11.352
119.6	11.337
130.1	11.321
139.6	11.306
150.0	11.289

fregs52b :=

0.15
0.152
0.142
0.142
0.135
0.139
0.131
0.132
0.129
0.132
0.128
0.12
0.118
0.123

The percent error in the prediction of the antiresonant frequencies of Trial #52b crystal #52 (YXwl)0,28.2 LEO is:

$$\text{errorfA0\_52b}_j := \frac{fA0\_52b_j \cdot 10^{-6} - \text{fregs52b}_j}{\text{fregs52b}_j} \cdot 100$$

For Trial #61, crystal #61, (YXw)45,56 LE0:

$$th45\_56(temp) := 203.8 \cdot 10^{-6} \cdot (1 + \alpha45\_56 \cdot temp + \alpha45\_56^2 \cdot temp^2)$$

$$\rho\_61(temp) := 2414.6 \cdot (1 + \rho\_1 \cdot temp + \rho\_2 \cdot temp^2)$$

Using the eigenvalue expression for (YXw)45,56 LE0 and Equation (2.4) to find the antiresonant frequencies:

$$fA0\_61\_j := \frac{1}{2 \cdot th45\_56(temp61\_j)} \sqrt{\frac{\cos\left(\frac{56.1 \cdot \pi}{180}\right)^2 \cdot (.5 \cdot cE11(temp61\_j) - .5 \cdot cE12(temp61\_j)) + \sin\left(\frac{56.1 \cdot \pi}{180}\right)^2 \cdot cE44(temp61\_j)}{\rho\_61(temp61\_j)}}$$

Measured Data:

24.4	12.229
30.8	12.227
40.2	12.223
49.8	12.218
59.4	12.214
69.9	12.208
79.5	12.203
90.0	12.197
99.7	12.192
110.1	12.185
119.8	12.179
130.2	12.173
139.7	12.167
150.2	12.160

The percent error in the prediction of the antiresonant frequencies of Trial #61 crystal #61 (YXw)45,56 LE0 is:

$$errorfA0\_61\_j := \frac{fA0\_61\_j \cdot 10^{-6} - freqs61\_j}{freqs61\_j} \cdot 100$$

0.444
0.439
0.437
0.441
0.435
0.44
0.438
0.439
0.434
0.44
0.44
0.436
0.435
0.436

For Trial #61b, crystal #61, (YXwl)45,56 LE0:

$$th45\_56(temp) := 203.8 \cdot 10^{-6} \cdot (1 + \alpha45\_56 \cdot 1 \cdot temp + \alpha45\_56 \cdot 2 \cdot temp^2)$$

$$\rho\_61(temp) := 2414.6 \cdot (1 + \rho \cdot 1 \cdot temp + \rho \cdot 2 \cdot temp^2)$$

Using the eigenvalue expression for (YXwl)45,56 LE0 and Equation (2.4) to find the antiresonant frequencies:

$$fA0\_61b_j := \frac{1}{2 \cdot th45\_56(temp61b_j)} \sqrt{\frac{\cos\left(\frac{56.1 \cdot \pi}{180}\right) \cdot (.5 \cdot cE11(temp61b_j) - .5 \cdot cE12(temp61b_j)) + \sin\left(\frac{56.1 \cdot \pi}{180}\right) \cdot cE44(temp61b_j)}{\rho\_61(temp61b_j)}}$$

temps61b :=

23.3
30.8
40.3
49.8
59.4
69.0
79.5
90.1
100.6
110.1
119.6
130.1
139.6
150.0

freqs61b :=

12.230
12.227
12.223
12.218
12.213
12.209
12.203
12.197
12.191
12.185
12.180
12.173
12.167
12.160

Measured Data:

The percent error in the prediction of the antiresonant frequencies of Trial #61b crystal #61 (YXwl)45,56 LE0 is:

$$errorfA0\_61b_j := \frac{fA0\_61b_j \cdot 10^{-6} - freqs61b_j}{freqs61b_j} \cdot 100 \text{ errorfA0\_61b} =$$

0.44
0.439
0.437
0.441
0.443
0.435
0.438
0.439
0.438
0.44
0.433
0.436
0.435
0.437

For Trial #62, crystal #62, (YXwl)45,56 LEO:

$$th45\_56(temp) := 203.8 \cdot 10^{-6} \cdot (1 + \alpha45\_56 \cdot temp + \alpha45\_56^2 \cdot temp^2)$$

$$\rho\_62(temp) := 2433.3 \cdot (1 + \rho\_1 \cdot temp + \rho\_2 \cdot temp^2)$$

Using the eigenvalue expression for (YXwl)45,56 LEO and Equation (2.4) to find the antiresonant frequencies:

$$fA0\_62\_j := \frac{1}{2 \cdot th45\_56(temp62\_j)} \sqrt{\frac{\cos\left(\frac{56.1 \cdot \pi}{180}\right)^2 \cdot (.5 \cdot cE11(temp62\_j) - .5 \cdot cE12(temp62\_j)) + \sin\left(\frac{56.1 \cdot \pi}{180}\right)^2 \cdot cE44(temp62\_j)}{\rho\_62(temp62\_j)}}$$

Measured Data:

24.4	12.183
30.8	12.181
40.2	12.176
49.8	12.172
59.4	12.167
69.9	12.162
79.5	12.157
90.0	12.151
99.7	12.145
110.1	12.139
119.8	12.133
130.2	12.127
139.7	12.121
150.2	12.114

temps62 :=

freqs62 :=

The percent error in the prediction of the antiresonant frequencies of Trial #62 crystal #62 (YXwl)45,56 LEO is:

$$errorfA0\_62\_j := \frac{fA0\_62\_j \cdot 10^{-6} - freqs62\_j}{freqs62\_j} \cdot 100 \quad errorfA0\_62 =$$

0.435
0.43
0.437
0.433
0.435
0.432
0.43
0.431
0.434
0.432
0.433
0.428
0.428
0.429



For Trial #62b, crystal #62, (YXwl)45,56 LEO:

$$th45\_56(temp) := 203.8 \cdot 10^{-6} \cdot (1 + \alpha45\_56 \cdot temp + \alpha45\_56 \cdot temp^2)$$

$$\rho\_62(temp) := 2433.3 \cdot (1 + \rho \cdot temp + \rho \cdot temp^2)$$

Using the eigenvalue expression for (YXwl)45,56 LEO and Equation (2.4) to find the antiresonant frequencies:

$$fA0\_62b\_j := \frac{1}{2 \cdot th45\_56(temp62b\_j)} \cdot \sqrt{\frac{\cos\left(\frac{56.1 \cdot \pi}{180}\right)^2 \cdot (.5 \cdot cE11(temp62b\_j) - .5 \cdot cE12(temp62b\_j)) + \sin\left(\frac{56.1 \cdot \pi}{180}\right)^2 \cdot cE44(temp62b\_j)}{\rho\_62(temp62b\_j)}}$$

temps62b :=

23.3
30.8
40.3
49.8
59.4
69.0
79.5
90.1
100.6
110.1
119.6
130.1
139.6
150.0

freqs62b :=

12.184
12.181
12.176
12.172
12.167
12.162
12.157
12.151
12.145
12.139
12.133
12.127
12.121
12.114

Measured Data:

The percent error in the prediction of the antiresonant frequencies of Trial #62b crystal #62 (YXwl)45,56 LEO is:

$$errorfA0\_62b\_j := \frac{fA0\_62b \cdot 10^{-6} - freqs62b\_j}{freqs62b\_j} \cdot 100 \text{ errorfA0\_62b} =$$

0.431
0.43
0.436
0.433
0.435
0.435
0.43
0.431
0.43
0.432
0.434
0.429
0.428
0.43

For Trial #63, crystal #63, (YXwl)45,56 LEO:

$$th_{45\_56}(temp) := 203.8 \cdot 10^{-6} \cdot (1 + \alpha_{45\_56} \cdot temp + \alpha_{45\_56}^2 \cdot temp^2)$$

$$\rho_{63}(temp) := 2423.9 \cdot (1 + \rho_1 \cdot temp + \rho_2 \cdot temp^2)$$

Using the eigenvalue expression for (YXwl)45,56 LEO and Equation (2.4) to find the antiresonant frequencies:

$$f_{A0\_63\_j} := \frac{1}{2 \cdot th_{45\_56}(temps63_j)} \sqrt{\frac{\cos\left(\frac{56.1 \cdot \pi}{180}\right)^2 \cdot (.5 \cdot cE11(temps63_j) - .5 \cdot cE12(temps63_j)) + \sin\left(\frac{56.1 \cdot \pi}{180}\right)^2 \cdot cE44(temps63_j)}{\rho_{63}(temps63_j)}}$$

Measured Data:

24.4	12.195
30.8	12.193
40.2	12.188
49.8	12.184
59.4	12.179
69.9	12.174
79.5	12.169
90.0	12.163
99.7	12.157
110.1	12.151
119.8	12.145
130.2	12.139
139.7	12.132
150.2	12.125

The percent error in the prediction of the antiresonant frequencies of Trial #63 crystal #63 (YXwl)45,56 LEO is:

$$errorf_{A0\_63\_j} := \frac{f_{A0\_63\_j} \cdot 10^{-6} - freqs63_j}{freqs63_j} \cdot 100 \quad errorf_{A0\_63} =$$

0.531
0.525
0.532
0.528
0.53
0.527
0.525
0.526
0.529
0.528
0.528
0.523
0.531
0.532

For Trial #63b, crystal #63, (YXwl)45,56 LEO:

$$th45\_56(temp) := 203.8 \cdot 10^{-6} \cdot (1 + \alpha45\_56_1 \cdot temp + \alpha45\_56_2 \cdot temp^2)$$

$$\rho\_63(temp) := 2423.9 \cdot (1 + \rho_1 \cdot temp + \rho_2 \cdot temp^2)$$

Using the eigenvalue expression for (YXwl)45,56 LEO and Equation (2.4) to find the antiresonant frequencies:

$$fA0\_63b_j := \frac{1}{2 \cdot th45\_56(temp63b_j)} \sqrt{\frac{\cos\left(\frac{56.1 \cdot \pi}{180}\right)^2 \cdot (.5 \cdot cE11(temp63b_j) - .5 \cdot cE12(temp63b_j)) + \sin\left(\frac{56.1 \cdot \pi}{180}\right)^2 \cdot cE44(temp63b_j)}{\rho\_63(temp63b_j)}}$$

Measured Data:

23.3	12.196
30.8	12.192
40.3	12.188
49.8	12.184
59.4	12.179
69.0	12.174
79.5	12.169
90.1	12.163
100.6	12.157
110.1	12.151
119.6	12.145
130.1	12.139
139.6	12.133
150.0	12.126

The percent error in the prediction of the antiresonant frequencies of Trial #63b crystal #63 (YXwl)45,56 LEO is:

$$errorfA0\_63b_j := \frac{fA0\_63b_j \cdot 10^{-6} - freqs63b_j}{freqs63b_j} \cdot 100$$

0.526
0.534
0.532
0.528
0.53
0.531
0.525
0.526
0.525
0.528
0.529
0.524
0.523
0.525

For Trial #64, crystal #64, (YXwl)45,56 LE0:

$$th_{45\_56}(temp) := 203.8 \cdot 10^{-6} \cdot (1 + \alpha_{45\_56_1} \cdot temp + \alpha_{45\_56_2} \cdot temp^2)$$

$$\rho_{64}(temp) := 2429.5 \cdot (1 + \rho_{1_1} \cdot temp + \rho_{2_1} \cdot temp^2)$$

Using the eigenvalue expression for (YXwl)45,56 LE0 and Equation (2.4) to find the antiresonant frequencies:

$$f_{A0\_64\_j} := \frac{1}{2 \cdot th_{45\_56}(temps64\_j)} \sqrt{\frac{\cos\left(\frac{56.1 \cdot \pi}{180}\right)^2 \cdot (.5 \cdot cE11(temps64\_j) - .5 \cdot cE12(temps64\_j)) + \sin\left(\frac{56.1 \cdot \pi}{180}\right)^2 \cdot cE44(temps64\_j)}{\rho_{64}(temps64\_j)}}$$

Measured Data:

24.4	12.217
30.8	12.215
40.2	12.211
49.8	12.206
59.4	12.202
69.9	12.196
79.5	12.191
90.0	12.185
99.7	12.180
110.1	12.173
119.8	12.167
130.2	12.161
139.7	12.155
150.2	12.148

The percent error in the prediction of the antiresonant frequencies of Trial #64 crystal #64 (YXwl)45,56 LE0 is:

$$errorf_{A0\_64\_j} := \frac{f_{A0\_64\_j} \cdot 10^{-6} - freqs64\_j}{freqs64\_j} \cdot 100 \quad errorf_{A0\_64} =$$

0.234
0.229
0.227
0.231
0.225
0.23
0.228
0.229
0.224
0.23
0.23
0.226
0.225
0.226

For Trial #64b, crystal #64, (YXwl)45,56 LEO:

$$th_{45\_56}(temp) := 203.8 \cdot 10^{-6} \cdot (1 + \alpha_{45\_56} \cdot temp + \alpha_{45\_56} \cdot temp^2)$$

$$\rho_{64}(temp) := 2429.5 \cdot (1 + \rho_1 \cdot temp + \rho_2 \cdot temp^2)$$

Using the eigenvalue expression for (YXwl)45,56 LEO and Equation (2.4) to find the antiresonant frequencies:

$$f_{A0\_64b\_j} := \frac{1}{2 \cdot th_{45\_56}(temps64b\_j)} \sqrt{\frac{\cos\left(\frac{56.1 \cdot \pi}{180}\right)^2 \cdot (.5 \cdot cE11(temps64b\_j) - .5 \cdot cE12(temps64b\_j)) + \sin\left(\frac{56.1 \cdot \pi}{180}\right)^2 \cdot cE44(temps64b\_j)}{\rho_{64}(temps64b\_j)}}$$

temps64b :=

23.3
30.8
40.3
49.8
59.4
69.0
79.5
90.1
100.6
110.1
119.6
130.1
139.6
150.0

freqs64b :=

12.218
12.215
12.211
12.206
12.202
12.197
12.191
12.185
12.179
12.173
12.168
12.161
12.155
12.148

Measured Data:

0.23
0.229
0.227
0.231
0.225
0.226
0.228
0.229
0.228
0.23
0.223
0.226
0.226
0.227

The percent error in the prediction of the antiresonant frequencies of Trial #64b crystal #64 (YXwl)45,56 LEO is:

$$errorf_{A0\_64b\_j} := \frac{f_{A0\_64b\_j} \cdot 10^{-6} - freqs64b\_j}{freqs64b\_j} \cdot 100 \text{ errorf}_{A0\_64b\_j}$$

## Bibliography

- [1] G. S. Kino, *Acoustic Waves*. Prentice-Hall, Inc., New Jersey, 1987.
- [2] J. A. Kosinski, "Pure-Mode Loci for Dilithium Tetraborate Piezoelectric Resonators and Transducers." Doctorate Dissertation, The State University of New Jersey, New Brunswick, New Jersey, May 1993.
- [3] J. R. Vig, *A Tutorial: Quartz Crystal Resonators and Oscillators*. Submitted to U.S. Army Electronics Technology and Devices Laboratory, Fort Monmouth, NJ, July 1992.
- [4] A. Ballato, J. Kosinski, S. Mallikarjun, and T. Lucaszek, "A comparison of predicted and measured properties of doubly-rotated lithium tetraborate resonators," Proceedings of the 45th Annual Frequency Control Symposium, pp. 217-221, May 1991.
- [5] J. Krogh-Moe, "The crystal structure of lithium diborate,  $\text{Li}_2\text{O}\cdot 2\text{B}_2\text{O}_3$ ," Acta Crystallographica, Vol. 15, pp. 190-193, 1962.
- [6] W. Voigt, *Lehrbuch der Kristallphysik*. B. G. Teubner, Leipzig, 1928.
- [7] J. F. Nye, *Physical Properties of Crystals*. Oxford University Press, London, 1957.
- [8] K. Fukuta, J. Ushizawa, H. Suzuki, Y. Ebata, and S. Matsumura, "Growth and properties of  $\text{Li}_2\text{B}_4\text{O}_7$  single crystal for SAW device applications," Japanese Journal of Applied Physics, Vol. 22, Supplement 22-2, pp. 140-142, 1983.
- [9] C. D. J. Emin and J. F. Werner, "The bulk acoustic wave properties of lithium tetraborate," Proceedings of the 37th Annual Frequency Control Symposium, pp. 136-143, June 1983.
- [10] T. Shiosaki, M. Adachi, H. Kobayashi, K. Araki, and A. Kawabata, "Elastic, piezoelectric, acousto-optic and electro-optic properties of  $\text{Li}_2\text{B}_4\text{O}_7$ ," Proceedings of the 5th Symposium on Ultrasonic Electronics, pp. 5-8, 1984.

- [11] A. S. Bhalla, L. E. Cross, and R. W. Whatmore, "Pyroelectric and piezoelectric properties of lithium tetraborate single crystal," Japanese Journal of Applied Physics, Vol. 24, Supplement 24-2, pp. 727-729, 1985.
- [12] L. Bohaty, S. Haussühl, and J. Liebertz, "Electrooptical coefficients and temperature and pressure derivatives of the elastic constants of tetragonal  $\text{Li}_2\text{B}_4\text{O}_7$ ," Crystal Research and Technology, Vol. 24, No. 11, pp. 1159-1163, November 1989.
- [13] H. A. A. Sidek, G. A. Saunders, and B. James, "The pressure and temperature dependences of the elastic behavior of lithium tetraborate," Journal of the Physics and Chemistry of Solids, Vol. 51, No. 5, pp. 457-465, 1990.
- [14] K. Ya. Borman and Ya. V. Burak, "Characteristics of the thermal expansion of  $\text{Li}_2\text{B}_4\text{O}_7$ ," Inorganic Materials, Vol. 26, No. 2, pp. 372-373, February 1990.  
Translated from Izvestiya Akademii Nauk SSSR, Neorganische Materialy, Vol. 26, No. 2, pp. 440-442, February 1990.
- [15] H. F. Tiersten, "Thickness vibrations of piezoelectric plates," Journal of the Acoustical Society of America, Vol. 35, No. 1, pp. 53-58, January 1963.
- [16] B. A. Auld, *Acoustic Fields and Waves in Solids*. Vol. I, John Wiley & Sons, Inc., New York, 1973.
- [17] "IEEE Standard on Piezoelectricity: ANSI/IEEE Std 176-1987," available from IEEE, 345 East 47th Street, New York, NY 10017.
- [18] A. Ballato, H. L. Bertoni, and T. Tamir, "Transmission-line analogs for stacked crystals with piezoelectric excitation," presented at the 83rd meeting of the Acoustical Society of America, Buffalo, New York, 18-21 April 1972, paper NN3. Abstract: Journal of the Acoustical Society of America, Vol. 52, No. 1 (Part 1), p. 178, July 1972.
- [19] A. Ballato, "Transmission-line analogs for stacked piezoelectric crystal devices," Proceedings of the 26th Annual Frequency Control Symposium, pp. 86-91, June 1972.

- [20] A. Ballato, "Transmission-line analogs for piezoelectric structures," Doctorate Dissertation, Polytechnic Institute of Brooklyn, June 1972.
- [21] A. Ballato, H. L. Bertoni, and T. Tamir, "Systematic network approach for piezoelectrically driven crystal plates and stacks," presented at the 1972 IEEE Ultrasonics Symposium, 4-7 October 1972, Boston, MA, paper B-2. Abstract: IEEE Transactions on Sonics and Ultrasonics, Vol. SU-20, No. 1, p. 43, January 1973.
- [22] A. Ballato, "Networks for crossed-field and in-line excitation of bulk and surface acoustic waves," Proceedings of the Symposium on Optical and Acoustical Micro-Electronics, Polytechnic Institute of New York, pp. 599-615, April 1974.
- [23] A. Ballato, "Bulk and surface acoustic wave excitation and network representation," Proceedings of the 28th Annual Frequency Control Symposium, pp. 270-279, May 1974.
- [24] E. R. Hatch and A. Ballato, "Lateral-field excitation of quartz plates," 1983 IEEE Ultrasonics Symposium Proceedings, pp. 512-515, October-November 1983.
- [25] A. Ballato, "Doubly rotated thickness mode plate vibrators," *Physical Acoustics*, Vol. 13 (W. P. Mason and R. N. Thurston eds.). New York: Academic Press, pp. 114-181, 1977.
- [26] J. A. Kosinski, A. Ballato, and Yicheng Lu, "An improved method for the determination of piezoelectric material constants," 1994 IEEE International Frequency Control Symposium, pp. 85-90, January 1994.
- [27] J. Zelenka, *Piezoelectric Resonators and Their Applications*. Elsevier, Amsterdam, 1986.
- [28] MathCAD Plus 5.0, available from MathSoft Inc., 101 Main Street, Cambridge, MA 02142.



- [29] N. M. Shorrocks, R. W. Whatmore, F. W. Ainger, and I. M. Young, "Lithium tetraborate - a new temperature compensated piezoelectric substrate material for surface acoustic wave devices," 1981 IEEE Ultrasonic Symposium Proceedings, pp. 337-340, October 1981.
- [30] R. W. Whatmore and I. M. Young, "Application of lithium tetraborate to SAW devices," U. S. Patent 4,523,119, issued June 11, 1985.
- [31] M. Adachi, T. Shiosaki, H. Kobayashi, O. Ohnishi, and A. Kawabata, "Temperature compensated piezoelectric lithium tetraborate crystal for high frequency surface acoustic wave and bulk wave device applications," IEEE Ultrasonics Symposium Proceedings, pp. 228-232, October 1985.
- [32] I. M. Sil'vestrova, P. A. Senyushenkov, V. A. Lomonov, and Yu. V. Pisarevskii, "Anomalies of the temperature dependences of the elastic properties of lithium tetraborate under thermal cycling conditions," Soviet Physics - Solid State, Vol. 31, No. 10, pp. 1836-1837, Oct. 1989. Translated from Fizika Tverdogo Tela, Vol. 31, No. 10, pp. 311-313, October 1989.
- [33] Wang Jinfen, Zhang Lei, Qin Zikai, Wang Hong, He Dazhen, and Hu Shaoqin, "Measurements of electro-elastic constants of lithium tetraborate ( $\text{Li}_2\text{B}_4\text{O}_7$ ) crystal," Acta Acustica, Vol. 15, No. 6, pp. 425-431, November 1990.
- [34] T. Shiosaki, M. Adachi, and A. Kawabata, "Growth and properties of piezoelectric lithium tetraborate crystal for BAW and SAW devices," IEEE International Symposium on Applications of Ferroelectrics (ISAF) Proceedings, pp. 455-464, June 1986.
- [35] J. A. Kosinski, personal communication, March 1994.

## Vita

Gregory Scott Weaver was born in 1970 in Lebanon, Pennsylvania, and grew up in Dallas, Texas. He graduated in 1988 with high honors from Skyline High School in Dallas and entered the Air Force Academy that year. He attended Purdue University during the 1990-1991 academic year. He returned to the Air Force Academy in 1991, and graduated in 1993 with a B.S. in physics. He graduated from the Air Force Institute of Technology, WPAFB, OH, with an M.S. in electrical engineering in June 1995.

# REPORT DOCUMENTATION PAGE

Form Approved  
OMB No. 0704-0188

Public reporting burden for this collection of information is estimated to average 1 hour per response, including the time for reviewing instructions, searching existing data sources, gathering and maintaining the data needed, and completing and reviewing the collection of information. Send comments regarding this burden estimate or any other aspect of this collection of information, including suggestions for reducing this burden, to Washington Headquarters Services, Directorate for Information Operations and Reports, 1215 Jefferson Davis Highway, Suite 1204, Arlington, VA 22202-4302, and to the Office of Management and Budget, Paperwork Reduction Project (0704-0188), Washington, DC 20503.

<b>1. AGENCY USE ONLY (Leave blank)</b>		<b>2. REPORT DATE</b> June 1995	<b>3. REPORT TYPE AND DATES COVERED</b> Master's Thesis	
<b>4. TITLE AND SUBTITLE</b> DETERMINATION OF THE TEMPERATURE COEFFICIENTS OF SELECTED MATERIAL CONSTANTS OF DILITHIUM TETRABORATE			<b>5. FUNDING NUMBERS</b>	
<b>6. AUTHOR(S)</b>  Gregory S. Weaver, 2nd Lieutenant, USAF				
<b>7. PERFORMING ORGANIZATION NAME(S) AND ADDRESS(ES)</b>  Air Force Institute of Technology, WPAFB OH 45433-6583			<b>8. PERFORMING ORGANIZATION REPORT NUMBER</b>  AFIT/GE/ENG/95J-04	
<b>9. SPONSORING/MONITORING AGENCY NAME(S) AND ADDRESS(ES)</b>  Dr. John A. Kosinski, US Army Research Laboratory (AMSRL-PS-ED) USARL, Bldg 2700, Fort Monmouth, NJ 07703-5601			<b>10. SPONSORING/MONITORING AGENCY REPORT NUMBER</b>	
<b>11. SUPPLEMENTARY NOTES</b>				
<b>12a. DISTRIBUTION / AVAILABILITY STATEMENT</b>  Distribution Unlimited			<b>12b. DISTRIBUTION CODE</b>	
<b>13. ABSTRACT (Maximum 200 words)</b>  The first and second order temperature coefficients of the material constant $c_{11}^E$ , $c_{12}^E$ , $c_{44}^E$ , $c_{66}^E$ , and $e_{15}$ of dilithium tetraborate ( $\text{Li}_2\text{B}_4\text{O}_7$ ) have been measured over a temperature range of 20°C to 150°C. An improved resonator method was used to measure the fundamental zero mass loading antiresonant frequencies of selected pure-mode orientation of $\text{Li}_2\text{B}_4\text{O}_7$ . Material constants extraction was performed using a linear least squares matrix method. The resulting material constant curves were fit with a third order power series to obtain their corresponding temperature coefficients. The calculated temperature coefficients of the material constants $c_{11}^E$ , $c_{12}^E$ , $c_{44}^E$ , $c_{66}^E$ , and $e_{15}$ of $\text{Li}_2\text{B}_4\text{O}_7$ were used to predict the zero mass loading antiresonant frequencies of the crystal samples with average errors of 1.20% for thickness excitation and 0.285% for lateral excitation.				
<b>14. SUBJECT TERMS</b> dilithium tetraborate, temperature coefficients, material constants, mass loading, zero temperature coefficient orientation.			<b>15. NUMBER OF PAGES</b> 179	
			<b>16. PRICE CODE</b>	
<b>17. SECURITY CLASSIFICATION OF REPORT</b> UNCLASSIFIED	<b>18. SECURITY CLASSIFICATION OF THIS PAGE</b> UNCLASSIFIED	<b>19. SECURITY CLASSIFICATION OF ABSTRACT</b> UNCLASSIFIED	<b>20. LIMITATION OF ABSTRACT</b> UL	